

**Telescopic model of groundwater and surface
water interactions near San Antonio, NM**

**by
Laura J. Wilcox**

**Submitted in Partial Fulfillment
of the Requirements for the**

Masters of Science in Hydrology

**New Mexico Institute of Mining and Technology
Department of Earth and Environmental Science**

Socorro, NM

2003

ACKNOWLEDGEMENTS

My committee, composed of Robert Bowman, Nabil Shafike, and Brian McPherson, deserves recognition for collaborating on the project. Robert provided thoughtful support and ideas regarding water level and chemistry analysis. Nabil's guidance and problem solving tactics were crucial to the creation and calibration of the telescopic model. Brian gave helpful expertise in modeling and an outsider's view of Rio Grande issues. Funding agencies for the project were the Interstate Stream Commission and the Army Corps of Engineers. Other key contributors were the Bureau of Reclamation, and the Middle Rio Grande Conservancy District that provided information and access to wells, drains, and canals used in the study. Peggy Johnson and Dave Love, New Mexico Bureau of Mining and Mineral Resources, assisted with information regarding local geology and hydrogeology. Fieldwork assistance was performed by Page Pegram, Talon Newton, Kate Richards, Ryan Jakubowski, Christian Krueger, Michele Pate, Robert Bowman, Bryce Johnson, and Bayani Cardenas. Eunice Wilcox, Christian Krueger, and the committee conducted proofreading of the thesis. S.S. Papadopoulos and Associates, namely Bryan Grigsby, Steve Lindblom, Greg Pargas, Stephanie Kuhn, and Peter Lang, are recognized for their company's many recent publications regarding the Rio Grande water supply, and providing their result data from geologic log analysis and pump tests.

TABLE OF CONTENTS

	Page
LIST OF FIGURES	v
LIST OF TABLES	viii
LIST OF ABBREVIATIONS	ix
1. INTRODUCTION	1
1.1 MOTIVATION FOR THIS STUDY	1
1.2 THE RIO GRANDE COMPACT	2
1.3 WATER DEMANDS IN THE SOCORRO REACH OF THE RIO GRANDE	4
1.4 OBJECTIVES	5
2. REGIONAL OVERVIEW	8
2.1 LOCATION	8
2.2 CLIMATE	9
2.3 GEOLOGY	12
2.4 HYDROLOGY	13
2.4.1 The Rio Grande	14
2.4.2 The Low Flow Conveyance Channel	15
2.4.3 Agricultural Canals and Drains	16
2.4.4 Tributaries	17
2.4.5 Elephant Butte Reservoir	18
2.4.6 Groundwater	18
2.5 FLORA	19
2.6 FAUNA	20
3. PREVIOUS/ONGOING WORK	21
3.1 RIVER SEEPAGE ANALYSIS	21
3.2 WATER LEVEL DATA	23
3.3 ONGOING MODELING EFFORTS	26
3.4 ADDITIONAL STUDIES	27
3.4.1 Groundwater/Surface Water Interactions	27
3.4.2 Groundwater Resources	28
4. METHODS	29
4.1 CHARACTERIZATION OF STUDY AREA	29
4.1.1 Groundwater Elevations	29
4.1.2 Surface Water Elevations	39

	Page
4.1.3 Flood Plain Geology.....	41
4.1.4 Aquifer Tests.....	41
4.2 MODEL CONSTRUCTION.....	49
4.2.1 Grid.....	49
4.2.2 Hydrostratigraphic Layers.....	49
4.2.3 Vegetation.....	53
4.2.4 Surface Water System.....	56
4.2.5 Initial Conditions.....	59
4.3 STEADY-STATE MODEL.....	60
4.4 TRANSIENT-STATE MODEL.....	64
5. SENSITIVITY ANALYSES.....	69
5.1 HOMOGENEOUS ANISOTROPIC HYDROSTRATIGRAPHY.....	70
5.2 HETEROGENOUS ISOTROPIC HYDROSTRATIGRAPHY.....	73
5.3 ALTERATIONS TO HYDRAULIC CONDUCTIVITY.....	76
6. MANAGEMENT ALTERNATIVES.....	82
6.1 EVALUATION OF THE SYSTEM PRIOR TO THE LFCC.....	82
6.1.1 Steady-state.....	82
6.1.2 Transient-state.....	86
6.2 DECREASED RIPARIAN EVAPOTRANSPIRATION.....	89
6.3 EVALUATION OF RELOCATION OF RIVER CHANNEL.....	93
7. CONCLUSIONS.....	99
8. RECOMMENDATIONS FOR FUTURE WORK.....	103
8.1 MODEL CONSTRUCTION.....	103
8.2 INPUT DATA.....	104
8.3 LINKING REGIONAL AND TELESCOPIC MODELS.....	105
REFERENCES.....	107
APPENDICES.....	110
APPENDIX A: Surface water system - San Acacia to San Marcial.....	A-1
APPENDIX B: Additional water level data.....	A-8
APPENDIX C: BOR monitoring well locations.....	A-13
APPENDIX D: Well and surface water elevations.....	A-14
APPENDIX E: NMISC monitoring well locations.....	A-30
APPENDIX F: Surface water measurement locations.....	A-31
APPENDIX G: Borehole logs for NMISC wells.....	A-32

LIST OF FIGURES

	Page
Figure 1-1: Regional (inset) and local scale study area maps	3
Figure 1-2: Average consumptive use from San Acacia to San Marcial	4
Figure 2-1: Average annual precipitation recorded 1914-2002	10
Figure 2-2: Average annual snowfall recorded 1914-2002	10
Figure 2-3: Cumulative monthly precipitation recorded at Socorro.....	11
Figure 2-4: Cumulative monthly snowfall recorded at Socorro	11
Figure 2-5: Digital elevation model (DEM) of the Socorro reach	13
Figure 2-6: Average monthly Rio Grande discharge	15
Figure 2-7: Conceptual model of the shallow groundwater flow system	16
Figure 3-1: Ranges of seepage loss/gain along the Rio Grande	22
Figure 3-2: Locations of existing and newly installed well transects	24
Figure 4-1: Locations of model domain, area landmarks, and wells	30
Figure 4-2: Time series of water level elevations at cross-section RM 91.28	32
Figure 4-3: Time series of water level elevations at cross-section RM 87.62	33
Figure 4-4: Cross section of water level elevations at RM 91.28.....	34
Figure 4-5: Cross section of water level elevations at RM 87.62.....	34
Figure 4-6: Locations of ISC well transects at Brown Arroyo and Highway 380	36
Figure 4-7: Map view of well and staff gage locations at Brown Arroyo.....	37
Figure 4-8: Cross section of well and staff gage locations at Brown Arroyo	37
Figure 4-9: Map view of well and staff gage locations at Highway 380	38
Figure 4-10: Cross section of well and staff gage locations at Highway 380	38
Figure 4-11: Locations of the Rio Grande, LFCC, and drains	40
Figure 4-12: Grain size distribution at HWY-W07C	42
Figure 4-13: Split spoon sampling results at Brown Arroyo	43
Figure 4-14: Split spoon sampling results at Highway 380	44
Figure 4-15: Time vs. drawdown data for the 24-hour pump test at W-Sichler .	45
Figure 4-16: Layout of wells at Highway 380 pump test	46
Figure 4-17: Time vs. drawdown data for well HWY-W07	47
Figure 4-18: Time vs. drawdown data	48
Figure 4-19: Locations of active and inactive cells in the telescopic model grid	50
Figure 4-20: Hypothetical cross section of Rio Grande floodplain	51
Figure 4-21: Thickness distribution of telescopic model layers one and three...	52
Figure 4-22: Landcover classification from July 2000 IKONOS image	54

Figure 4-23: Gage reading at San Marcial vs. stage height applied in model....	59
Figure 4-24: Simulated water table maps	61
Figure 4-25: Cross-sectional view of water table elevations	62
Figure 4-26: Observed and simulated heads for the steady-state model	63
Figure 4-27: Simulated and observed heads at cross-section 91.28	66
Figure 4-28: Simulated monthly average Rio Grande loss and LFCC gain	68
Figure 4-29: Simulated losses from the system due to evapotranspiration	68
Figure 5-1: Simulated steady-state water table maps with homogeneous and heterogeneous models	71
Figure 5-2: Cross-section of water level elevations at row 260 with simulations of homogeneous and heterogeneous geology	72
Figure 5-3: Steady-state simulated vs. observed water level elevations for the model with homogeneous geology	73
Figure 5-4: Simulated steady-state water table maps with isotropic and anisotropic models	75
Figure 5-5: Simulated water table map using decreased, increased, and initial values of hydraulic conductivity	78
Figure 5-6: Cross-section of water level elevations at row 260 with simulations of decreased, increased, and initial values of hydraulic conductivity	79
Figure 5-7: Cross-section of water level elevations in layers 1, 2, and 3 at row 260 when hydraulic conductivities of the sediments are decreased	79
Figure 5-8: Seepage response to changes in hydraulic conductivity	79
Figure 5-9: Steady-state simulated vs. observed water level elevations for the model with decreased hydraulic conductivity.....	80
Figure 6-1: Simulated water table maps generated with and without the presence of the LFCC	83
Figure 6-2: Cross-section of water level elevations at row 260 with and without the presence of the LFCC	84
Figure 6-3: Cross-section of water level elevations in layers 1, 2, and 3 at row 260 in the absence of the LFCC.....	85
Figure 6-4: Steady-state observed and simulated heads in the absence of the LFCC	85
Figure 6-5: Transient-state observed and simulated water level elevations with and without the presence of the LFCC	87
Figure 6-6: Time series plot of Rio Grande seepage loss with and without the presence of the LFCC	88
Figure 6-7: Cross-section of water level elevations at row 260 with varied rates of riparian evapotranspiration	91
Figure 6-8: Simulated water table maps generated with decreased evapotranspiration rates	92
Figure 6-9: Steady-state observed and simulated water level elevations with reduced evapotranspiration rate.....	93

	Page
Figure 6-10: Present day and simulated locations of the Rio Grande channel ..	94
Figure 6-11: Simulated and observed water elevations for current and proposed river channel locations.....	96
Figure 6-12: Simulated Rio Grande seepage for relocated and original river channel locations.....	97
Figure 6-13: Simulated LFCC seepage for relocated and original river channel locations	98

LIST OF TABLES

	Page
Table 3-1: Rio Grande seepage between Escondida and Highway 380.....	23
Table 3-2: LFCC seepage between Brown Arroyo and Highway 380.....	23
Table 4-1: Monthly evapotranspiration rates for riparian vegetation	55
Table 4-2: Stage variation and crop evapotranspiration input	58
Table 4-3: Predicted groundwater inputs and outputs	62
Table 4-4: Inputs and outputs to the water budget	67
Table 5-1: Steady-state water budget with homogeneous geology	70
Table 5-2: Steady-state water budget with isotropic geology	74
Table 5-3: Steady-state water budget with altered hydraulic conductivity	77
Table 6-1: Inputs and output to the system prior to LFCC construction.....	82
Table 6-2: Inputs and outputs to the system in the absence of the LFCC	88
Table 6-3: Inputs and output to the system with decreased evapotranspiration	90
Table 6-4: Inputs and output to the system with a new river channel location...	95

LIST OF ABBREVIATIONS

af	acre-feet
af/a/yr	acre-feet per acre per year
amsl	above mean sea level
BDA	Bosque del Apache
bgs	below ground surface
BOR	Bureau of Reclamation
cfs	cubic feet per second
d	day
DEM	Digital Elevation Model
ft	feet
ft/day	feet per day
ft ² /day	feet squared per day
gpm	gallons per minute
gsd	grain size distribution
km	kilometers
LFCC	Low Flow Conveyance Channel
m	meters
min	minute
mo	month
MRGCD	Middle Rio Grande Conservancy District
NMBGMR	New Mexico Bureau of Geology and Mineral Resources
NMED	New Mexico Environment Department
NMIMT	New Mexico Institute of Mining and Technology
NMISC	New Mexico Interstate Stream Commission
NWR	National Wildlife Refuge
RM	river mile
s	second
SSPA	S.S. Papadopoulos and Associates, INC.
USCOE	United States Army Corps of Engineers
USGS	United States Geological Survey
yr	year

1. INTRODUCTION

1.1 MOTIVATION FOR THIS STUDY

Rivers of the southwest play a key role in sustaining life in arid regions. The Rio Grande flows through Colorado, New Mexico, and Texas and is the 24th longest river in the world, with a watershed covering 11% of the continental US surface area. Many demands are made of this finite resource including urban, agricultural, and industrial depletions. Concerned environmentalists fight to maintain river flows for fish habitat and groundwater replenishment. In addition to anthropogenic diversions from the Rio Grande, natural losses can be attributed to leakage from the river channel (seepage) and evaporation.

Balancing the demands on the Rio Grande is a primary concern for management agencies such as the New Mexico Interstate Stream Commission (NMISC), the United States Army Corps of Engineers (USCOE), and the U.S. Bureau of Reclamation (BOR). In order to improve our ability to predict river flows in response to changes in given environmental conditions we must gain a better understanding of groundwater and surface water systems and their interaction with one another. Examinations of the subsurface geology, groundwater flow paths, riverbed characteristics, and modeling of specific reaches of the river requires expanded monitoring networks and extended

research. When the interactions between surface water and groundwater become better understood, informed management decisions of water resources will help optimize the overall conveyance efficiency of the Rio Grande.

The purpose of this study was to develop a working model of a reach of the Rio Grande experiencing high losses in order to evaluate management alternatives that could maximize local river conveyance efficiency.

1.2 THE RIO GRANDE COMPACT

Rio Grande water is allocated according to the Rio Grande Compact, signed in 1938 by Colorado, New Mexico, and Texas. The 76th Congress passed this document as Public Act No. 96 in 1939 and its goal is to ensure equitable allocation of water among the three states. The first paragraph of the Rio Grande Compact reads:

“The State of Colorado, the State of New Mexico, and the State of Texas, desiring to remove all causes of present and future controversy among these States and between citizens of one of these States and citizens of another State with respect to the use of the waters of the Rio Grande above Fort Quitman, Texas, and being moved by considerations of interstate comity, and for the purpose of effecting an equitable apportionment of such waters, have resolved to conclude a Compact for the attainment of these purposes.”

In order to meet requirements of the compact, New Mexico is obligated to deliver a percentage of the river flow at United States Geological Survey (USGS) Otowi gage to Elephant Butte Reservoir, termed Elephant Butte Scheduled Delivery. The difference between this delivery and the flow at Otowi, plus tributary and groundwater inflows, is the volume of water available for use by the Middle Rio Grande region extending from Cochiti Dam to Elephant Butte. Locations of

Elephant Butte Reservoir and Otowi gage are shown in the inset to Figure 1-1.

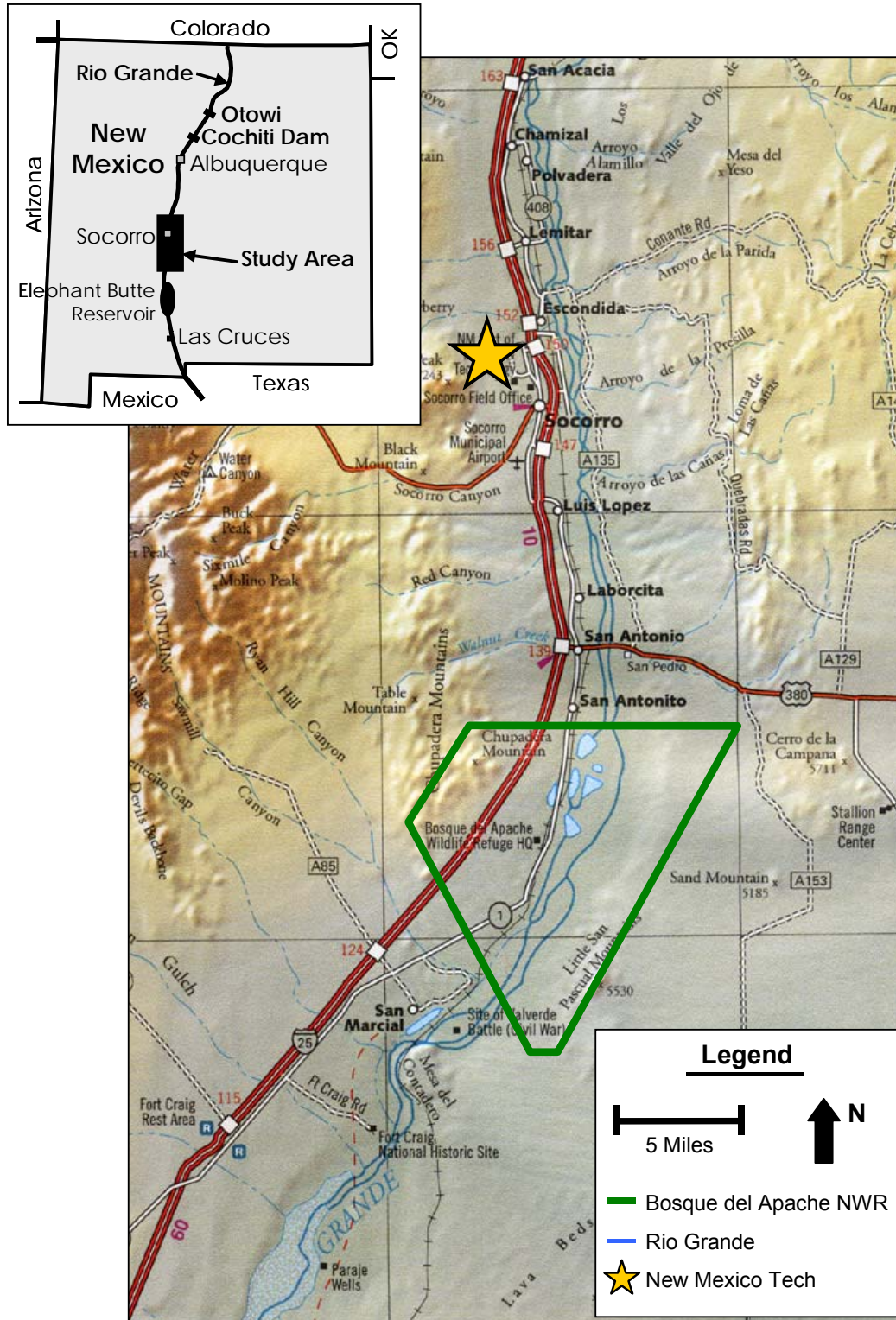


Figure 1-1: Regional (inset) and local scale study area maps (roadmap courtesy of the NMBGMR library).

1.3 WATER DEMANDS IN THE SOCORRO REACH OF THE RIO GRANDE

The Socorro reach of the Rio Grande extends from San Acacia to San Marcial (Figure 1-1). Diversions for irrigation of crops are the largest anthropogenic depletion from the Rio Grande (Shafike, personal communication, July 2003). Non-depleted water recharges the shallow aquifer and eventually returns to the Rio Grande. Reductions in river flow in the Socorro reach include 52% to riparian evapotranspiration, 8% to open water evaporation, 12% to groundwater outflow, and 27% to crop evapotranspiration (Shafike et al., 2002, p. F30) (Figure 1-2).

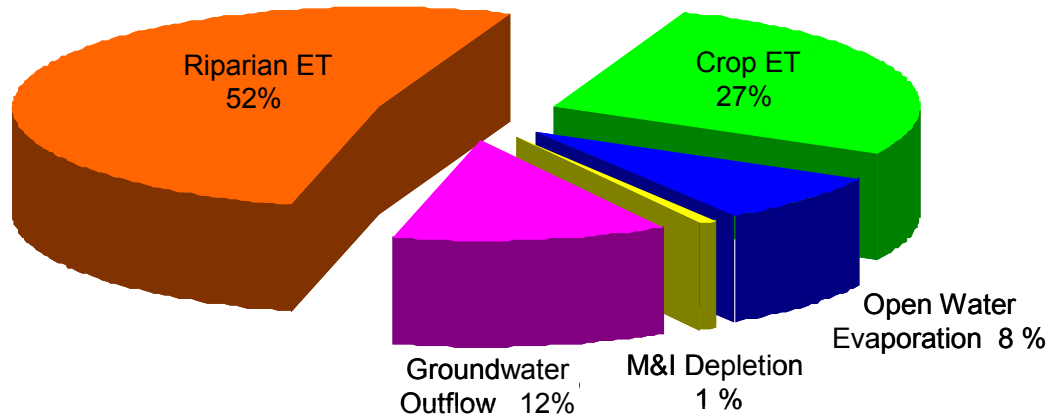


Figure 1-2: Average consumptive use from San Acacia to San Marcial (Shafike, 2002).

The Rio Grande serves as a habitat for many species of flora and fauna. Among these are the Rio Grande silvery minnow and southwestern willow flycatcher, two species that are protected by the Endangered Species Act. Maintaining sustained river flow is one approach proposed to preserve habitat for fish and birds.

Population growth in urban centers has placed additional demands on water resources in the state of New Mexico. Controversy surrounds the issue

concerning depletions from the river for municipal use. The City of Socorro reported groundwater withdrawals of 741 acre-feet (af) or 9.14×10^5 cubic meters (m^3) per year in 1972, with approximately 50 percent return flow to the hydrologic system through the wastewater treatment plant (Anderholm, 1987, p. 53). In 2001, withdrawals made by the City of Socorro, the New Mexico Institute of Mining and Technology (NMIMT), and the NMIMT Golf Course totaled 3184 af or $3.93 \times 10^6 m^3$ per year (430 percent increase), with an average of 42 percent return to the system via the wastewater treatment plant (Dixie Daniels of City of Socorro and Jim Shaffner of NMIMT, personal communication, July 2003).

1.4 OBJECTIVES

The primary objectives for this thesis were to improve our understanding of groundwater and surface water interactions and investigate methods for maximizing river conveyance. To achieve this, conceptual and numerical modeling of water levels and flow patterns in the subsurface aquifer, Rio Grande, and associated agricultural drains was performed. Detailed models were used to simulate the behavior of groundwater and surface water systems and to analyze competing management scenarios.

An existing regional-scale model constructed by the NMISC extends from San Acacia to San Marcial (Figure 1-1). Preliminary results from the regional model indicate high losses from the river between Luis Lopez and San Antonio (Figure 1-1) (Shafike et al., 2002). Field data obtained in 2000 and 2001 for the same reach support the regional model and indicate high variability in seepage rates (SSPA, 2002). A smaller-scale (telescopic) model with a refined grid was

targeted at this six-mile (ten-kilometer (km)) long reach of the Rio Grande with the following specific objectives:

- 1) Develop understanding of the groundwater/surface water interactions in the area
- 2) Integrate recently collected geologic and hydrologic information into conceptual and numerical models
- 3) Simulate management alternatives to develop strategies for optimizing river conveyance efficiency including river channel re-location and riparian vegetation changes

The telescopic model was constructed to be an inset model with increased horizontal and vertical resolution. It was designed to obtain boundary conditions from the regional model at the beginning of every stress period, although this feature was not applied for the purposes of this research.

This thesis was organized as follows. Chapter 2 begins with a general description of the Socorro reach including information regarding climate, geology, hydrology, flora, and fauna. An overview of past and ongoing work is summarized in Chapter 3, with a presentation of related seepage studies, water level data, groundwater/surface water interaction reports, and ongoing modeling efforts. In Chapter 4 the thesis focuses on the reach of the Rio Grande between Luis Lopez and San Antonio, the area simulated by the higher-resolution model. The study area is described through presentation and analysis of groundwater, surface water, geologic logging, and pump test data. Model construction is explained in detail, followed by calibrated steady-state and transient-state results. Sensitivity analyses were performed with the model to observe effects of changes in subsurface geology and are described in Chapter 5. Chapter 6

evaluates three management alternatives tested using simulations of the system with

- 1) The absence of the Low Flow Conveyance Channel (LFCC), a conveyance drain that lies directly west of the Rio Grande
- 2) A relocated and widened river channel
- 3) Decreased evapotranspiration from riparian vegetation and bare ground

A summary of conclusions and recommendations for future work are presented in Chapters 7 and 8.

2. REGIONAL OVERVIEW

2.1 LOCATION

This study focuses on the reach of the Rio Grande between Socorro and San Marcial. The major town in the study area is San Antonio which is located 87 miles (140 km) south of Albuquerque, near the geographical center of Socorro county (Figure 1-1). Socorro County was home to 18,043 residents as of July 1, 2002, with major population centers being Socorro, Magdalena, San Antonio, Lemitar, and Polvadera (U.S. Census Bureau, 2003). The economy is based on agriculture, ranching, and employment with many federal and state agencies including the BOR, Middle Rio Grande Conservancy District (MRGCD), and NMIMT.

The Rio Grande flows North-South and is paralleled to the West by the LFCC, a drain that runs from San Acacia to Elephant Butte reservoir and was constructed to more efficiently convey water to Elephant Butte Reservoir. The LFCC is the topographic low in the system. A riparian habitat surrounds both channels and provides a refuge for local flora and fauna. Agricultural fields, irrigation ditches, and residential homes dominate the landscape to the west of the Rio Grande. Little development has occurred to the east of the Rio Grande due to limited access, and the floodplain there contains primarily riparian vegetation. The Bosque del Apache National Wildlife Refuge (BDA NWR) is

located five miles south of San Antonio, straddles the LFCC and Rio Grande, and is part of the Chihuahuan desert (Figure 1-1). It is a haven for more than 340 species of birds such as migratory snow geese and sandhill cranes. Socorro division MRGCD water diverted from the LFCC and agricultural drains is used to irrigate crops necessary for bird habitat.

2.2 CLIMATE

Socorro County is characterized by a typical high desert semiarid climate. Elevations range from 4,500 feet (1,372 m) in the valley to greater than 10,000 feet (3,048 m) along the Magdalena mountain crest. Prior to the signing of the Rio Grande Compact in 1938, precipitation was average or above average. Between 1942 and 1956, New Mexico experienced below average precipitation, an era marked by drought and increased water conservation (WRCC, 2003) (Figures 2-1 and 2-2). The year 1972 marked the first significant rainfall after the onset of the 1950's drought and precipitation has remained above or average since that time. Recent years have shown average rainfalls, with 1999, 2001, and 2002 reported at 9.86, 9.08, and 10.64 inches (25, 23, and 27 centimeters (cm)) respectively. The year 2000 was the first to have below average rainfall of 8.8 inches (22 cm) since 1996.

During the period from 1914 to 2002 average annual temperatures measured 20 miles east of Socorro ranged from a low of 40.9 to a high of 74.1 degrees Fahrenheit (5 to 23 degrees Celsius) (WRCC, 2003). Average annual precipitation for the same 88-year period was 9.39 inches (24 cm) including 6.7 inches (17 cm) of snowfall. Sixty percent of precipitation fell over Socorro during

the months of July, August, September, and October (Figure 2-3). Average snowfall peaks were during the months of December, January, and February (Figure 2-4).

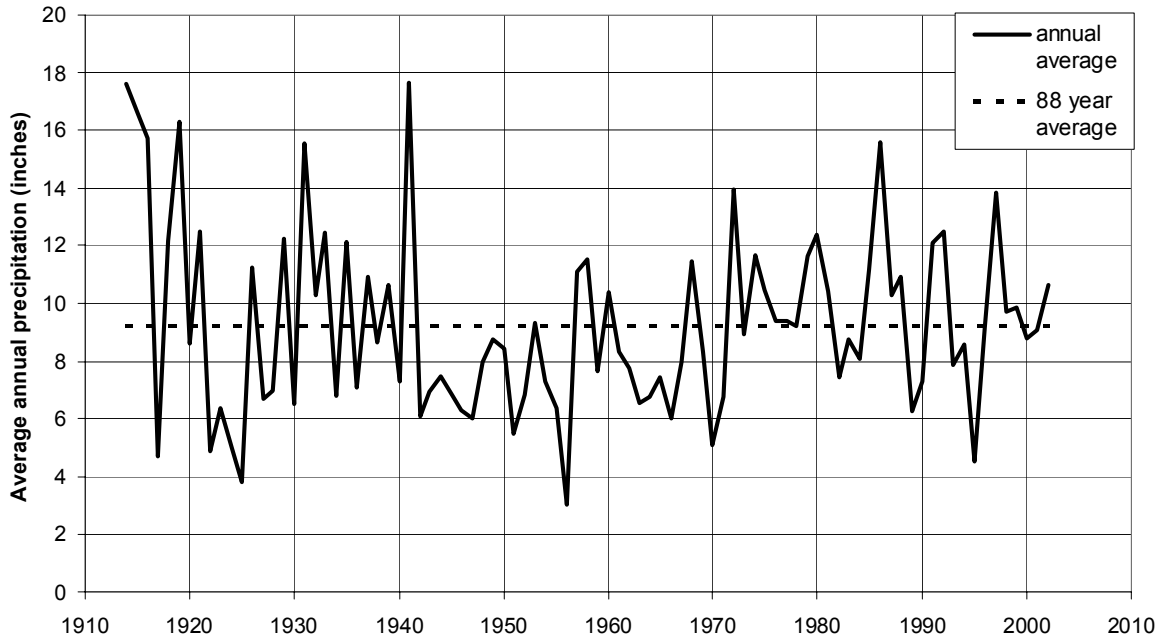


Figure 2-1: Average annual precipitation recorded 1914-2002 in Socorro, New Mexico (WRCC, 2003).

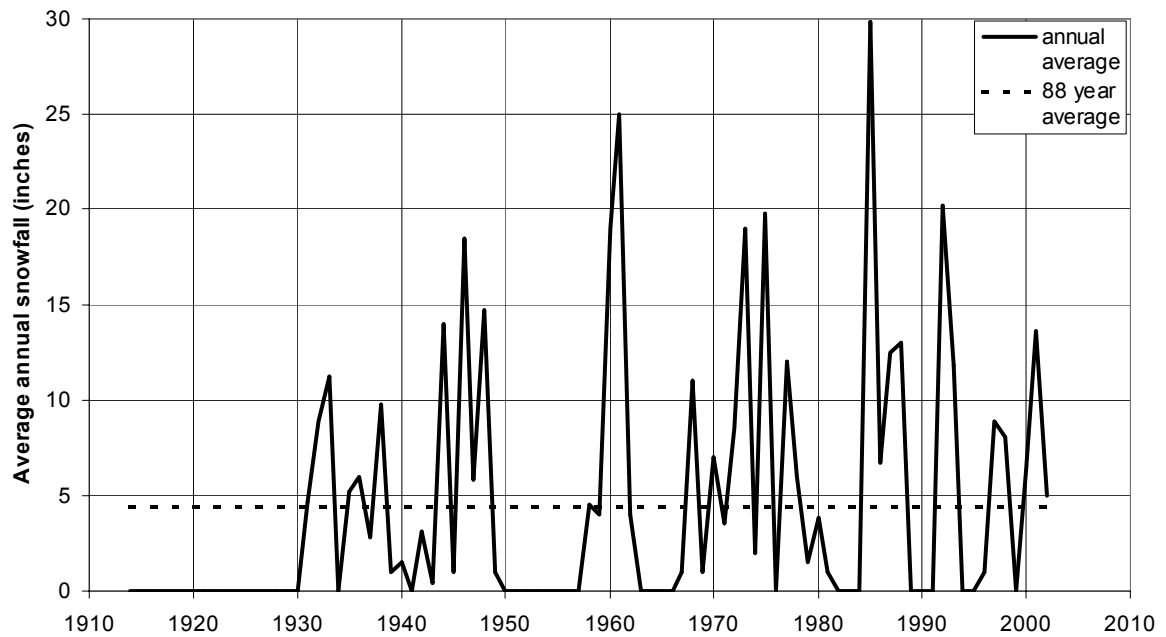


Figure 2-2: Average annual snowfall recorded 1914-2002 in Socorro, New Mexico (WRCC, 2003).

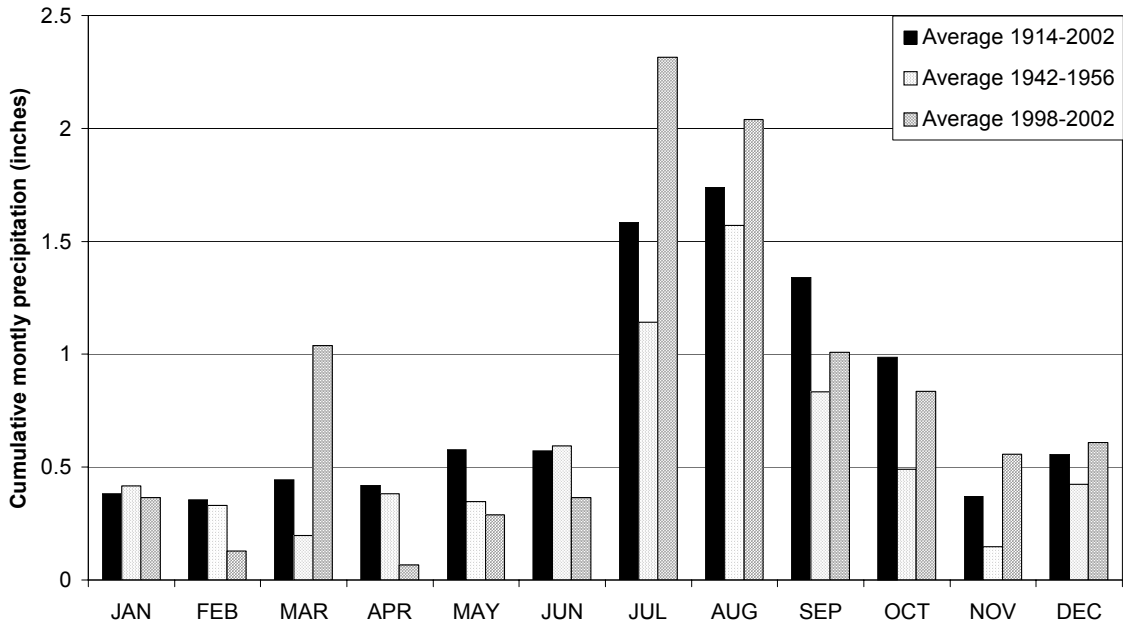


Figure 2-3: Cumulative monthly precipitation recorded at Socorro, New Mexico (WRCC, 2003).

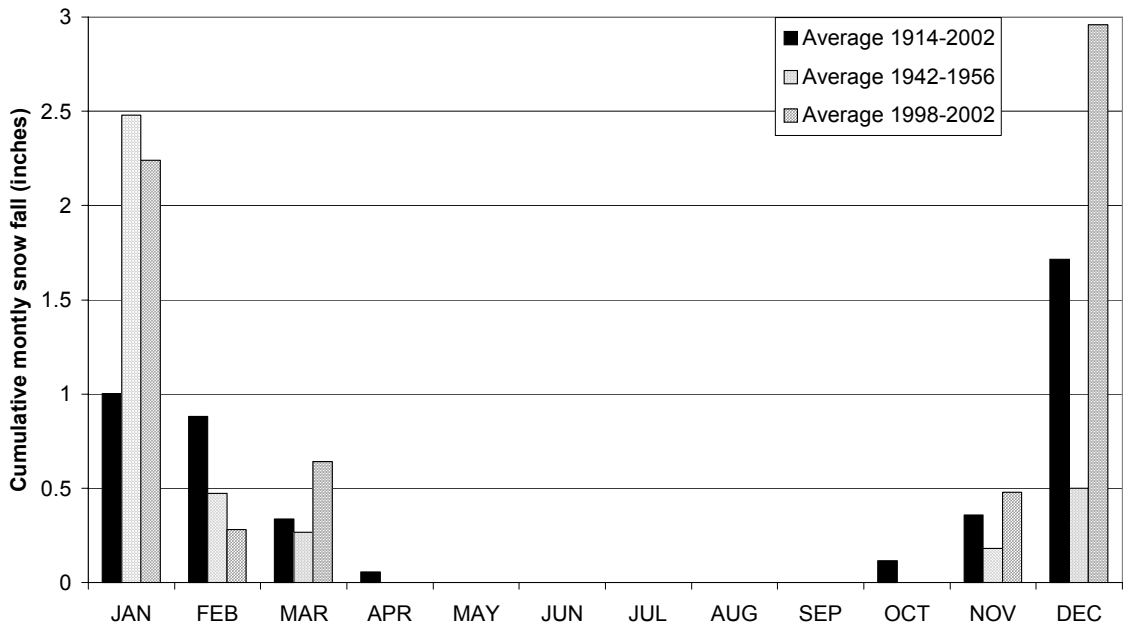


Figure 2-4: Cumulative monthly snowfall recorded at Socorro, New Mexico (WRCC, 2003).

2.3 GEOLOGY

In Socorro county the Rio Grande River follows a path along the active Rio Grande rift. The Socorro basin is one of many sub-basins along the Rio Grande and is marked at its northern and southern termini by San Acacia and Elephant Butte. To the east of the Socorro Basin lies the Lomas de las Canas Uplift, Cerro Colorado, and Little San Pascual Mountain (Anderholm, 1987, p.5). To the west are Socorro Peak and the Magdalena, Lemitar, and Chupadera Mountains.

Rocks range from Precambrian to Holocene, but only those younger than Oligocene are considered to be water-yielding units (Anderholm, 1987, p. 9). The Santa Fe Formation is the primary geologic unit between the basin bedrock and surficial alluvium deposits and consists mainly of aggradational basin fill sourced from Rio Grande rift deposits. Estimates of its thickness in different locations range from zero to 5,000 feet (1,524 m) and were determined from gravity maps collected prior to 1968 (Sanford, 1968 and Shafike et al., 2002). The thickest section within the Socorro reach underlies the floodplain alluvium near San Antonio. Here, the Santa Fe Formation is composed primarily of the Popotosa and Sierra Ladrones Formations. The Popotosa includes interfingering fanlomerate and playa facies. The Sierra Ladrones Formation consists of piedmont slope, alluvial fan, alluvial flat, local basalt, floodplain, and axial stream deposits (Anderholm, 1987, p. 13). The Santa Fe Formation represents the principal aquifer in the state of New Mexico and is defined with an unconformity between the overlying fluvial quaternary deposits (Cather, 1997, p. 15). These fluvial deposits exhibit characteristics of the Sierra Ladrones Formation, have a

maximum thickness of 100 feet (31 m), and will be discussed further in the next section.

2.4 HYDROLOGY

The Rio Grande sustains a corridor of life extending from its headwaters in southern Colorado to its termination into the Gulf of Mexico along the Texas/Mexico border. The Socorro reach of the Rio Grande lies directly north of Elephant Butte Reservoir and several features make this reach of the river unique, including the LFCC and the Bosque del Apache NWR (Figure 2-5).

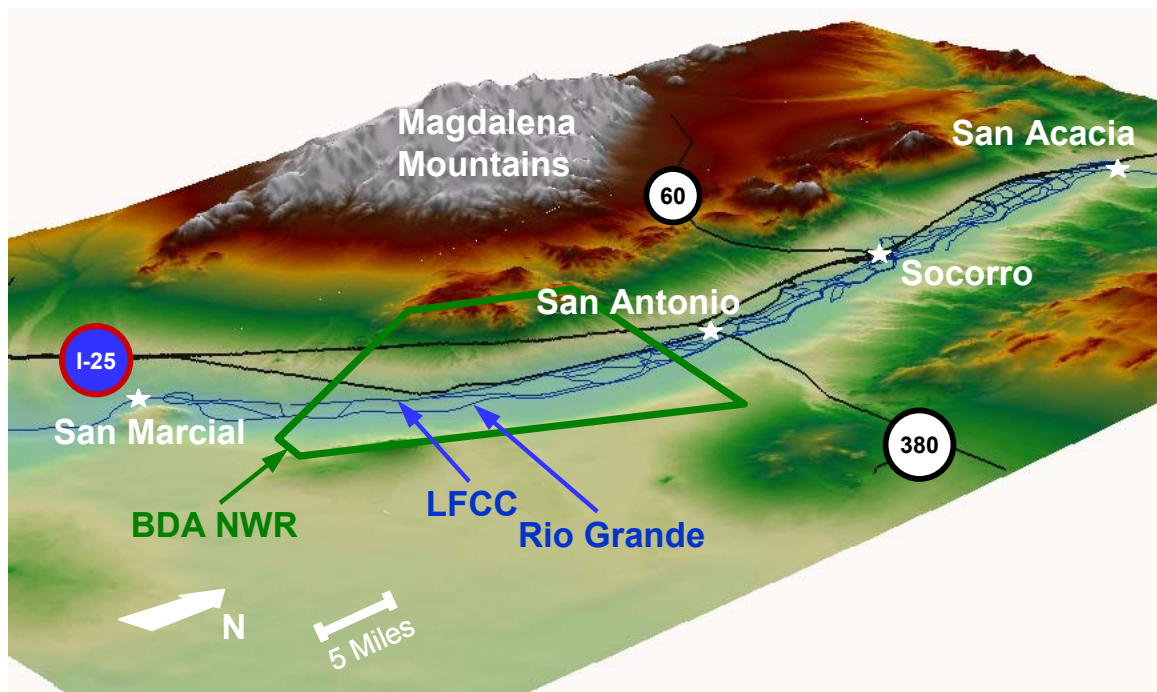


Figure 2-5: Digital elevation model (DEM) of the Socorro reach of the Rio Grande.

Numerous man-made drains enter and exit the system, supplying water to agriculture and livestock (Appendix A) (SSPA, 2002). Surface water enters the region from the Rio Grande, surface water run-off, and Drain Unit 7, a drain that

runs from Bernardo to San Acacia. Groundwater is replenished from the Rio Grande, precipitation, and mountain front recharge.

2.4.1 The Rio Grande

Historically characterized as a naturally meandering channel, the Rio Grande has become a controlled river, being intercepted by many dams and diversion structures along its path through Colorado, New Mexico, and Texas. One of these dams is located at San Acacia where flows are regulated and diverted into the main irrigation canal and, previously, the LFCC. United States Geological Survey real-time telemetry stream flow data are available for the Rio Grande and LFCC at San Acacia and San Marcial. Data quality from these stations are rated “fair” by the USGS and are collected at points 0.25 miles (0.4 km) downstream of the San Acacia dam and the San Marcial railroad bridge. Average monthly discharge data collected between 1951 and 2002 indicate losses from the Rio Grande between the two locations are at a maximum in May and a minimum in December (Figure 2-6). These trends are supported by results from seepage-run studies that are explained further in Chapter 3.1.

During the summer the Rio Grande often runs dry in the Socorro reach, despite efforts to maintain the endangered Rio Grande silvery minnow habitat. At the south end of the reach near Elephant Butte Reservoir, the river flows slower because of a decreased gradient in the topography. Here, the connection between the river and reservoir is often broken because of silting in the river channel.

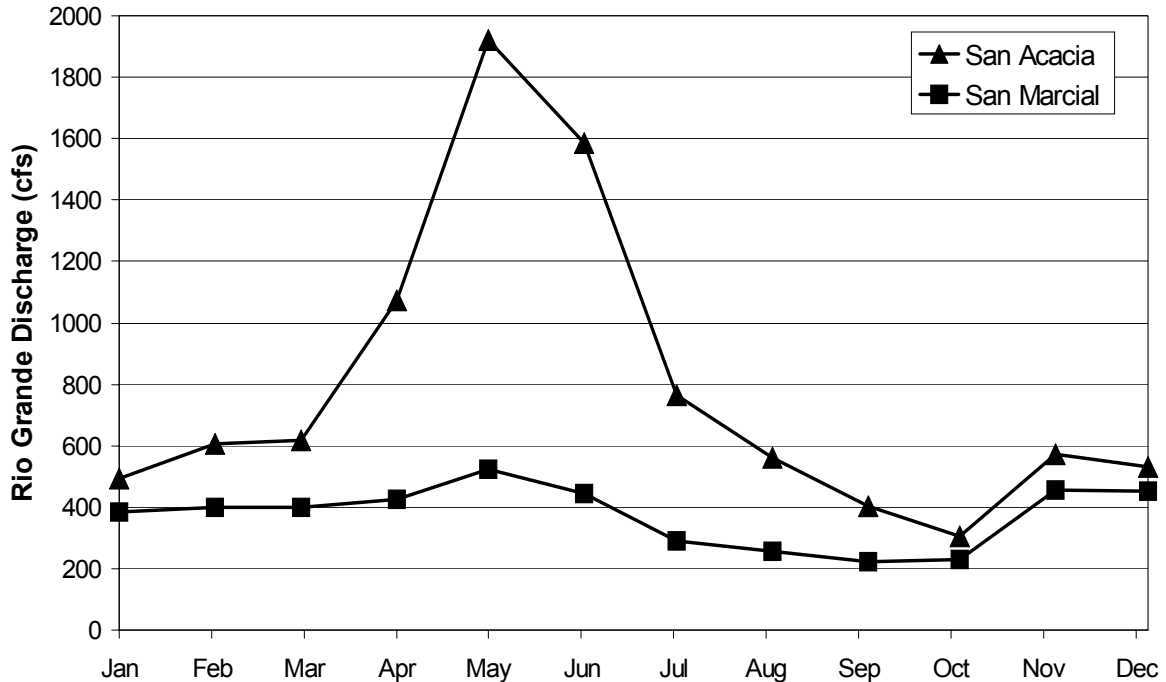


Figure 2-6: Average monthly Rio Grande discharge between 1951 and 2002 at San Acacia and San Marcial.

2.4.2 The Low Flow Conveyance Channel

During the drought of the 1950's, concerns were raised regarding delivery obligations to Elephant Butte Reservoir. It was hypothesized that the Socorro reach was responsible for large portions of river depletions. In addition, fluctuations in reservoir levels and high sediment load of the river caused the river channel to clog and often surface flows did not reach the reservoir. In response to these losses, the USCOE and BOR completed construction of the LFCC west of the Rio Grande in 1959 to convey water more efficiently to the reservoir. The LFCC is a 50-foot (15-meter) wide, rock-lined channel with a bottom elevation below the river bottom elevation. It is the topographic low point in the system for the majority of its length (Figure 2-7). During LFCC construction, the Rio Grande was re-channeled in some locations and sediments

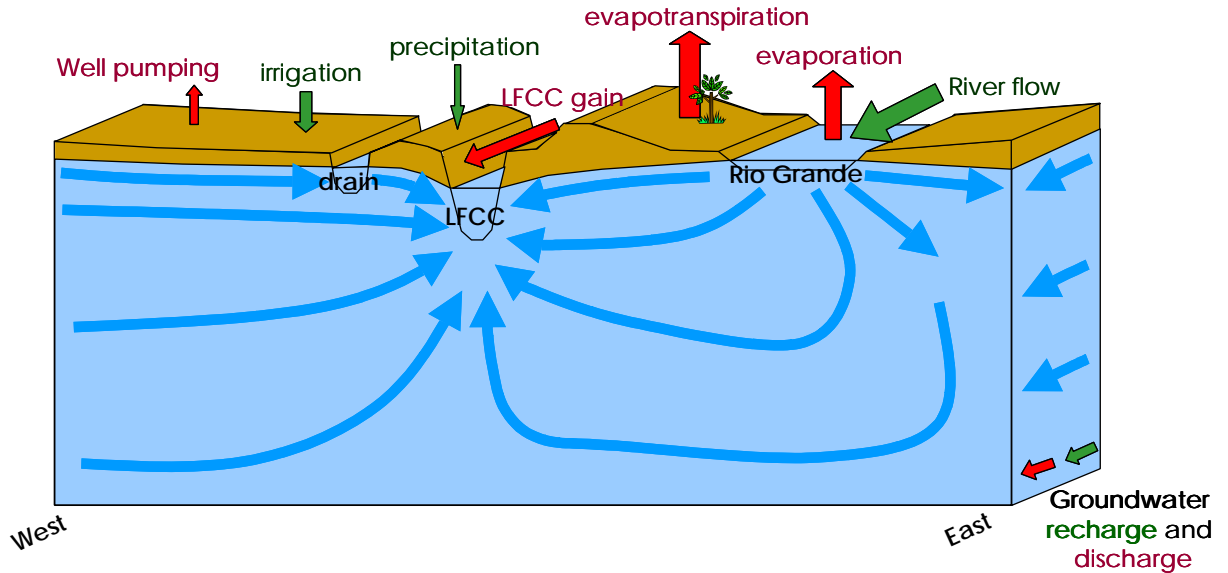


Figure 2-7: Conceptual model of the shallow groundwater flow system near San Antonio. between the river and LFCC were disturbed. The LFCC increased water conveyance efficiency to Elephant Butte Reservoir, but the canal terminus eventually began to silt in and lose its connection to the reservoir, much like the Rio Grande channel. In March 1985, diversions from the Rio Grande into the LFCC at San Acacia were terminated and to this day the channel acts as a drain for groundwater. It also serves as a conveyance for irrigation canals and drainage water. During the summer, water is often pumped from the LFCC into the river channel to maintain habitat for the endangered Rio Grande silvery minnow.

2.4.3 Agricultural Canals and Drains

In addition to the LFCC, drains and canals play major roles in the hydrologic system between San Acacia and Elephant Butte (Appendix A). The Elmendorf Drain south of San Antonio and Highway 380 is responsible for returning irrigation and BDA NWR water to the LFCC.

Socorro Main Canal conveys water diverted from the Rio Grande at San Acacia and ultimately meets the Elemendorf Drain. Additional water from the north enters the Socorro Main Canal from Drain Unit 7. During the winter months Socorro Main is dry because it receives no diverted water. Diversions into agricultural canals begin during the first week of March and continue until the end of October, depending on annual river flow conditions.

The Socorro Riverside Drain parallels Socorro Main Canal for most of the reach. The drain is substantially lower than the Socorro Main and flows for the entire year, gaining water from the surrounding aquifer. It begins approximately 0.1 miles (0.16 km) south of the San Acacia dam and flows between the LFCC and the Socorro Main Canal until it joins with the Elmendorf Drain.

A network of secondary irrigation canals, ditches, and drains exist throughout the study area, and are listed in Appendix A. Those located within the model domain are described in detail in Chapter 4.1.2.

2.4.4 Tributaries

Two ephemeral streams feed the Rio Grande a short distance north of San Acacia. The Rio Salado flows during heavy rainstorms and contributes sediment-laden surface runoff from the west-lying Ladron Mountains to the Rio Grande approximately two miles north of San Acacia. Thirteen miles (20 km) north of San Acacia the Rio Puerco enters the Rio Grande, draining a watershed covering roughly 9,942 square miles (16,000 km²) of northwestern New Mexico. It supplies more than 70% of suspended sediment to the Rio Grande above Elephant Butte reservoir (Gellis, 1992).

Several minor ungaged tributaries between San Acacia and San Marcial contribute flows to the Rio Grande during storms and other precipitation events. Those that contribute flows to the east of the Rio Grande, from north to south, include San Lorenzo Arroyo, Arroyo de la Parida, Arroyo de los Pinos, Arroyo de Tio Bartolo, Arroyo de la Presilla, and Arroyo de las Canas. Contributions from the west, from north to south, include Escondida Arroyo, Brown Arroyo, and Walnut Creek (Appendix A).

2.4.5 Elephant Butte Reservoir

The northernmost extent of Elephant Butte Reservoir lies 40 miles (64 km) south of Socorro and has been storing water since 1915. It is the largest lake in New Mexico and primary designated uses include irrigation water storage for downstream parties in New Mexico, Texas, and Mexico, and hydroelectric power production at the dam. Recently, the reservoir began developing symptoms of eutrophication with algal blooms, prolonged hypolimnetic oxygen depletion, and odor from hydrogen sulfide evolution (Chapman and Canavan, 2002). These problems are associated with low reservoir levels following a period of higher levels.

2.4.6 Groundwater

A conceptual model of the groundwater flow scheme in the study area shows river water following a topographic gradient flowing toward the LFCC (Figure 2-7) (Anderholm, 1987, p.22). Regional flow patterns and water levels are largely affected by irrigation drains that are considered to be the main factor

controlling water levels in the Rio Grande valley (Anderholm, 1987, p.23).

Recharge to the shallow aquifer and underlying sediments comes from the Rio Grande and mountain front recharge from the east and west in areas adjacent to mountain ranges (Roybal, 1991, p.11). Precipitation that falls on the mountain slopes flows over somewhat impermeable watersheds and encounters relatively permeable alluvial basin-fill deposits, recharging the groundwater system (Roybal, 1991, p.11).

2.5 FLORA

The majority of cropland near San Antonio is cultivated for alfalfa production with other crops including chile, corn, and grazing land for horses, cattle, and goats. Riparian vegetation is dominant in the area surrounding the Rio Grande and LFCC (Tetra Tech Inc., 2003, p. v). The vegetation consists primarily of saltcedar (*Tamarix ramosissima*) and cottonwood trees (*Populus deltoids and angustifolia*), along with Russian olive (*Eleagnus angustifolia*) and honey mesquite (*Prosopis glandulosa*). All species are important to the ecosystem because they provide food, habitat, and shade for many creatures.

Saltcedar was introduced in the early 1900's to help with riverbank stability and has eventually come to dominate the riparian zone. It has a high evapotranspiration rate with some estimates of a single mature tree consuming up to 200 gallons (757 liters) of water per day (Smith, 2002). Saltcedars also increase river channelization, water and soil salinity, and the frequency of fires and floods (Tetra Tech Inc., 2003).

Cottonwood trees are a species native to the Rio Grande valley and dominated the low riparian forests of the southwest before the late 16th century. Since then, Rio Grande dams, re-channelization, and stream flow regulation have resulted in decreased water levels and water quality, and minimized the cottonwoods' ability to reproduce.

2.6 FAUNA

Many species inhabit the area surrounding the river. Two creatures of interest to this study include the Rio Grande silvery minnow (*Hybognathus amarus*) and the southwestern willow flycatcher (*Empidonax traillii extimus*) (Tetra Tech Inc., 2003, p. v). Laws with special regulatory measures to enforce preservation of their habitat during nesting and spawning seasons protect these endangered species.

Populations of the Rio Grande silvery minnow have diminished since changes were first made to its habitat. Such changes include decreased sediment load and unnatural flow pulses caused by manmade structures along the river. The Socorro reach is one of the remaining locations where the silvery minnow chooses to reside and spawn. It is also a reach of the river that historically runs dry in the summertime. Many fish do not survive this period and rescue efforts are often made to trap and re-locate many of the silvery minnow fish and eggs.

3. PREVIOUS/ONGOING WORK

The Rio Grande between San Acacia and San Marcial has been one of the least studied reaches of the river and is thought to be where many depletions occur before Elephant Butte reservoir. It is critical to gain a better understanding of the groundwater and surface water interactions that occur within this reach in order to maximize overall river conveyance efficiency. Prior and ongoing studies along the Rio Grande between San Acacia and Elephant Butte Reservoir include calculations of river and LFCC seepage, water level elevation data, groundwater surface water interaction studies, and various modeling efforts.

3.1 RIVER SEEPAGE ANALYSIS

During the summers of 2000 and 2001 the ISC conducted seepage runs along the Rio Grande from Belen to San Marcial (SSPA, June 2002). These measurements of changes in flow between two points were made in an effort to quantify losses from the river and LFCC. Procedures were based on standard USGS methods in which flow rates were determined at incremental widths along a cross section (SSPA, June 2002, Appendix K). Widths were determined so that incremental discharge would be less than five percent of the total discharge across the cross section. After obtaining flow rates at various locations along a

reach, inflows and outflows were quantified to yield calculations of gains and losses for the reach.

Seepage losses from the river between Brown Arroyo and San Antonio ranged from 3.3 to 24.8 cubic feet per second (cfs)/mile (9.3×10^{-2} to 7.0×10^{-1} $m^3/s/mile$) (Figure 3-1, Tables 3-1 and 3-2). When discussing seepage, positive values are gains to the aquifer and negative values are losses from the aquifer.

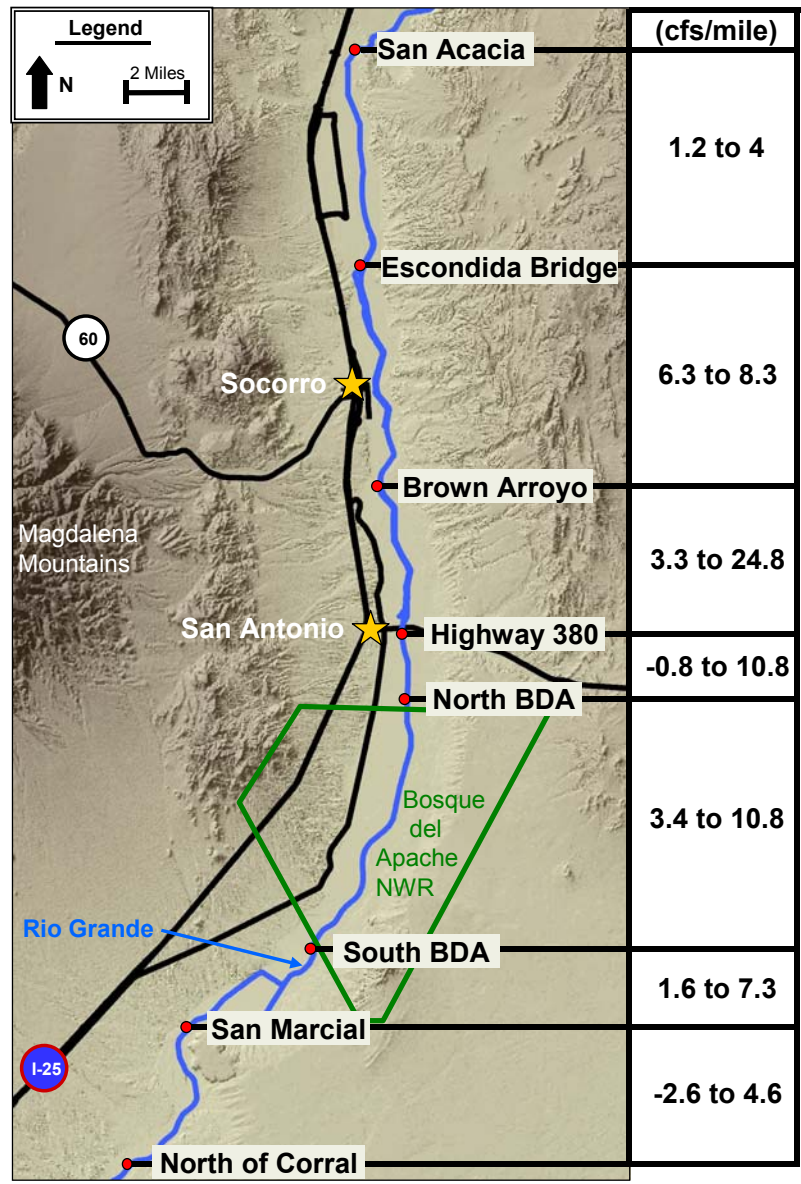


Figure 3-1: Ranges of seepage loss/gain along the Rio Grande within the San Acacia reach measured in the summer of 2000 and 2001 (SSPA, 2002).

	Rio Grande Seepage (cfs per mile)								
	Irrigation Season 2000				Post Irrigation	Winter 2001	Irrigation Season 2001		
Rio Grande Reach	Aug 18	Sep 9	Sep 14	Sep 22	Oct 19	Jan 30	Jun 9	Jun 27	Aug 3
Escondida to HWY 380 (15.61 miles)	8.4	6.9	11.5	7.4	11.6	11.3	6.6	8.9	6.5
Brown Arroyo to Neel Cupp (2.55 miles)						21.0		24.8	8.4
Neel Cupp to HWY 380 (3.80 miles)						18.9	-6.9	3.3	3.6
Brown Arroyo to HWY 380 (6.35 miles)			13.1	8.1	16.0	19.7			

Table 3-1: Rio Grande seepage between Escondida and Highway 380 (SSPA, 2002).

	LFCC Seepage (cfs per mile)						
	Irrigation Season 2000			Post Irrigation	Winter 2001	Irrigation Season 2001	
LFCC Reach	Aug 18	Sep 9	Sep 22	Oct 11	Jan 30	Jun 10	Aug 8
Below Brown Arroyo to downstream of HWY 380 (6.35 miles)	-6.8	-8.0	-8.0	-7.0	-6.1	-6.2	-4.8

Table 3-2: LFCC seepage between Brown Arroyo and Highway 380 (SSPA, 2002).

3.2 WATER LEVEL DATA

The NMISC and the USCOE supports a large-scale study officially entitled “The Rio Grande Watershed Study – San Acacia Surface Water/Groundwater Investigation.” This study began in 2001 and its main objectives were to characterize the shallow groundwater aquifer and the interaction between surface water and groundwater in this reach, in order to allocate more effectively water resources in New Mexico south of San Acacia and north of Elephant Butte Reservoir.

The initial phase of this project involved monthly measurement of depth to water in 38 groundwater wells owned by the BOR and was initiated in October of 2001. These wells were constructed in the early 1990’s and most are shallow piezometers screened at the water table. All wells lay within the floodplain between San Acacia and Elephant Butte delta, arranged in seven transects

across the Rio Grande and LFCC (Figure 3-2). Surface water levels in the LFCC

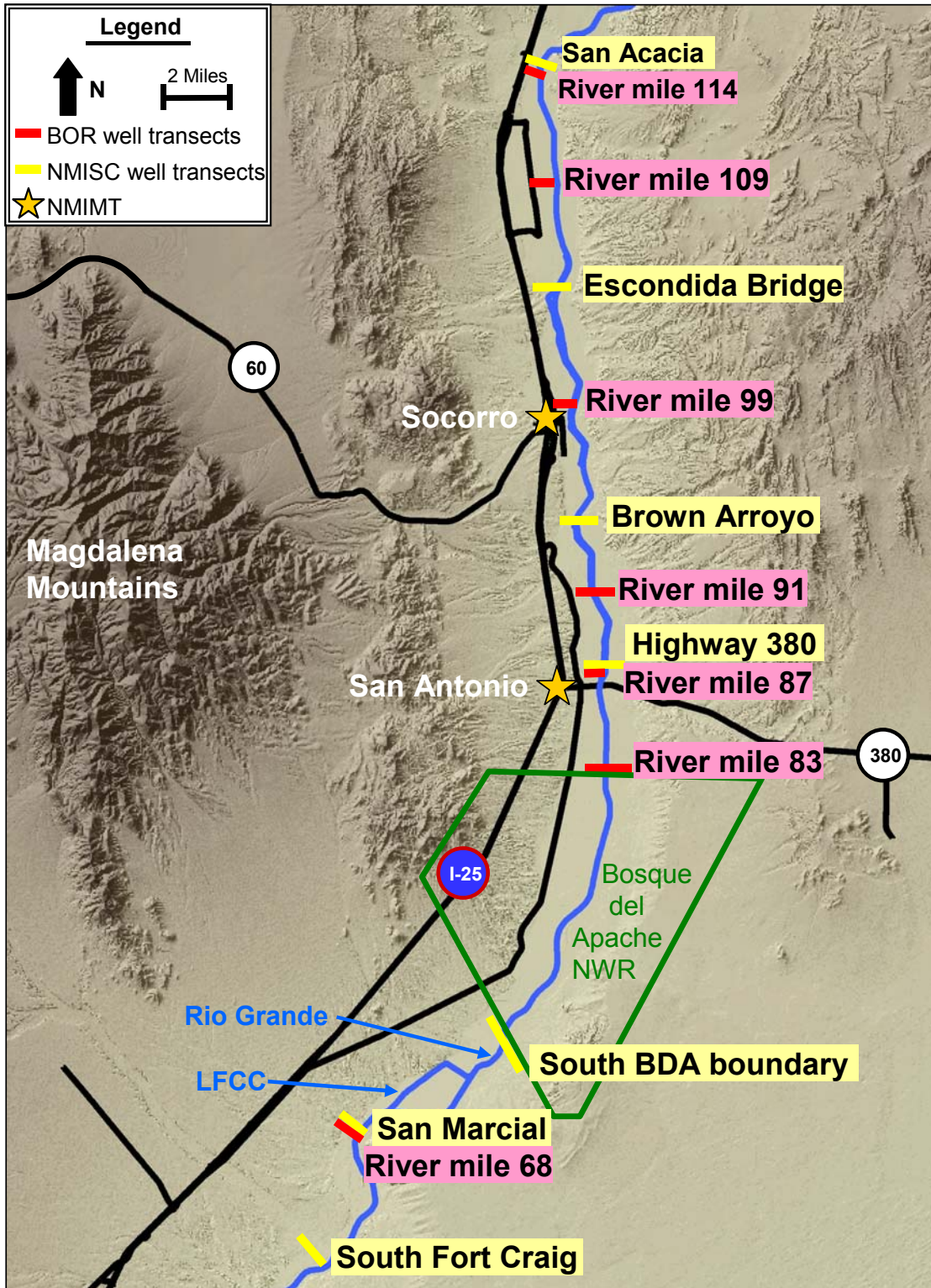


Figure 3-2: Locations of existing and newly installed well transects between San Acacia and Elephant Butte reservoir.

and Rio Grande at each transect were measured monthly, starting in January of 2002. In February of 2002 a plan was initiated to sample wells and surface water locations in the river and LFCC for baseline water quality including major anions and cations. This plan included six such water quality snapshots in February, June, and October of 2002, and February, June, and November of 2003. Several wells were added to the monitoring network as contacts with local agencies and private well owners were made.

To supplement this monitoring network, 114 nested piezometers were constructed from October 2002 through May 2003. These wells were arranged in 7 cross sections across the floodplain extending from San Acacia to Fort Craig (Figure 3-2). Staff gages were installed in the LFCC and Rio Grande at these transects. Each transect consisted of 1 deep well, drilled until its interception with the Santa Fe formation at about 100 feet (31 m). Approximately 18 additional piezometers were located at each cross section and were screened at three depths; 3 to 18 feet (1 to 6 m), 40 to 60 feet (12 to 18 m), and 60 to 80 feet (18 to 24 m). Larger diameter pumping wells were installed with screen intervals determined from geological log and grain size analysis. Split-spoon sampling was conducted at all borehole locations and grain size analyses and detailed geologic descriptions were made for all samples.

Monthly field measurement of water level data for the expanded well network was initiated in May 2003. During the months of May and June of 2003, 60 dataloggers were installed in wells and staff gages, set to record water levels at one-hour increments. Pump tests to determine aquifer hydraulic properties

were performed at the Escondida and Highway 380 cross sections. These data, along with water level elevation measurements collected since October 2001 from the existing BOR wells, are stored in an Access database developed by the ISC, NMIMT, and Intera, Inc. The most updated copy of this database resides with NMIMT and will be made publicly available via the Internet.

Several parties have collected additional water level data during the period from 1949-1996. These data are summarized in Appendix B.

3.3 ONGOING MODELING EFFORTS

The New Mexico Interstate Stream Commission developed a regional-scale surface water/groundwater model of the Rio Grande reach from San Acacia to Elephant Butte reservoir that included the entire Rio Grande basin sediments of the Santa Fe and Quaternary alluvium. The model's purpose was to evaluate potential system-wide depletions resulting from changes in management of the LFCC, riparian vegetation, and riverbed aggradation (Shafike et al., 2002). MODFLOW with extensions and supplemental programs Riv2 (Miller, 1988), stream package (Prudic, 1989), and MODBRANCH (Swain and Wexler, 1996) were used to simulate the interaction between the LFCC, Rio Grande, and Santa Fe Group and alluvial aquifers. These physical processes were portrayed in the model via surface water routing, surface water/groundwater interactions, discharge from springs, riparian and crop depletions, groundwater withdrawals, and groundwater levels.

Field ground-truthing of the regional model was done with water level, water chemistry, pump test, and tracer test data compiled from various

databases and current monitoring efforts. Preliminary results indicated high losses from the river to the shallow aquifer between Brown Arroyo and San Antonio (Shafike, 2002). River channel conveyance losses were also shown to decrease with aggradation of the riverbed (Shafike, 2002). Results from the steady-state regional model were used to determine initial head values for the boundaries of the telescopic model that is the focus of this study.

3.4 ADDITIONAL STUDIES

3.4.1 Groundwater/Surface Water Interactions

In August of 2001, Hydrosphere Resource Consultants prepared a surface water/groundwater report for the U.S. Bureau of Reclamation, largely drawn from compiled groundwater elevation levels, gaging stations, seepage runs, and pump test data in Socorro county. The main conclusions stated that:

- The surface water system and shallow groundwater system (top 100 ft or 31 m) were largely connected between San Acacia and San Marcial.
- Shallow aquifer hydraulic conductivities determined from slug and impulse-response testing range between 40 and 120 ft/d (12 to 37 m/d).
- Significant gains to the LFCC from the west occur during the March through October irrigation season.

(Hydrosphere, 2001, p. 70). The report made recommendations to perform additional seepage runs, pump tests, and slug tests, expand the monitoring network, and develop a physically based groundwater flow model of the Socorro basin.

3.4.2 Groundwater Resources

Several additional works of significance consider groundwater resources in Socorro County. Two of these include “Hydrogeology of the Socorro and La Jencia Basins, Socorro County, New Mexico” by Scott Anderholm (1987), and “Ground-Water Resources of Socorro County, New Mexico” by Eileen Roybal (1991). The first report was meant to develop a database of well-completion and water-quality information. These data were used to describe the general hydrogeology of the area and define goals for future investigations (Anderholm, 1987). The second report describes “the occurrence, availability, and quality of groundwater in Socorro County” (Roybal, 1991). Water elevation and chemical data were gathered and presented in this report.

4. METHODS

4.1 CHARACTERIZATION OF STUDY AREA

Telescopic modeling was conducted along a six-mile (ten-km) reach of the river between Brown Arroyo and San Antonio (Figure 4-1). The model width was roughly three miles (5 km) and included floodplain sediments ranging from 40 to 100 feet (12 to 31 m) in depth. Development along this reach was consistent with that of the broader region, with agriculture and settlement mostly lying to the west of the Rio Grande. This particular reach was chosen for intensive study because of high Rio Grande losses observed from the seepage run studies conducted in 2000 and 2001. Data collected for model calibration included estimated seepage values from the LFCC and Rio Grande, groundwater elevations from wells, canal and drain bottom elevations, geologic logs, and pump test results.

4.1.1 Groundwater Elevations

Monthly depth to water was measured and recorded by New Mexico Tech graduate students in ten wells within the model domain between October 2001 and August 2003 (Figure 4-1, Appendix C, and Appendix D). Eight of these wells were owned by the BOR, arranged in two transects consisting of four wells each, and screened at the water table. The southern cross section was located one-

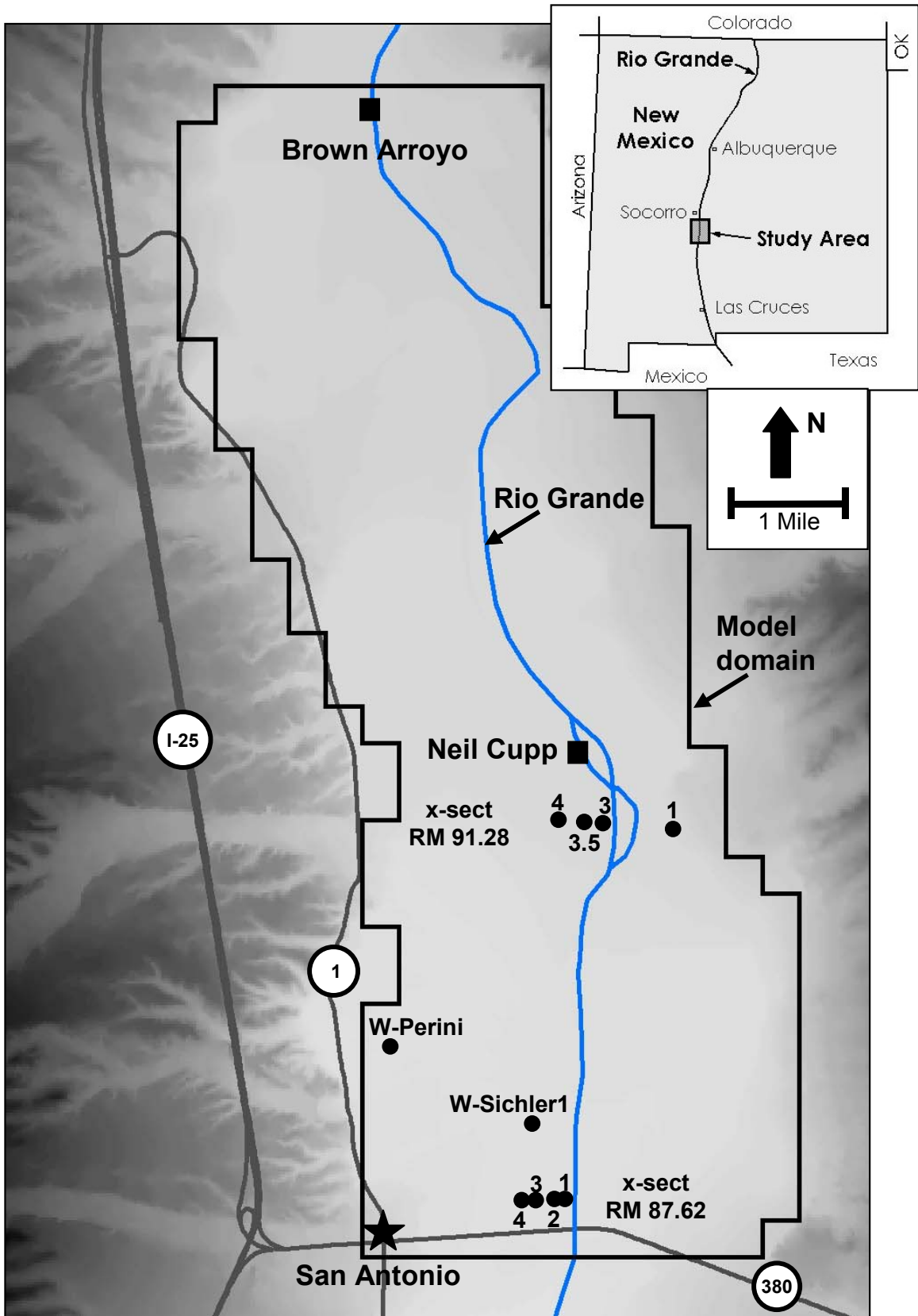


Figure 4-1: Locations of model domain, area landmarks, and BOR and private wells monitored October 2001 through July 2003.

quarter mile (0.4 km) north of Highway 380 and labeled river mile (RM) 87.62 to represent its distance in river miles north of Caballo Dam. Well W-87.62-1 was the eastern-most well with wells -2, -3, and -4 wells in increasing order to the west. The northern cross section was 0.5 miles (0.8 km) south of Neil Cupp at RM 91.28. It used the same labeling sequence as cross-section RM 87.62. Two additional private wells, labeled W-Perini and W-Sichler1, were monitored in 2002 and 2003. Well W-Perini was 81 feet (25 m) deep, fully screened, and located near the western edge of the floodplain one mile north of Highway 380. Well W-Sichler1 was a sand point piezometer installed for a pump test conducted in February 2002. It was located approximately 100 feet (31 m) west of Socorro Main Canal, aligned with the southern well transect, and screened from 35-40 feet (10 to 12 m) depth.

Time series plots of these cross sections showed winter recharge between September and April, with lower water levels during the summer months (Figures 4-2 and 4-3). This pattern was observed most distinctly in wells to the east of the river and between the river and the LFCC. Wells to the west of the LFCC showed dampened or reversed effects due to the application of water to agricultural fields during the irrigation season. The shallow water table appeared to be highly connected to the surface water system in this reach, with trends in LFCC water elevation closely mimicking those of the Rio Grande.

Cross-sectional views of the transects at RM 91.28 and RM 87.62 displayed relatively steep water table gradients to the east and west of the LFCC with the LFCC as the topographic low in the system (Figures 4-4 and 4-5).

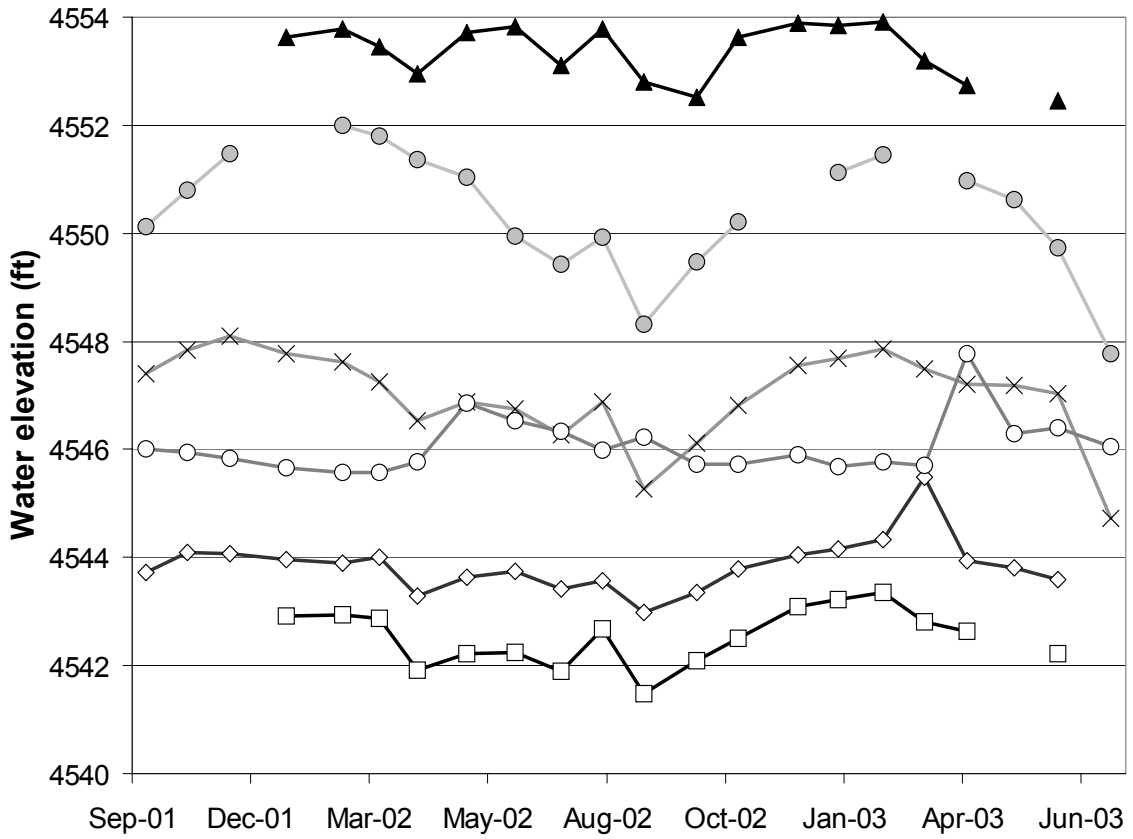
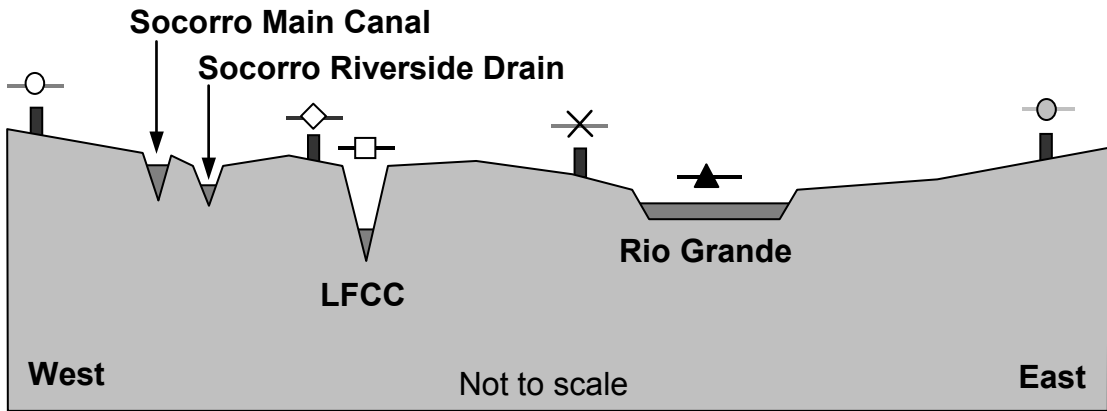


Figure 4-2: Time series of water level elevations at cross-section RM 91.28, October 2001 through August 2003.

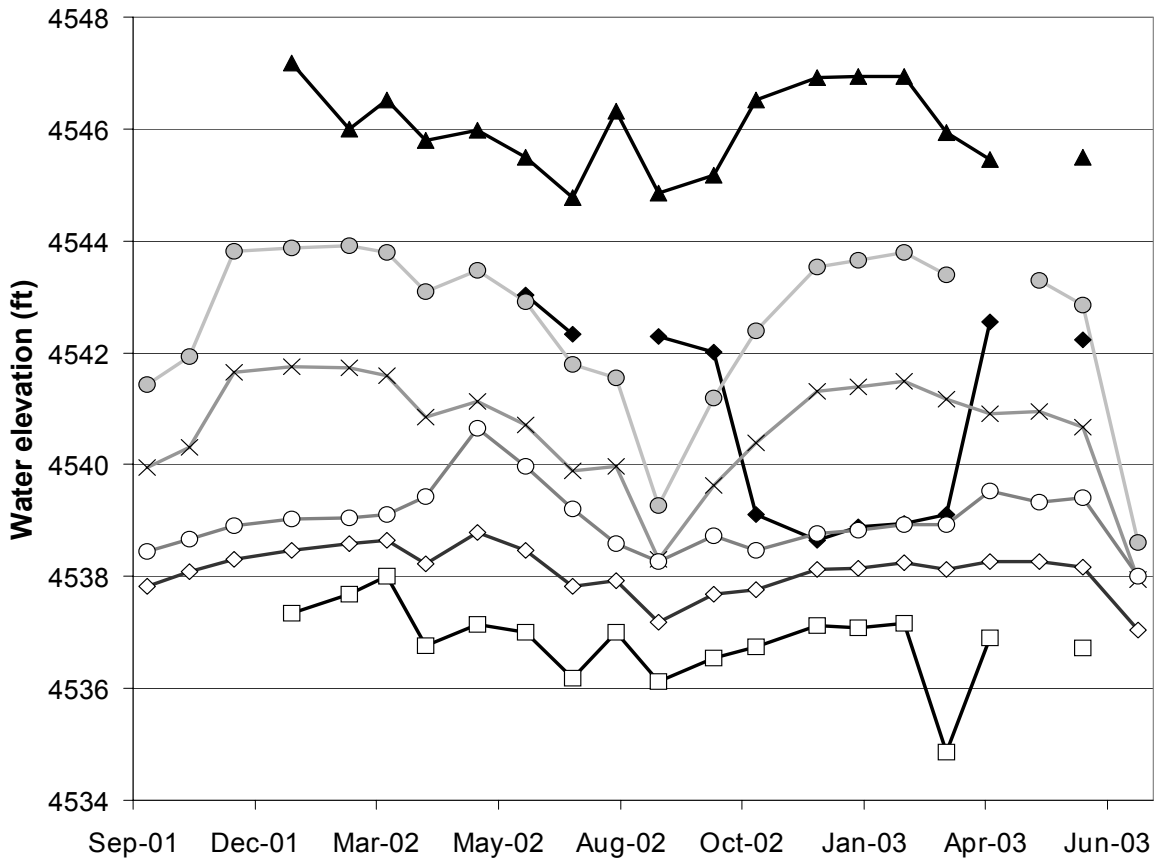
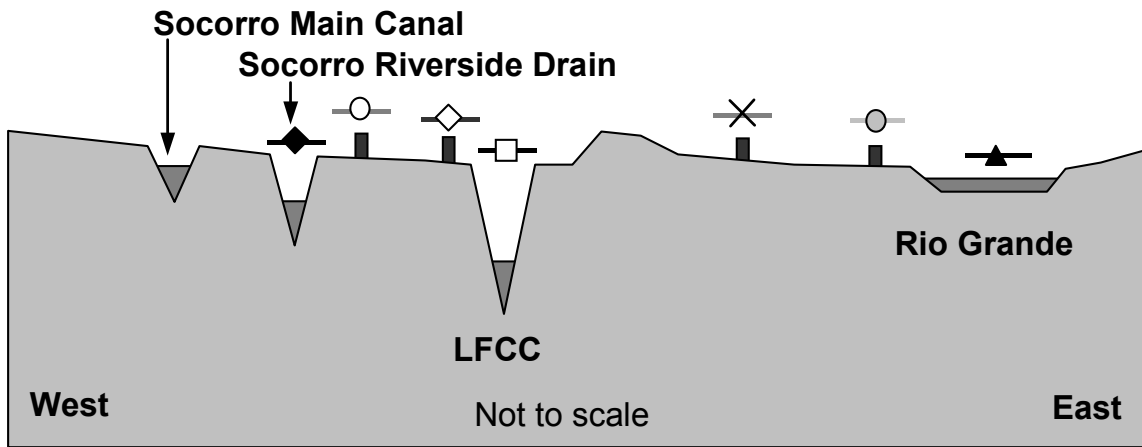


Figure 4-3: Time series of water level elevations at cross-section RM 87.62, October 2001 through August 2003.

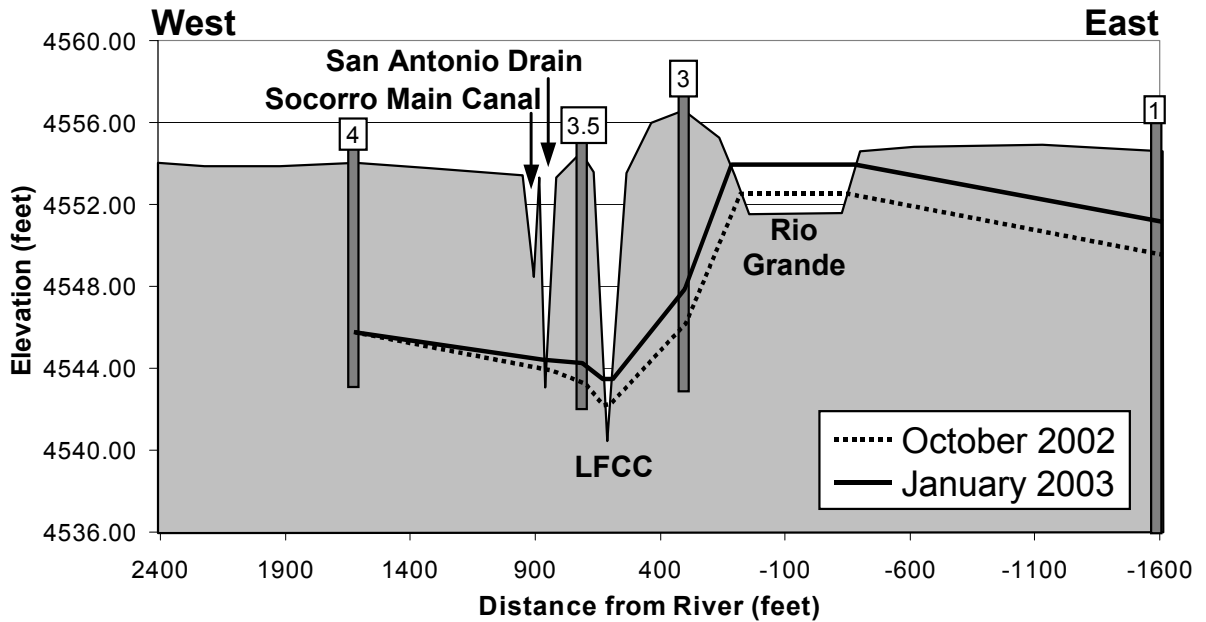


Figure 4-4: Cross section of water level elevations at RM 91.28.

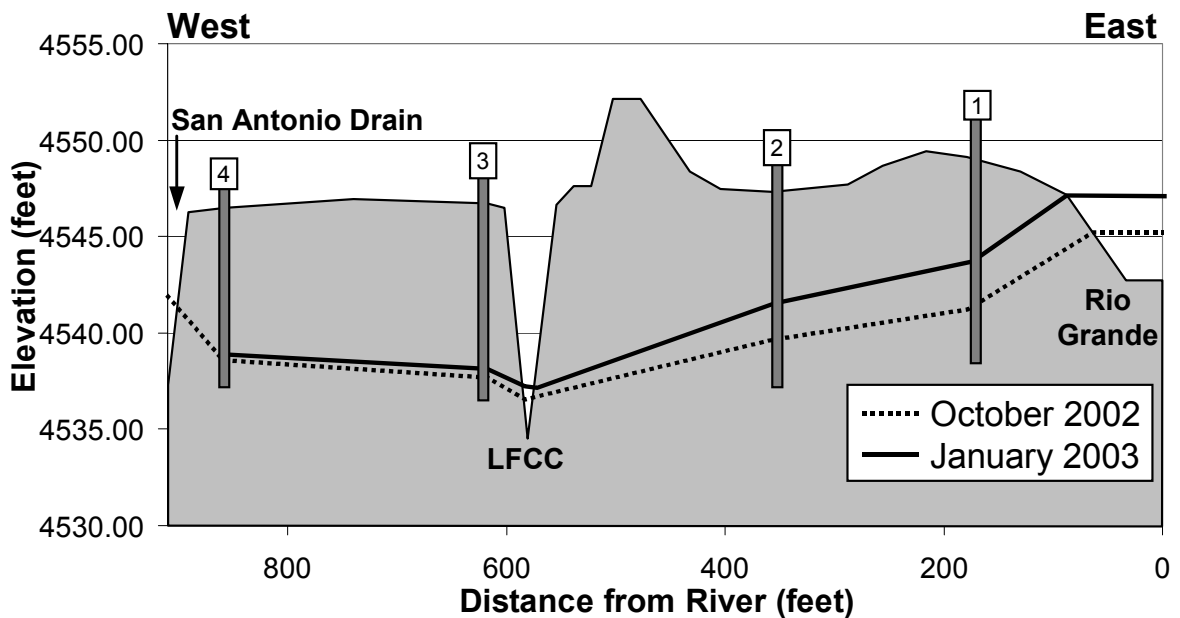


Figure 4-5: Cross section of water level elevations at RM 87.62.

These gradients were between the LFCC and the Rio Grande and the LFCC and agricultural drains. At RM 91.28 the LFCC bottom was 11 feet (3 m) below the river bottom and at RM 87.62 the difference was 8 feet (2 m). At both locations the LFCC was located approximately 600 feet (183 m) west of the Rio Grande

channel. Throughout this reach the Rio Grande was observed to lose water both to the east and west.

Forty-six wells were installed in two transects between October 2002 and May 2003 according to phase two of the NMISC “The Rio Grande Watershed Study – San Acacia Surface Water/Groundwater Investigation” (Figure 4-6) (Appendix E). The first transect marked the northern model boundary at Brown Arroyo, contained 22 wells in 11 borehole locations, and spanned a distance of approximately 5,000 feet (1.5 km) (Figures 4-7 and 4-8). East of the river the well transect split into two lines, one roughly 2,000 feet (0.6 km) south of the other. The second transect was located near the model’s southern boundary at Highway 380 (Figure 4-9). It contained 24 wells in 13 borehole locations and spanned a distance of 3,250 feet (1 km) (Figure 4-10). Each borehole location contained two piezometers, one screened from 15 to 20 feet (5-6 m), labeled “A”, and the other from 45 to 50 feet (12-15 m), labeled “B”. One deep well, screened from 80 to 90 feet (24 –27 m) and labeled “C”, was located at each transect. All piezometers were constructed from two-inch (five-cm) diameter pvc with the exception of one pumping well located at the Highway 380 transect that had a diameter of 12 inches (30 cm) (HWY-W08EX).

NMIMT graduate students initiated manual monthly measurements of depth to water in May 2003. Surveying of the NMISC wells was completed in October of 2003 by ASCI of Albuquerque, New Mexico. Detailed analyses of water level data obtained from these wells will be presented in future projects

conducted between San Acacia and San Marcial. Data are currently stored in the project database that is maintained by NMIMT graduate students.

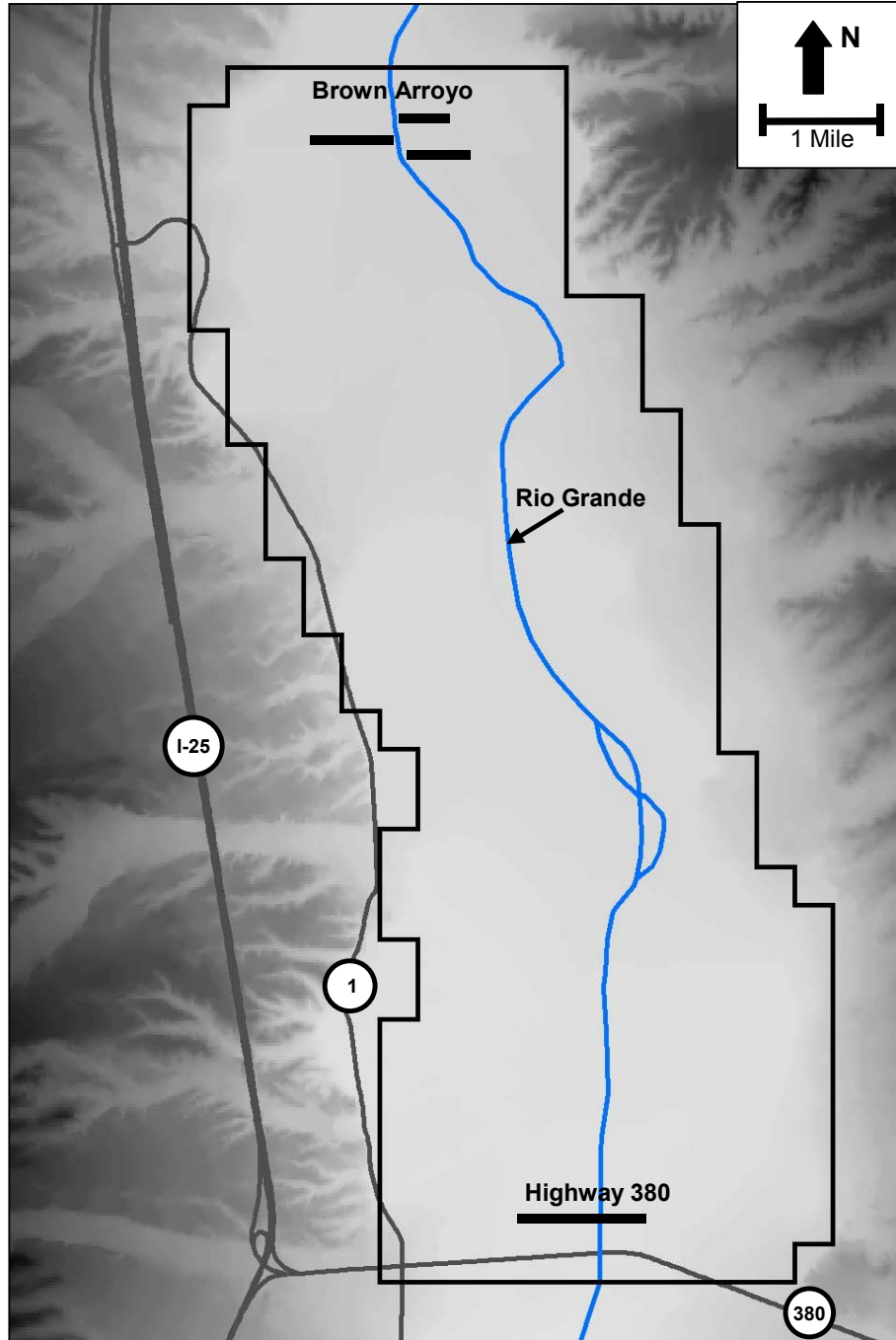


Figure 4-6: Locations of ISC well transects at Brown Arroyo and Highway 380.

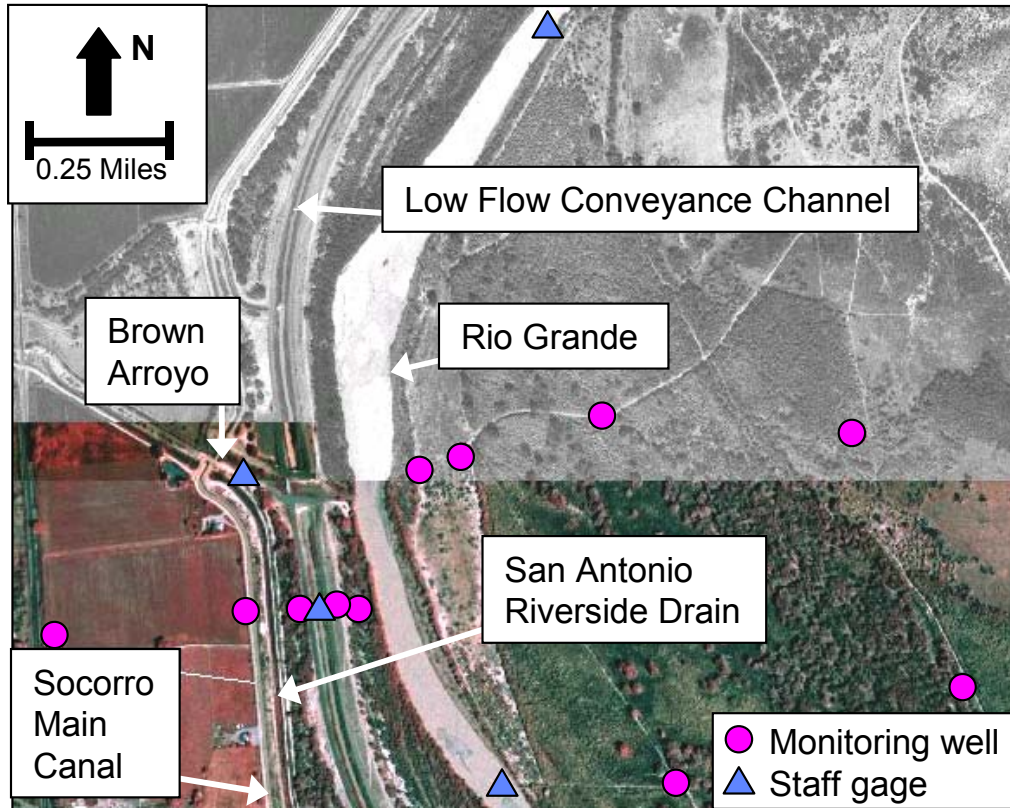


Figure 4-7: Map view of well and staff gage locations at Brown Arroyo. Image courtesy of SSPA, Inc.

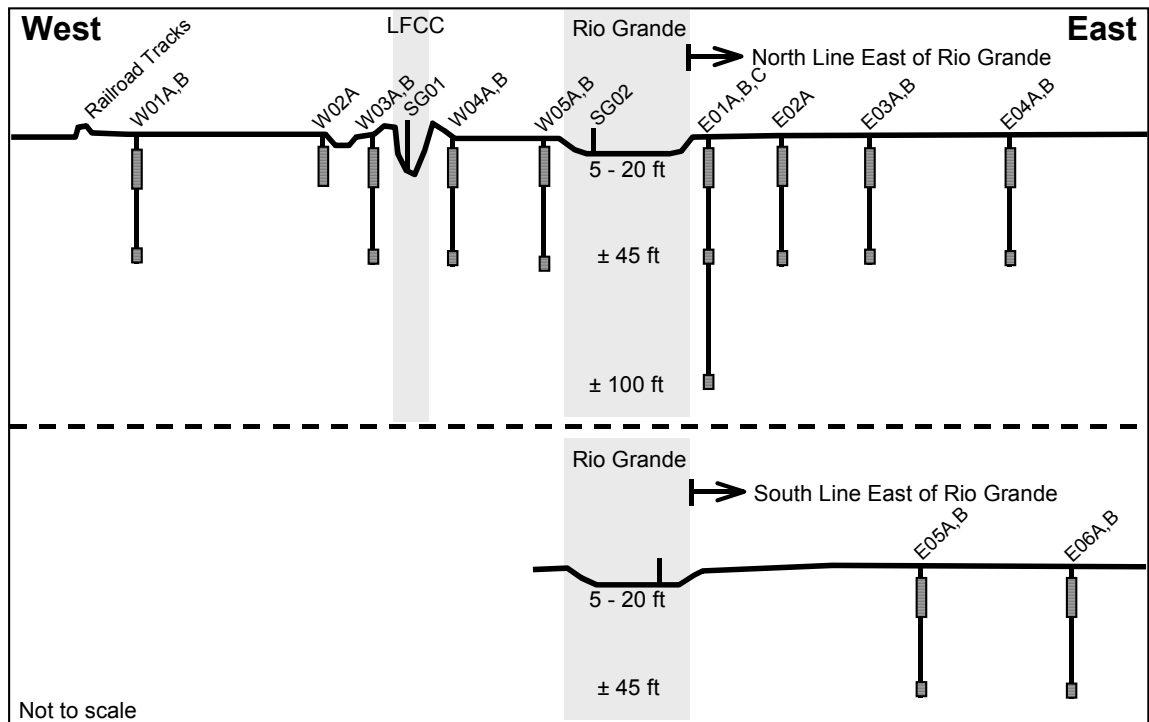


Figure 4-8: Cross section of well and staff gage locations at Brown Arroyo. Image courtesy of SSPA, Inc.

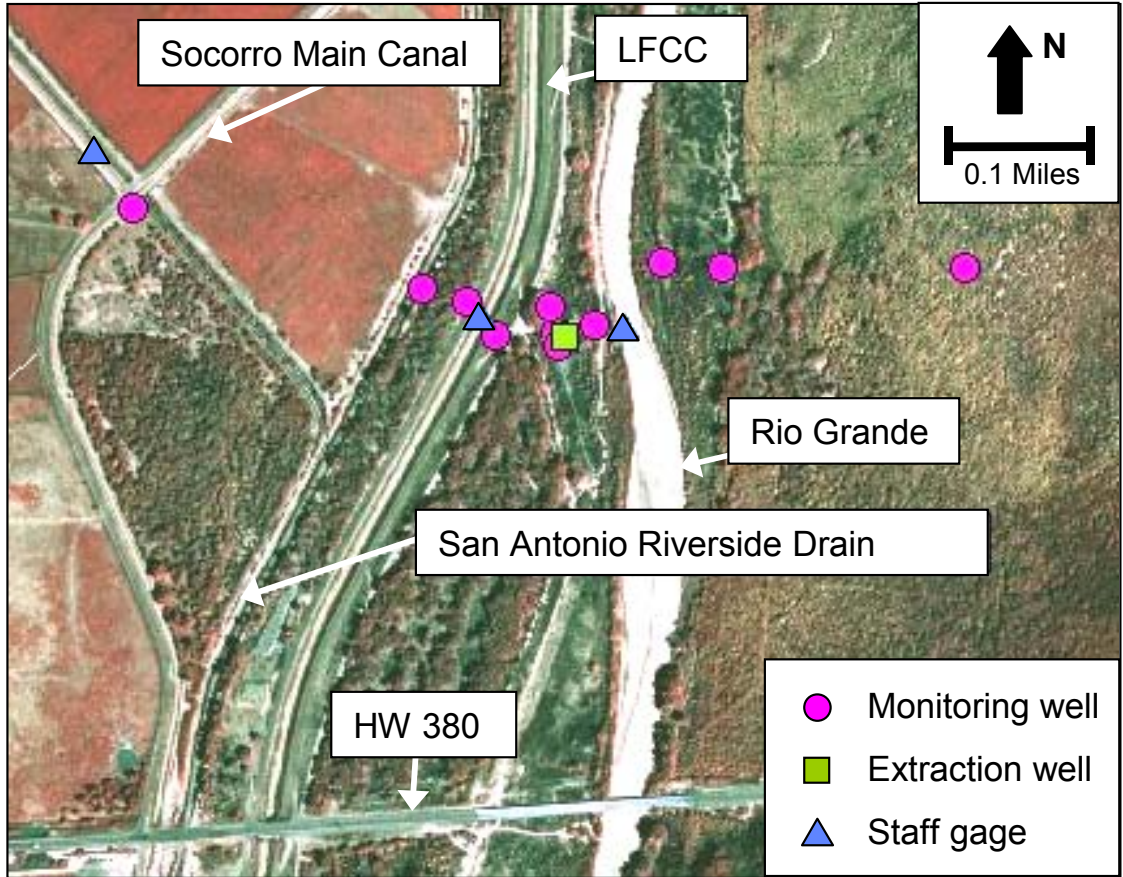


Figure 4-9: Map view of well and staff gage locations at Highway 380. Image courtesy of SSPA, Inc.

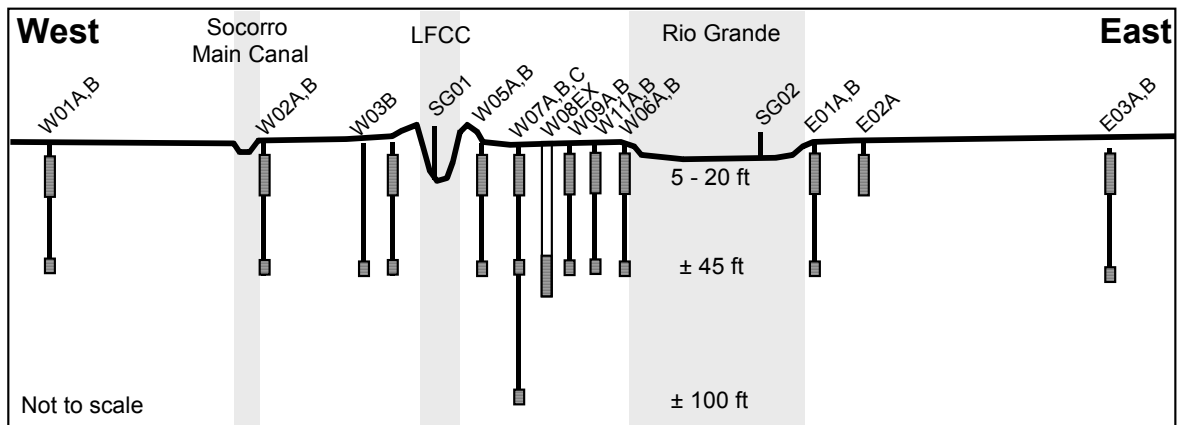


Figure 4-10: Cross section of well and staff gage locations at Highway 380. Image courtesy of SSPA, Inc.

4.1.2 Surface Water Elevations

Surface water elevations were collected at six locations along the LFCC and Rio Grande from January 2001 through August 2003. River and LFCC bed elevations were interpolated from regional model values.

In addition to the Rio Grande and LFCC, several drains and canals flowed through the model domain (Figure 4-11). The Socorro Main Canal and Socorro Riverside Drain paralleled the LFCC through the model area. Water flowed in the Socorro Main during the irrigation season (March through October), but in the winter months it was dry. Socorro Riverside Drain was located between Socorro Main Canal and the LFCC and was wet for most of the year.

Further west, several canals and drains were found that contained water only during the irrigation season. These included San Antonio Ditch, San Antonio Drain, Mosley Lateral, Apodaca Lateral, and Luis Lopez Ditch. Luis Lopez Drain was similar to Socorro Riverside Drain because it often contained water for the entire year. It began at the northern end of the model and terminated at its junction with Socorro Riverside Drain near the south. Monthly water levels were recorded at 32 points along these drains and ditches from August 2002 through July 2003 (Appendix F). Measurement locations were chosen to be approximately every one-mile (1.6 kilometers) along each drain and at all intersections.

In October 2002, seven staff gages were installed along the LFCC, Rio Grande, Luis Lopez Drain, and Brown Arroyo. Manual staff gage readings were recorded monthly and datalogger information was available at five locations.

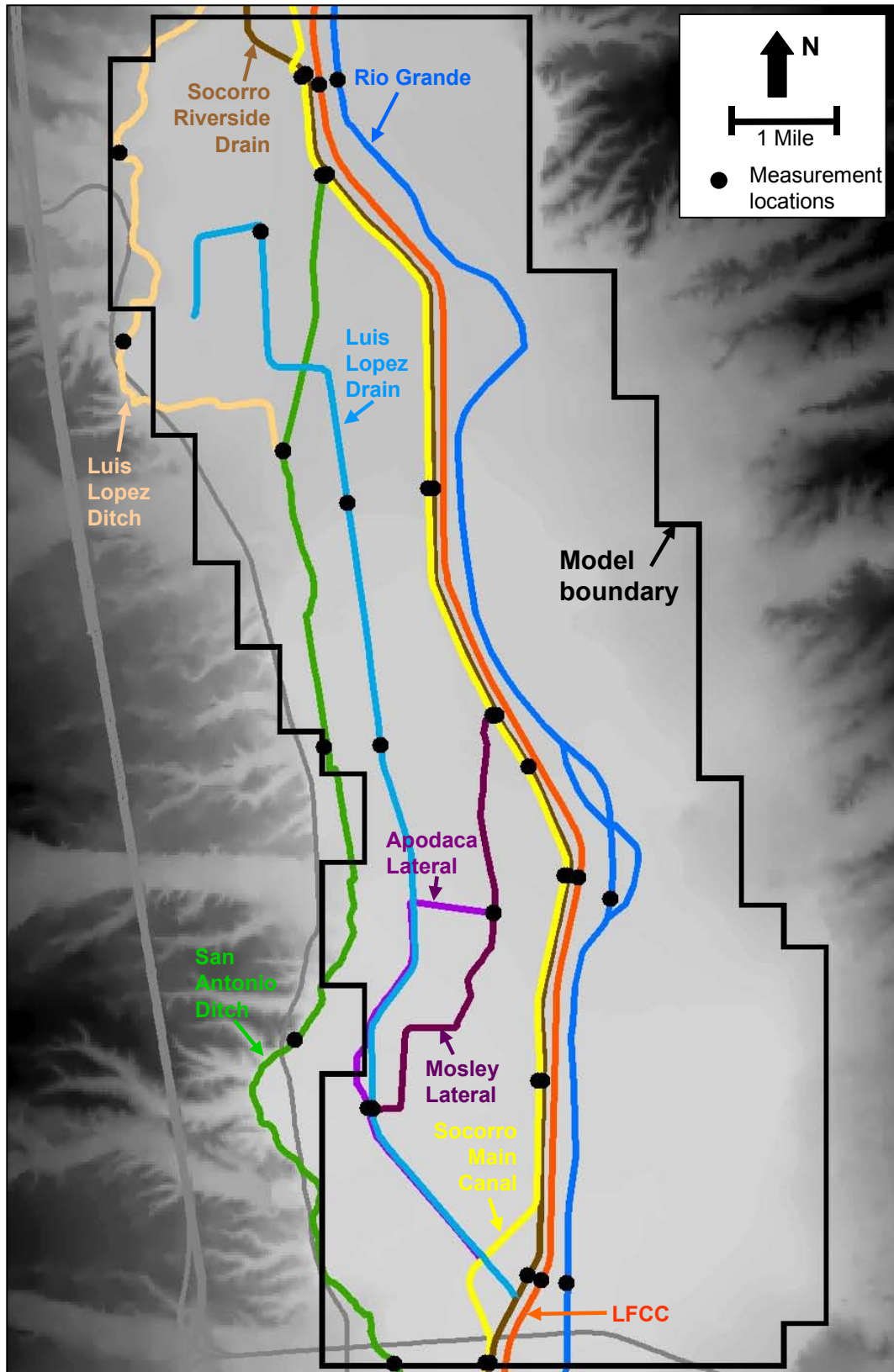


Figure 4-11: Locations of the Rio Grande, LFCC, and associated agricultural drains and canals.

4.1.3 Flood Plain Geology

Split spoon samples were collected and analyzed by SSPA in one-foot (0.3-m) increments at Brown Arroyo and Highway 380 well boreholes (Appendix G). Preliminary stratigraphic and grain size distribution analyses showed that the upper 100 feet (31 m) of sediment underlying the Rio Grande Floodplain was composed primarily of unconsolidated sand, gravel, and silt (Figure 4-12). The model domain was located entirely within the Quaternary Alluvium. Further analysis indicated a two-foot (0.6-m) thick discontinuous clay layer at roughly 30 feet (9 m) depth. The remaining sediments were coarse-grained sands and gravels (Figures 4-13 and 4-14).

No significant faults existed within the valley alluvium; however several existed within the Santa Fe Group below. These structures were mostly normal and high-angle with dips to the west ranging from 65 to 80 degrees (Cather, 1996, p. 23).

4.1.4 Aquifer Tests

Hydrosphere Resource Consultants and S.S. Papadopoulos, Inc. conducted aquifer tests within the model domain at two locations near Highway 380, wells W-Sichler (Figure 4-1) and HWY-W08EX. The first test was conducted over a period of 24 hours in February 2002 at an agricultural irrigation well owned by Chris Sichler (Figure 4-15). The pumping well depth was approximately 100 feet (31 m) below ground surface (bgs), fully screened, and pumped at a constant rate of 1,800 gallons per minute (gpm) ($6.8 \text{ m}^3/\text{min}$). Static water level in the well was approximately 8 feet (2 m) bgs and steady-state

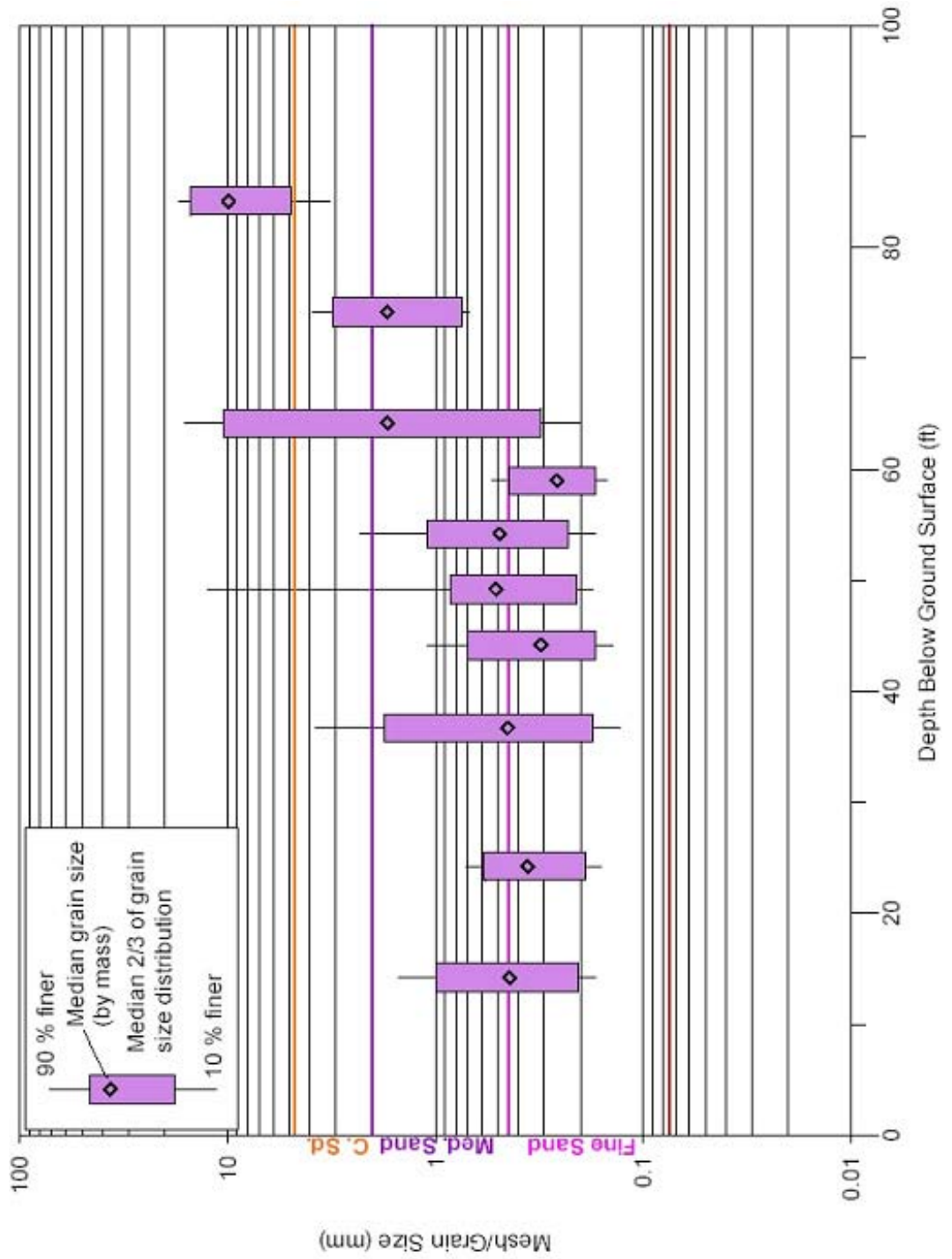


Figure 4-12: Grain size distribution at HWY-W07C. Image courtesy of SSPA.

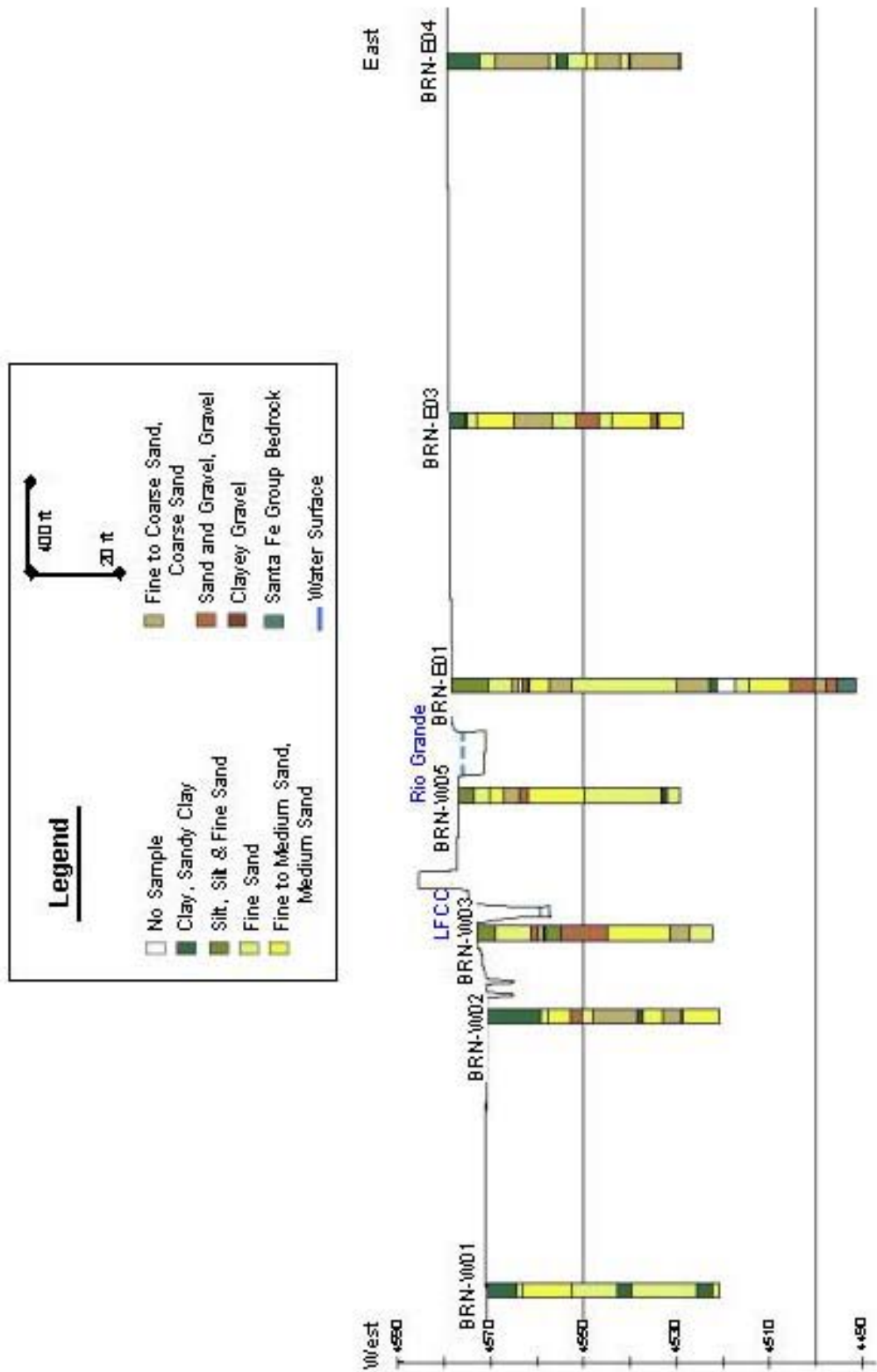


Figure 4-13: Split spoon sampling results at Brown Arroyo conducted by S.S. Papadopoulos and Associates, INC.

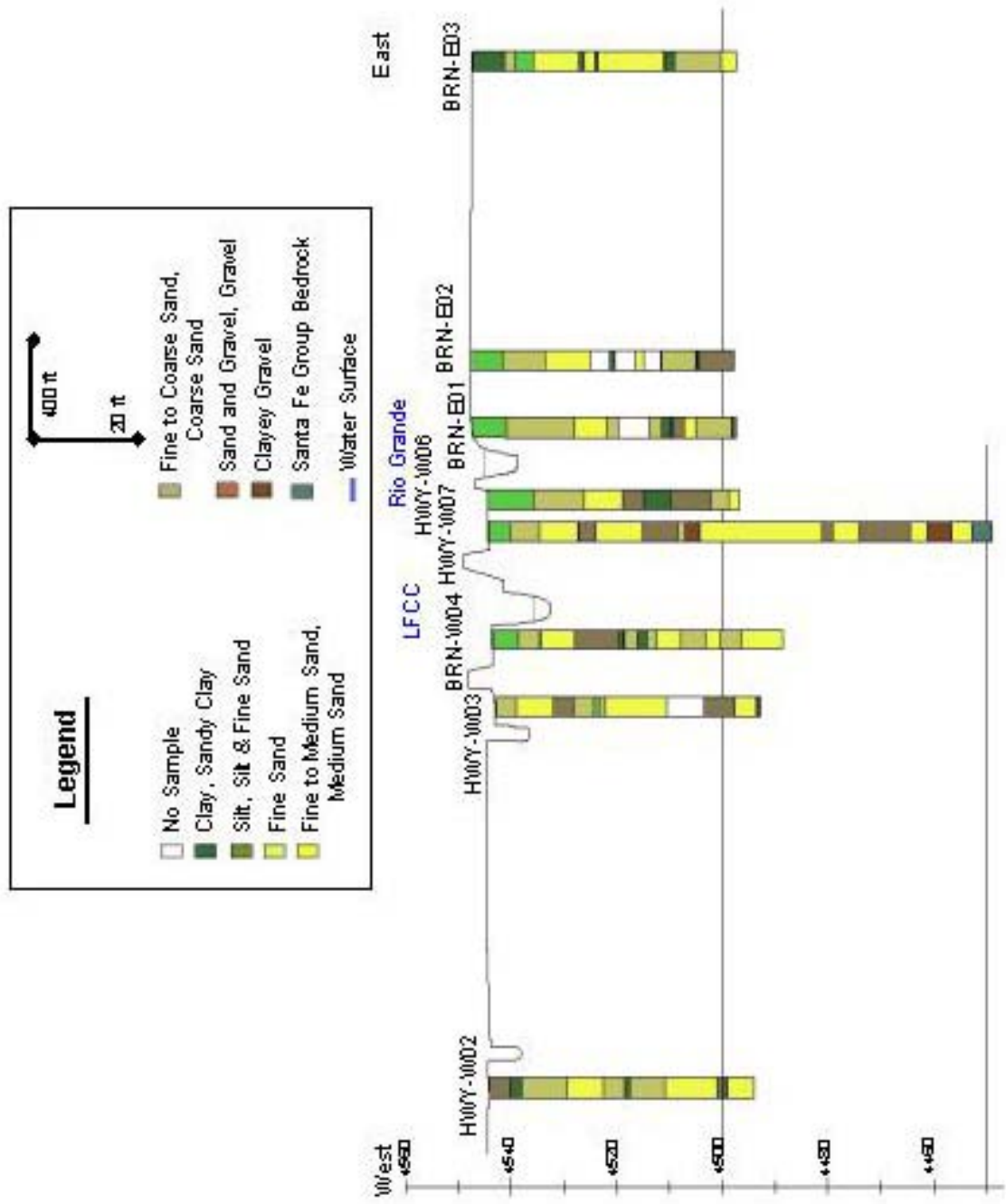


Figure 4-14: Split spoon sampling results at Highway 380 conducted by S.S. Papadopoulos and Associates, INC.

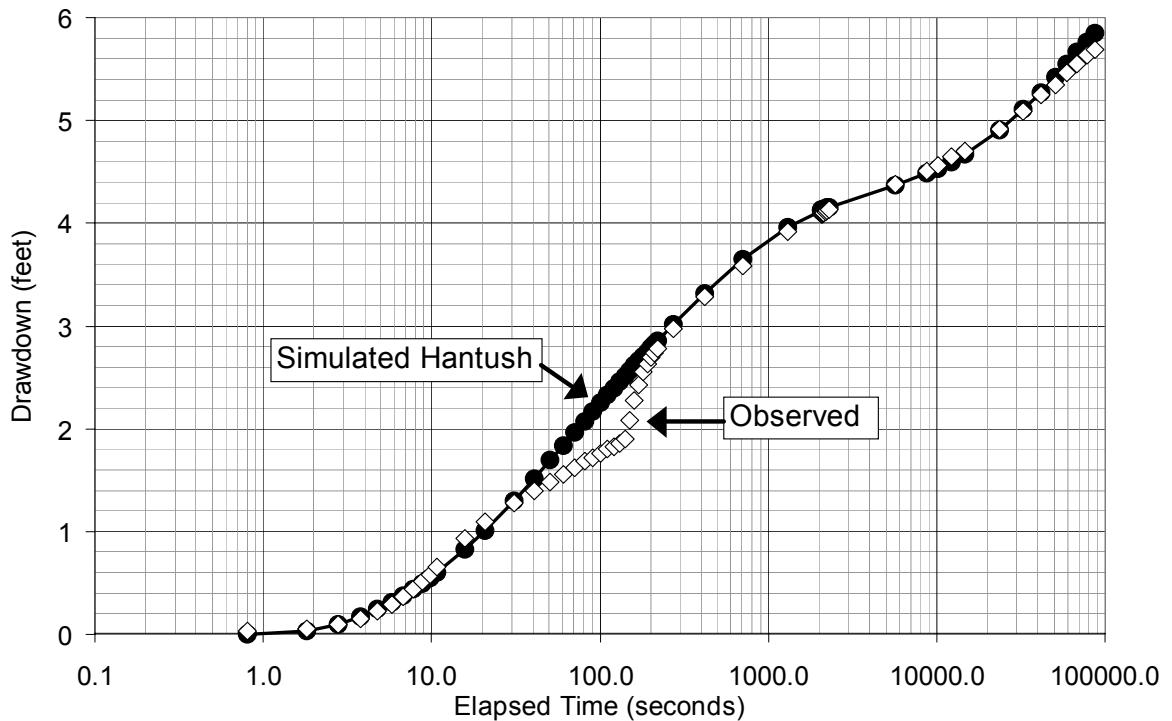


Figure 4-15: Time vs. drawdown data for the 24-hour pump test at W-Sichler (Shafike, personal communication, 2003).

drawdown was achieved at roughly 15 feet (5 m) bgs. Analysis by ISC staff using the Hantush method indicated horizontal and vertical hydraulic conductivity values of 240 and 200 feet/day (73 and 61 m/d), respectively (Hantush, 1956). Specific storage was determined to be 3.0×10^{-5} 1/feet (9.8×10^{-5} 1/m) and specific yield at 0.035. The sudden change in drawdown at 140 seconds was caused by an increase in pumping rate from 1,500 to 1,800 gpm (5.7 to 6.8 m³/min) (Shafike, personal communication, 2003).

The second test was performed at the Highway 380 cross section in June 2003 and was run for a period of 48 hours (Figure 4-6). Prior to construction of the pumping well, laboratory grain-size distribution (gsd) analysis was conducted on split spoon samples of borehole sediments (SSPA, 2003, p.4). This was done to determine an optimum screen interval of 35 to 60 feet (11 to 18 m) bgs with 0.030-slot screen and 10 to 20-filter sand. It was estimated that the well would

be able to pump up to 150 gpm ($0.6 \text{ m}^3/\text{min}$) for a constant rate test. Values of hydraulic conductivity for the sediments were estimated using the Hazen method and ranged from 14 to 1889 feet/day (4 to 576 m/day) (SSPA, 2003, p.18). The extraction well, HWY-W08EX, was 12 inches (31 cm) in diameter, screened at a depth of 35 to 59 feet (11 to 18 m) bgs, and pumped at 76 gallons/minute ($0.3 \text{ m}^3/\text{min}$). Monitoring wells were screened at 10 to 20 feet (3 to 6 m), 40 to 50 feet (12 to 15 m), and 80 to 90 feet (24 to 27 m) bgs (Figure 4-16).

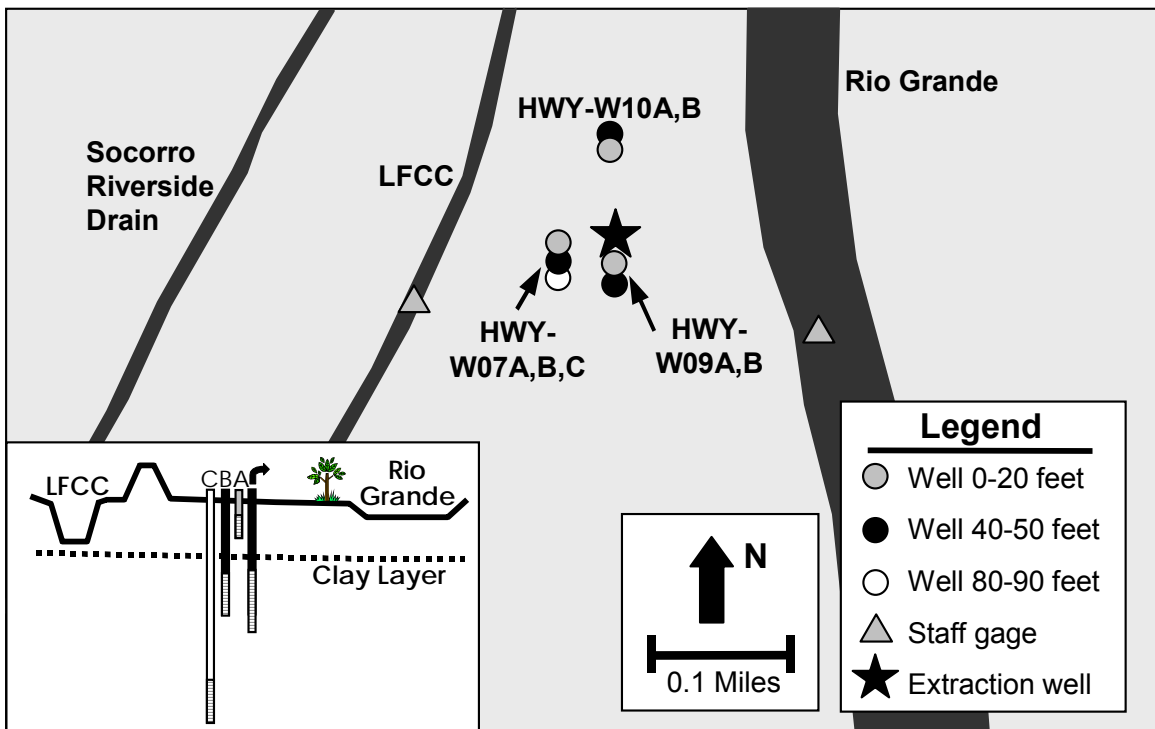


Figure 4-16: Layout of wells at Highway 380 pump test.

Time vs. drawdown plots indicated a strong connection between the pumping well and piezometers screened between 40 and 50 feet (12 and 15 m) bgs (Figure 4-17). These data supported the presence of a clay layer at 30 feet (9 m) depth because greater pumping effect was observed between the pumping well and deepest well (screen intervals were separated by 20 vertical ft or 6 m) than between the pumping well and the shallow well (screen intervals were

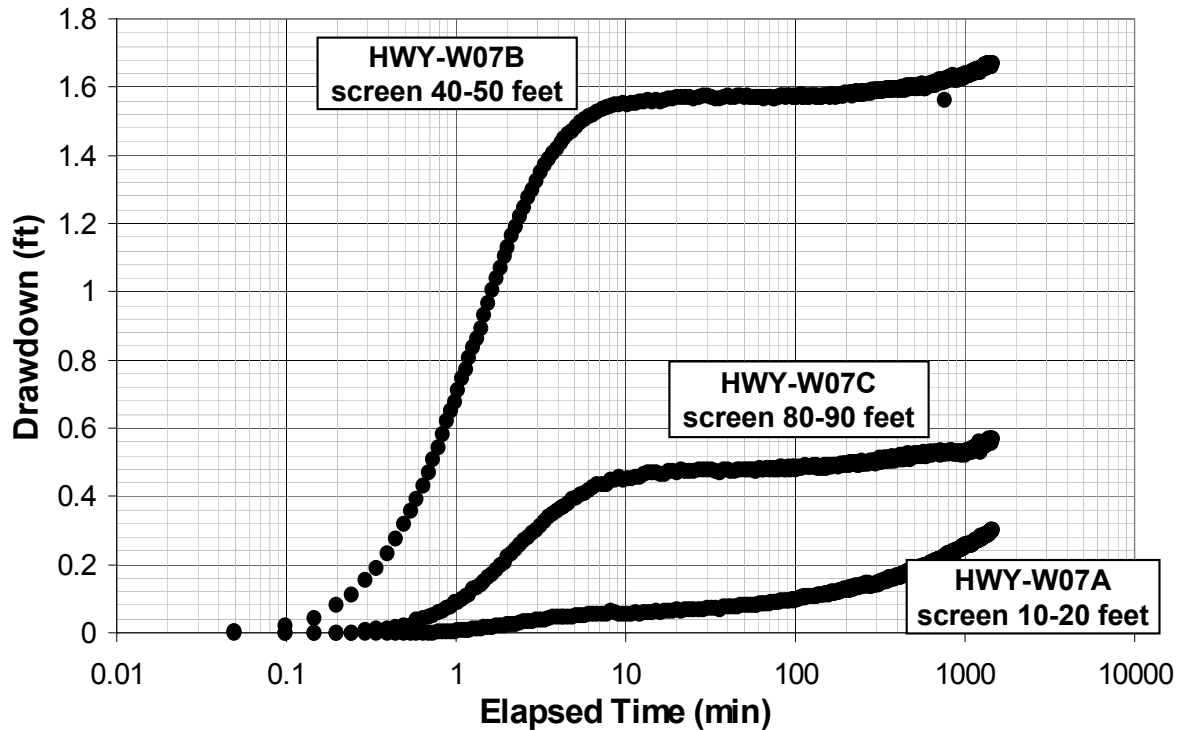


Figure 4-17: Time vs. drawdown data for well HWY-W07 showing nested well effects. separated by 15 vertical ft or 4.6 m). Connection between the pumping and shallow wells was dampened by the clay layer. Maximum pumping effect was observed in HWY-W09B, located five feet (1.5 m) south of HWY-W08EX and screened between 40 and 50 feet (12 and 15 m) depth (Figure 4-18). Less effect was noticed in wells screened from 40-50 feet (12 and 15 m) bgs as radius from the pumping well increased.

Initial analysis for Highway 380 pump test data was done using Theis-type and Cooper-Jacob equations resulting in horizontal hydraulic conductivity calculations of 34 and 42 feet/day (10 and 13 m/d), respectively (Figure 4-18). Transmissivity and storativity values ranged from 815 to 992 feet²/day (76 to 86 m²/d) and 0.012 to 0.013, respectively. These values suggested an alluvial material consisting of clean and silty sands (Freeze and Cherry, 1979, p. 29).

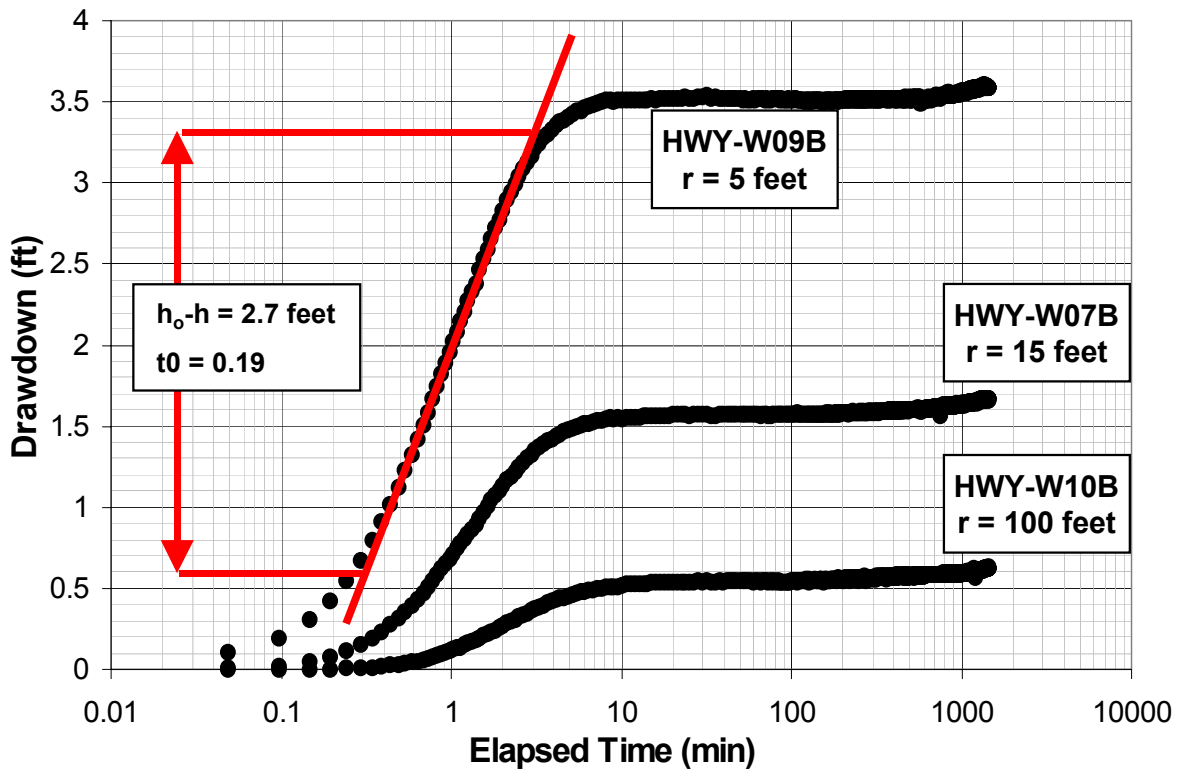


Figure 4-18: Time vs. drawdown data showing effects with distance from pumping well.

The lower values of hydraulic conductivity determined at Highway 380 compared to well W-Sichler reflected differences in geology between the LFCC and the Rio Grande and the surrounding area. Sediments containing higher percentages of fine particles and clay beds may have been more prevalent near the river than at the edges of the floodplain. In addition, construction of the LFCC and re-channeling of the Rio Grande greatly disturbed sediments between the two water bodies. This unnatural restructuring of the subsurface may have been responsible for observed differences in aquifer properties. Finally, values of hydraulic conductivity at well W-Sichler represented the upper 100 feet (31 m) of sediments in the floodplain. It is possible that several feet of the extraction well were screened within the Santa Fe Formation, historically known to have a higher hydraulic conductivity than floodplain sediments.

4.2 MODEL CONSTRUCTION

Steady-state simulations were performed to determine initial head values of layer one for all grid cells in the telescopic model. These simulations displayed changes in the water table in response to variations of aquifer properties and implementation of management scenarios. Steady-state initial head values were applied as input to the transient-state model. The transient-state model was used to show changes in water level elevations and water budget with time and for predictive analyses.

4.2.1 Grid

The regional model had a grid cell size of 1,000 feet by 1,000 feet (305 m), 265 rows, 118 columns, and extended 57 river miles in length from San Acacia to the Elephant Butte delta. The telescopic model grid was generated using Microsoft Excel and ESRI ArcView software. The 6-mile (10-km) long by 3-mile (5-km) wide domain consisted of 320 rows and 170 columns, for a total of 54,400 cells with a uniform grid cell size of 100 x 100 feet (31 m) (Figure 4-19). Only cells within the floodplain alluvium were active. Steady-state and transient-state simulations used the same model grid.

4.2.2 Hydrostratigraphic Layers

The regional model contained five layers, the uppermost being an alluvium that varied in thickness from 40 to 100 feet (12 to 31 m) bgs. Telescopic model construction was based on the regional model features, where the upper layer of the regional model was the total thickness of the telescopic model. Samples

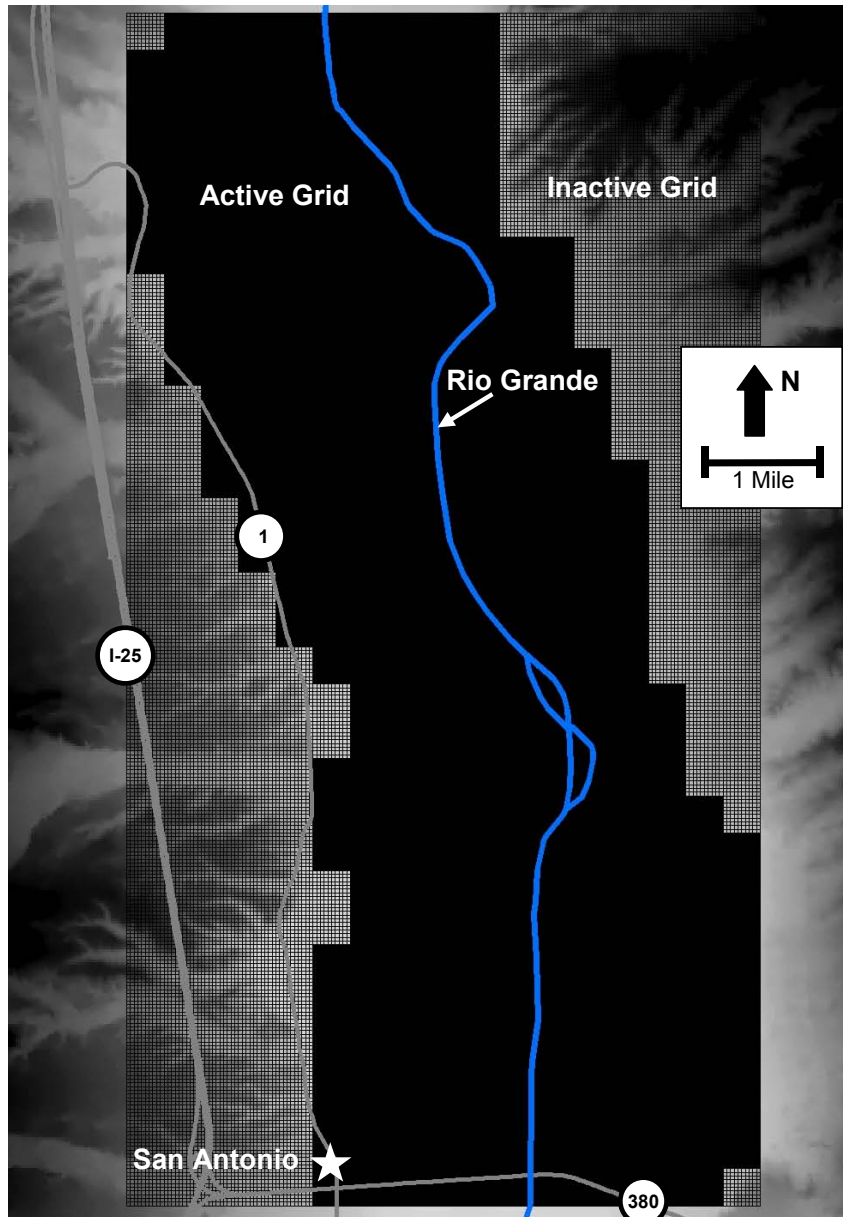


Figure 4-19: Locations of active and inactive cells in the telescopic model grid. taken from drill core were analyzed for geologic and hydrologic properties as described in Chapter 4.1.3. Three distinct units were identified including a clay layer at approximately 30 feet (9 m) depth sandwiched between two thicker, sand/gravel units (Figures 4-13 and 4-14). These units were conceptualized as shown in Figure 4-20. Model ground surface elevation was determined for each 100 by 100 foot (31 m) grid cell from a 32.8-foot (10-m) resolution digital

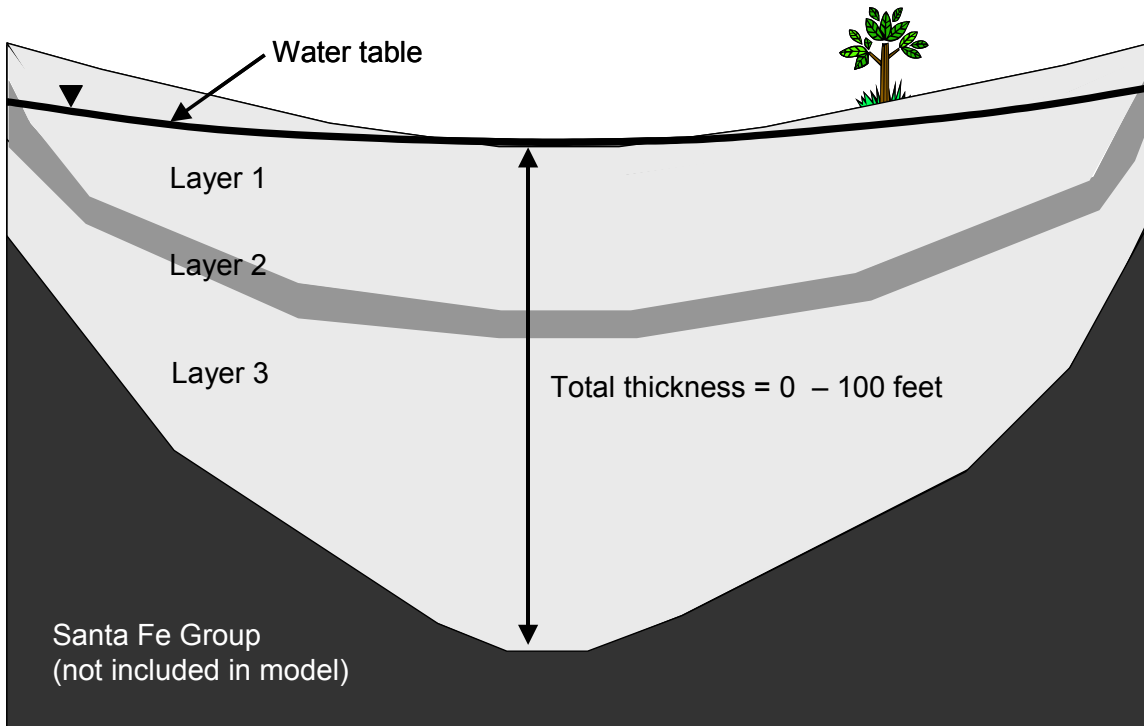


Figure 4-20: Hypothetical cross section of Rio Grande floodplain with confining layer 2. elevation model (DEM). Thickness of layer 1 was defined as the vertical distance between the land surface+ and the top of the clay layer. Linear interpolation between known clay layer depths was conducted across each of the two cross sections, and then applied longitudinally to assign a layer 1 thickness value to each cell. Layer 2, the identified clay layer, was assumed to be a constant thickness of two feet (0.6 m) throughout the model. Layer 3 was determined as the remainder of thickness from layer 1 of the regional model and extended from the bottom of the clay layer to the top of the Santa Fe Formation. Layers 1 and 2 were initially saturated throughout the domain except for select cells along the east and west boundaries where topographical changes forced the layer to exist above the water table. Layer 1 thickness ranged from 11 to 35 feet (3 to 11 m) with the thickest area occurring at the north beneath the present day river channel (Figure 4-21). At the base of the model, layer 3 was initially entirely

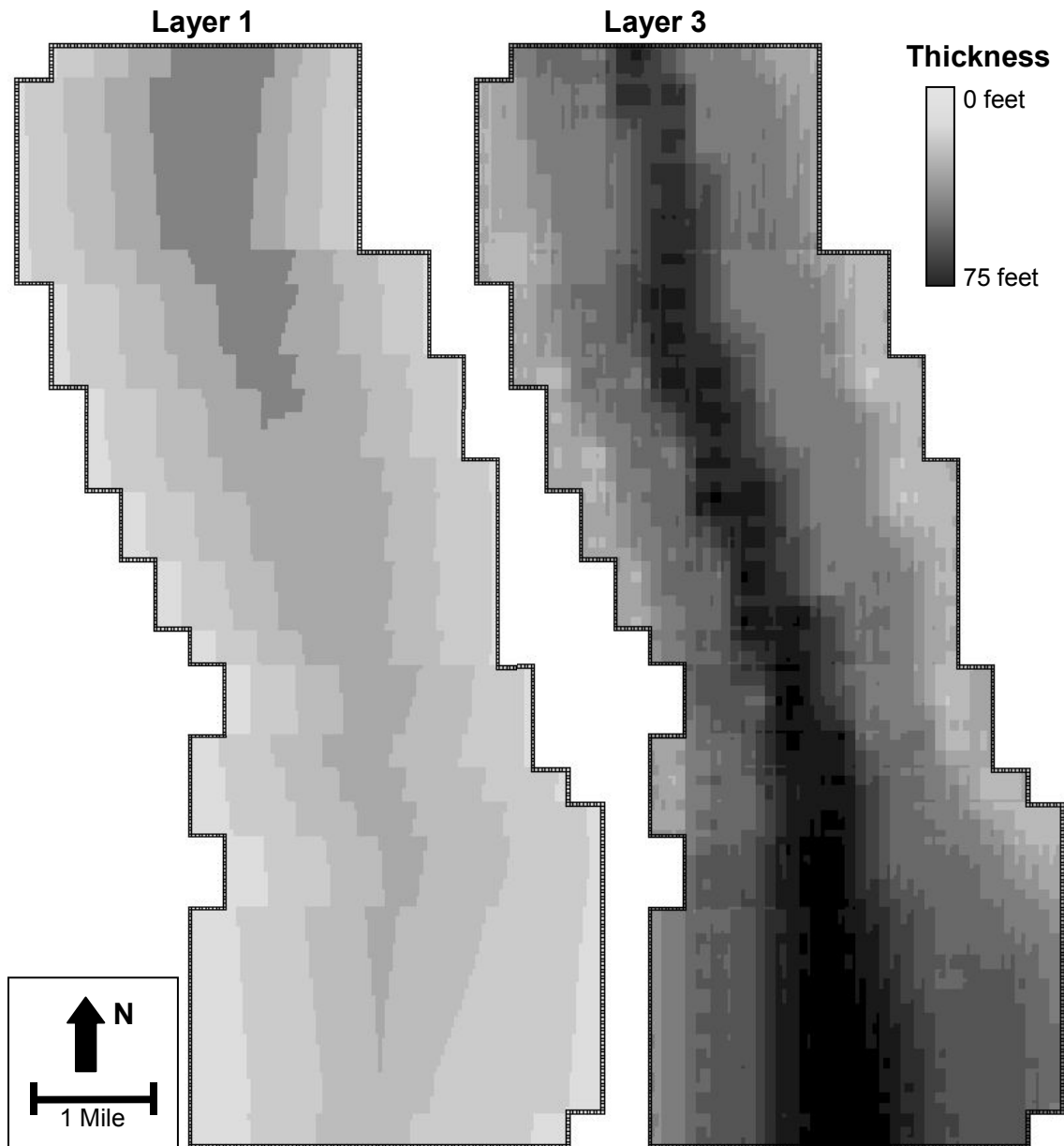


Figure 4-21: Thickness distribution of telescopic model layers one and three. saturated with thickness ranging from 19 feet (6 m) to a maximum of 75 feet (23 m) beneath the current river channel in the south.

Initially, layers 1 and 3 were assigned horizontal and vertical hydraulic conductivity values of 100 and 50 feet/day (31 and 15 m/d), respectively. These values were the same as those applied to the uppermost layer of the regional-scale model and were a representative average of the measured Highway 380

and Sichler pump test results (Chapter 4.1.4). Model simulations of varied anisotropies and magnitudes of horizontal hydraulic conductivity were conducted, although changes to initial values were not necessary for calibration. The steady-state model was calibrated when water table elevations and seepage values from the Rio Grande and LFCC matched the output of the regional-scale model and observed field data. Layer 2 was assigned standard values for silty sand with a horizontal conductivity of two feet/day (0.6 m/d) and vertical conductivity of 0.1 ft/day (3.0×10^{-2} m/d) (Freeze and Cherry, 1979, p.29). This information was included in the block centered flow (bcf) package of MODFLOW.

4.2.3 Vegetation

The evapotranspiration package (evt) of MODFLOW factored for direct evaporation and plant transpiration from the saturated water table. A finite difference approach was used to solve for the volumetric rate of loss (evapotranspiration) for each cell, $Q_{ETi,j}$, by multiplying the horizontal surface area, $DEL R_j * DEL C_i$, by the rate of loss per unit surface area of water table due to evapotranspiration, $R_{ETMi,j}$ (McDonald and Harbaugh, 1988, p. 10-2),

$$Q_{ETi,j} = R_{ETMi,j} * DEL R_j * DEL C_i$$

IKONOS satellite imagery from July 2000 was classified into crop, riparian, sandbar, and inactive regions (Figure 4-22) using ESRI ArcGIS (geographic information system) software (ISC and MRGDC, 2001). The classification included a percentage of grid cell surface area occupied by each vegetation type (cover area). Estimations of evapotranspiration rates for various vegetation types in the year 1999 were obtained from eddy covariance tower data collected

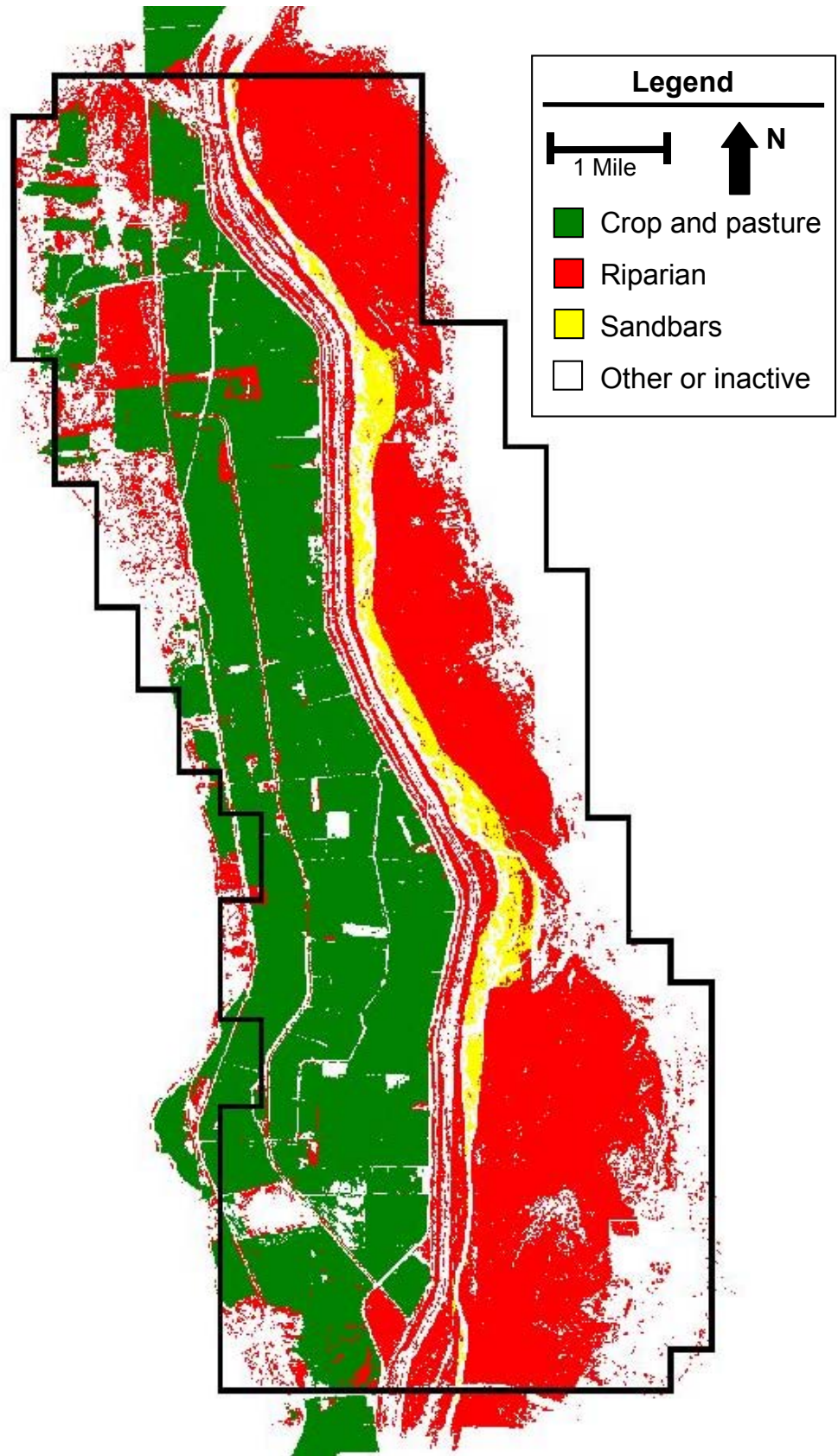


Figure 4-22: Landcover classification from July 2000 IKONOS image.

at the BDA NWR (Cleverly et al., 2001). Values were multiplied by the cover area of that vegetation type for each grid cell to yield input rates for MODFLOW.

To the east of the river and LFCC was riparian vegetation, consisting primarily of cottonwoods and saltcedar, while to the west was a mixture of cropland and riparian vegetation. For the telescopic steady-state model, riparian vegetation was assigned an evapotranspiration rate of 3.5 acre-feet per acre per year (af/a/yr) (1.1 m/yr), an average of monthly values collected at the BDA NWR in 1999. Open ground surrounding the river was averaged in the same manner with an evapotranspiration rate of three af/a/yr (0.9 m/yr) (Cleverly et al., 2001). These values were the same as those applied to the regional-scale model (Shafike, personal communication, 2003). For the telescopic transient model, open ground evapotranspiration rates were also maintained at three af/a/yr. Values were varied according to monthly averages of daily evapotranspiration tower data collected during 1999 (Table 4-1) (Cleverly et al., 2001).

	Evapotranspiration	
	af/a/mo	m/yr
October	4.44	1.35
November	1.43	0.44
December	1.21	0.37
January	1.08	0.33
February	1.12	0.34
March	1.62	0.49
April	1.72	0.52
May	4.76	1.45
June	9.18	2.80
July	9.18	2.80
August	8.82	2.69
September	7.36	2.24

Table 4-1: Monthly evapotranspiration rates for riparian vegetation recorded in 1999 applied to the transient model (Shafike, personal communication, 2003).

Evapotranspiration rates ranged from a maximum of 9 af/a/yr (2.7 m/yr) in June to a minimum of 1 af/a/yr (0.3 m/yr) in January.

The steady-state model did not include crop evapotranspiration because it was meant to coincide with the steady-state regional model and represent a period of inactive agriculture (no water in agricultural drains and no irrigation). For the transient model, evapotranspiration from crops was simulated during the months of April through October. March was not included in this time period because it was assumed that farmers did not use significant quantities of canal, ditch, and drain water for crop irrigation until late March or early April. Crop evapotranspiration was assumed to be less than applied irrigation and thus the sum was treated as a deep percolation recharge (.rch) term in MODFLOW. This difference or flood irrigation term was one af/a/yr (0.3 m/yr), defined as $Q_{Ri,j}$ (McDonald and Harbaugh, 1988 p. 7-1),

$$Q_{Ri,j} = I_{i,j} * DELR_j * DELC_i$$

In this equation the recharge flow rate applied to the model at horizontal cell location (i,j), $Q_{Ri,j}$, was equal to the product of the recharge flux, $I_{i,j}$, and map area of the cell, $DELR_j * DELC_i$.

4.2.4 Surface Water System

The Rio Grande, LFCC, and agricultural drains were connected to the shallow aquifer using the river package (.riv) of MODFLOW. This package was designed to simulate flow between surface water features and ground water systems. In order to do this, seepage terms to and from surface features were added to the groundwater flow equation given by,

$$CRIV = (K * L * W) / M \quad ,$$

$$QRIV = CRIV * (HRIV - h_{i,j,k}) \quad ,$$

where CRIV was the hydraulic conductance of the stream-aquifer interconnection, K was vertical hydraulic conductivity of the streambed, L was length of the stream within the cell, W was width of stream, M was thickness of streambed, QRIV was the stream-aquifer flow, HRIV was head in the stream (stage), and $h_{i,j,k}$ was the head at the node in the cell underlying the stream reach (McDonald and Harbaugh, 1988 p. 6-5).

A total of 4,185 grid cells represented agricultural drains and canals, the LFCC, and the Rio Grande, while 1,889 were designated Rio Grande cells and assigned widths and lengths of 100 feet (31 m) with a vertical hydraulic conductivity of one foot/day (0.3 m/d) (Shafike, personal communication, 2003). A total of 401 LFCC cells had a width of 50 feet (15 m) and all other drains (an additional 1,895 cells) were 10 feet (3 m) wide with lengths determined from ESRI ArcGIS software. Vertical hydraulic conductivity of LFCC and agricultural drain cells was two feet/day (0.6 m/d) (Shafike, personal communication, 2003). Riverbed vertical hydraulic conductivities were assigned so that they coincide with values applied in the regional steady-state model.

Drain bottom elevations were determined using linear interpolation between surveyed locations. Measurements were taken approximately every one-mile (1.6 km) along the drains and at intersection points. A drain width of ten feet (3 m) was applied to all drains, but in reality, this dimension varied slightly with respect to water level in the canal and construction differences.

For the steady-state simulation, only the LFCC and the Rio Grande were included in the river package. This was done to simulate a pre-irrigation system and coincided with the regional model that included only the LFCC and the river. All cells were assigned a stage value of two feet (0.6 m) above the river or LFCC bottom and a bed thickness of one foot (0.3 m). These values were determined from regional model calibrations.

Field observations indicate that the Rio Grande stage at Highway 380 and San Marcial was at a minimum in August (often zero feet with no river flows) and a maximum during the winter months. For the transient-state simulation, synthetic data was applied to represent Rio Grande stage variations in character and magnitude that were based on observed USGS gage readings at San Marcial (Table 4-2 and Figure 4-23). Stage values for the LFCC and agricultural drains and canals remained a constant value of two feet (0.6 m).

Month	Stage height	
	(feet)	(meters)
Oct-01	1.50	0.46
Nov-01	1.75	0.53
Dec-01	2.00	0.61
Jan-02	2.00	0.61
Feb-02	2.00	0.61
Mar-02	2.00	0.61
Apr-02	1.75	0.53
May-02	1.50	0.46
Jun-02	0.90	0.27
Jul-02	0.35	0.11
Aug-02	0.20	0.06
Sep-02	0.80	0.24

Table 4-2: Stage variation and crop evapotranspiration input for the transient-state model.

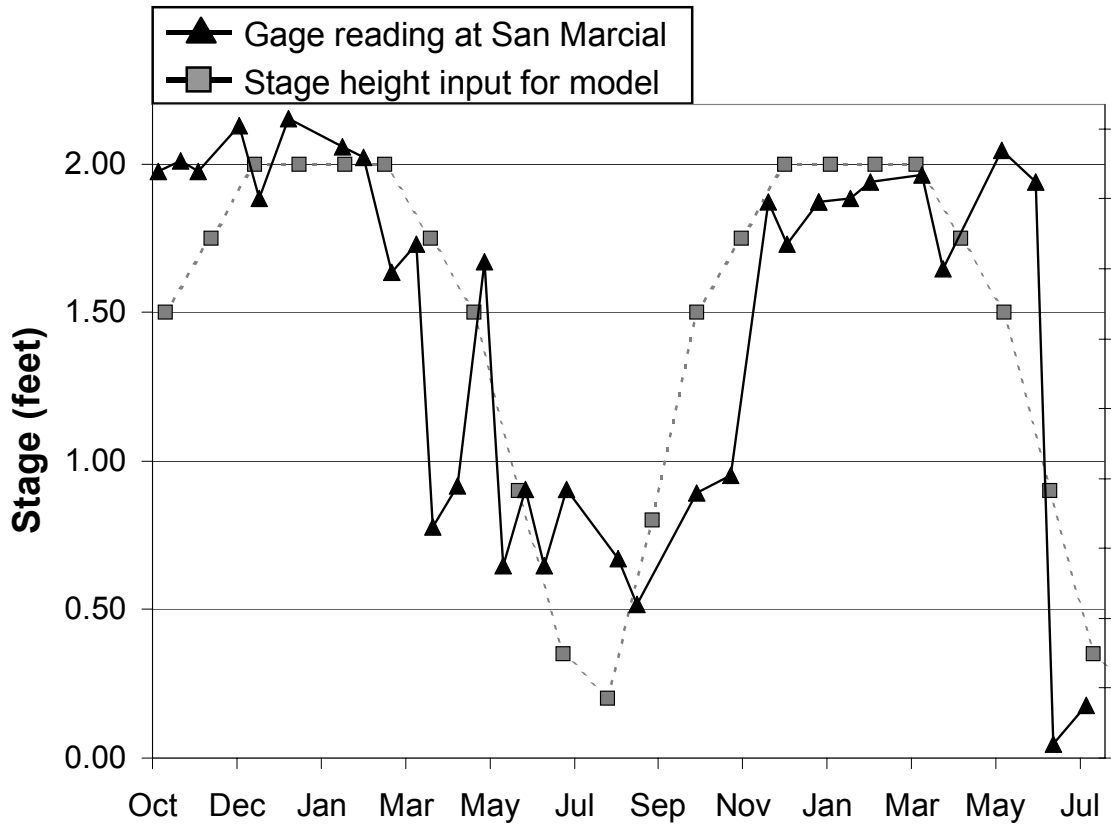


Figure 4-23: Gage reading at San Marcial vs. stage height applied in model.

4.2.5 Initial Conditions

The regional and telescopic models were linked through the prescribed head boundary. At the first stress period, prescribed head values for the boundary of the model domain were extracted from the regional model and imported into layer three of the telescopic model as a constant head file (.chd). Ideally, the regional model would be called on at the beginning of each stress period to determine an updated set of constant head boundaries. This continuous link between the regional model and the telescopic model would help ensure consistency for long-term simulations and maintain the link between the large-scale and refined systems. Because simulations for the purposes of this study did not exceed two years and head fluctuations were small (on the order of

one to two ft or 0.3 to 0.6 m), it was assumed that regional water table elevations would not vary drastically and that it was not necessary to continuously update this link.

4.3 STEADY-STATE MODEL

Modeling of the system under steady-state conditions was performed in order to simulate a water table consistent with steady-state regional model results and measured field data. The steady-state system included riparian and sandbar evapotranspiration and a constant stage value of two feet (0.6 m) for the LFCC and Rio Grande surface water systems.

Telescopic model steady-state results indicated patterns of seepage loss and gain that were consistent with the observed behavior of the river and the LFCC. Results were also in reasonable agreement with the regional model simulated water table (Figure 4-24). Differences between the two models such as smoother contouring and greater detail of the telescopic model results were because of finer grid spacing. At the south of the model at row 260, upward and downward gradients between layers 1, 2, and 3 coincide with areas of shallow aquifer recharge and discharge (Figure 4-25). Regional model aquifer and streambed property values applied to the telescopic model produced a calibrated higher resolution analysis tool between Luis Lopez and San Antonio.

Leakage values from each grid cell for the river and LFCC were tabulated to yield values of seepage. As previously discussed in Chapter 3.1, measured seepage from the river along the telescopic model reach ranges between 3.3 and 24.8 cfs/mile (9.4×10^{-2} and 7.0×10^{-1} m³/s/mile), depending on environmental

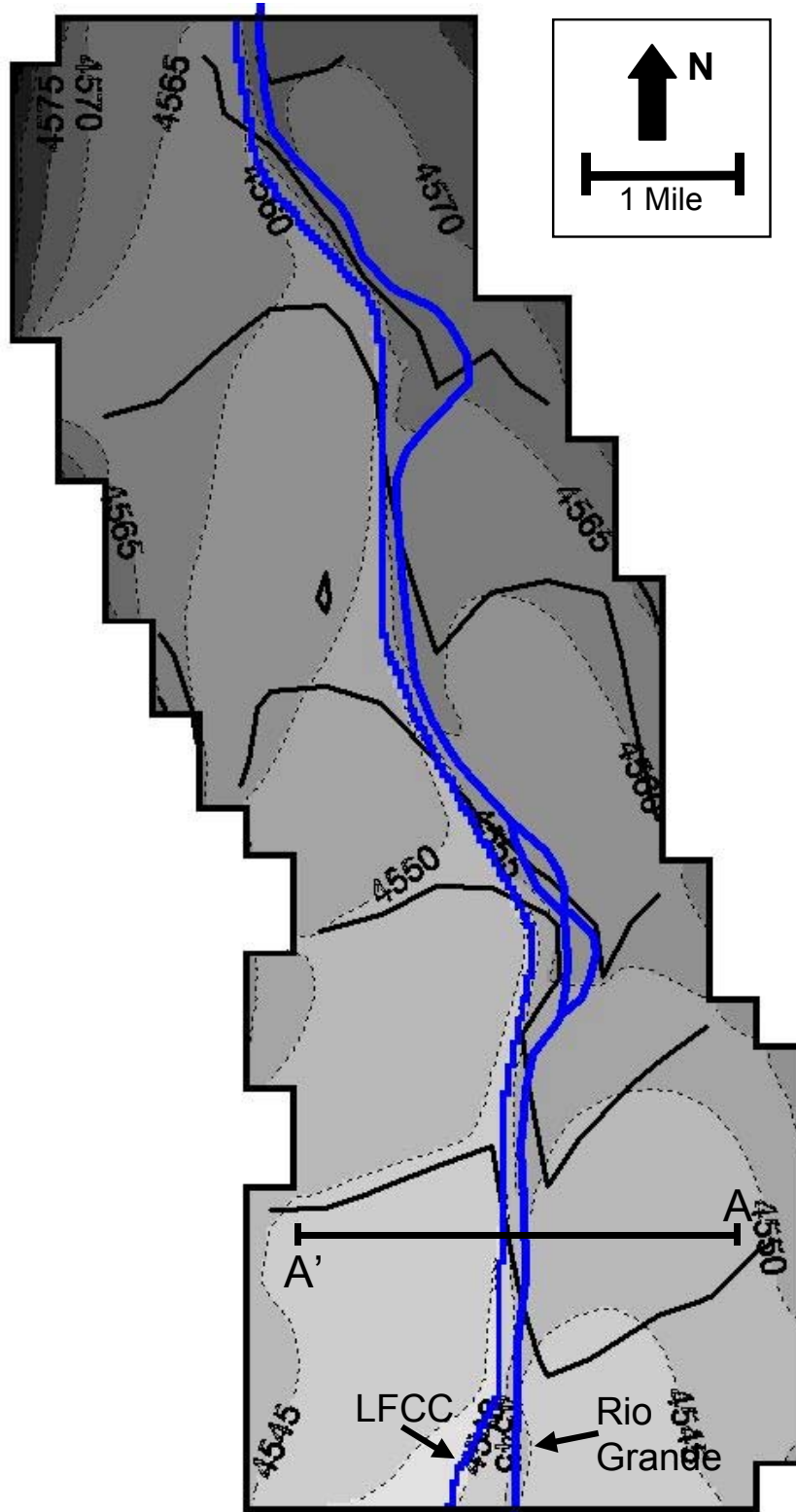


Figure 4-24: Simulated water table maps generated by telescopic (dashed) and regional (solid) models.

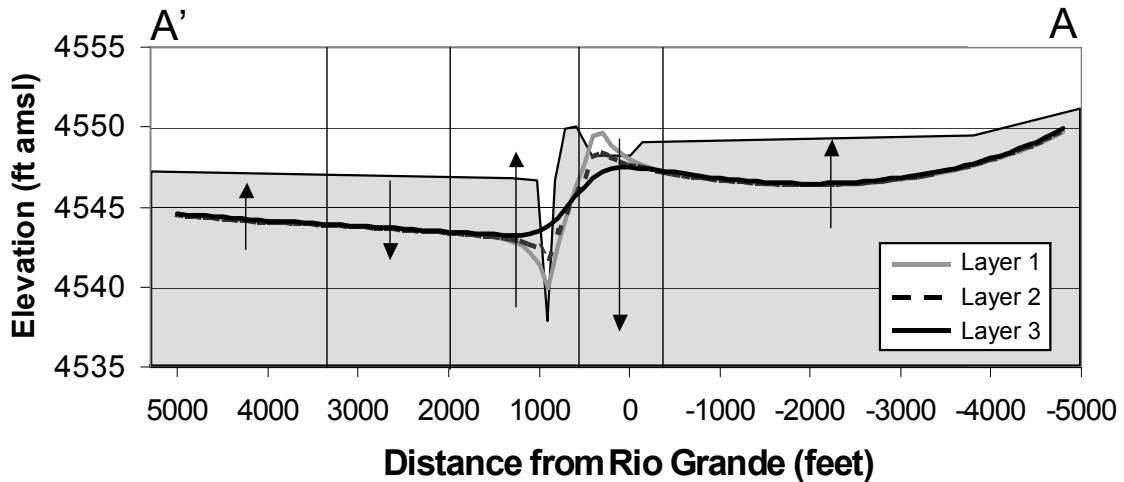


Figure 4-25: Cross-sectional view of water table elevations in Layers 1, 2, and 3 showing vertical gradients.

conditions. Field acquired seepage into the LFCC ranged from -6.1 to -8.0 cfs/mile (-1.7×10^{-1} and -2.3×10^{-1} $m^3/s/mile$). Steady-state model results for river and LFCC seepage were 7.8 cfs/mile (2.2×10^{-1} $m^3/s/mile$) and -7.4 cfs/mile (-2.1×10^{-1} $m^3/s/mile$), respectively. These values were within the ranges of the field data.

The steady-state model predicted river seepage of $34,037$ af/yr (4.2×10^7 m^3/yr) and net boundary inflow of $6,052$ af/yr (7.5×10^6 m^3/yr) (Table 4-3). Net boundary flows were flux values through the perimeter of the model. The model

Groundwater Inputs	af/yr	m^3/yr
River seepage	34,037	4.2E+07
Net boundary inflow	6,052	7.5E+06
TOTAL IN	40,089	4.9E+07
Groundwater Outputs		
LFCC seepage	31,930	3.9E+07
Evapotranspiration	8,191	1.0E+07
TOTAL OUT	40,121	4.9E+07
IN - OUT	-33	-4.0E+04

Table 4-3: Predicted groundwater inputs and outputs of the steady-state model.

predicted LFCC seepage of $-31,930$ af/yr (-3.9×10^7 m³/yr) and evapotranspiration from riparian vegetation and sandbars of $8,191$ af/yr (1.0×10^7 m³/yr). The difference between inputs and outputs was a -33 af/yr (-4.1×10^4 m³/yr) loss to the system. This was approximately 0.08 percent of the total water budget.

Simulated and observed head data collected in May 2003 are displayed in Figure 4-26. Root mean squared (RMS) and R-squared values of residuals were 5.22 feet (1.59 m) and 0.97, respectively, and indicated good correlation between the observed and simulated data. RMS is a measurement of difference between

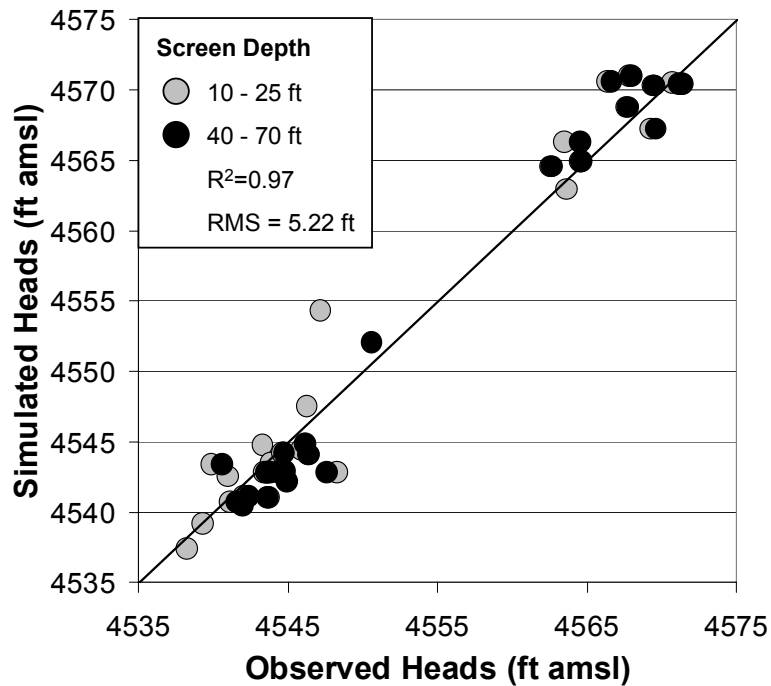


Figure 4-26: Observed and simulated heads for the steady-state model.

simulated and observed head elevations and was calculated using the equation,

$$RMS = \sqrt{\frac{1}{N} \sum_{1}^{N} (\text{obs} - \text{sim})^2}$$

where obs was the observed head elevation, sim was simulated head elevation, and N was the total number of points monitored in the system. For the steady-state model, RMS value calculations indicated that simulated heads are an average of 5.22 feet (1.59 m) different than observed heads. Measured seasonal fluctuations in water level elevations in ten BOR wells during 2002 had an RMS value of 2.6 feet (0.8 m). The larger RMS value observed for the steady-state model was an effect of using regional model input for the perimeter of the telescopic model. The regional model was calibrated using historical water level data spanning several decades and simulated slightly higher water levels than the telescopic model. The steady-state telescopic model was calibrated using water level data from October 2001 to August 2003, a period of drought. Also, May 2003 aquifer levels were lower than wintertime water levels that were simulated with the telescopic model. Measured wintertime water elevations were not used because May 2003 was the first month that a full dataset was available for the study area. At the time of publication, complete datasets were available only for the months of May 2003 through October 2003.

4.4 TRANSIENT-STATE MODEL

The transient model was run for two years with a time step of three days. Each stress period was set at one month (ten time steps) to facilitate inclusion of seasonal fluctuations in river stage and riparian evapotranspiration. Monthly field data from BOR wells at cross-sections 87.62 and 91.28 collected October 2001 through August 2003 were used to calibrate the model. Output heads generated by the steady-state model were used as initial head values for the

transient model. Aquifer and streambed properties applied in the steady-state telescopic model were maintained in the transient model. Riparian evapotranspiration and Rio Grande stage varied according to seasonal fluctuations (discussed in Chapters 4.2.3 and 4.2.4).

The irrigation season extended from the beginning of March through the end of October and was represented by activation of agricultural canals and drains to the west of the LFCC. It was assumed that the majority of crop irrigation did not begin until approximately one month after water became available. Because of this, a flood irrigation recharge factor of one af/yr was applied only during the months of April through October.

Observed water levels were compared to simulated data at ten well locations within the domain. Three plots of simulated versus observed head values were selected to show a representation of trends throughout the floodplain east of the river (well W-91.28-1), west of the LFCC (well W-91.28-4), and far west of the LFCC (well W-Perini) (Figure 4-1). Simulated water levels were consistently higher than observed levels because initial head values for the transient-state model were taken from output of the steady-state model simulation. Final calibration was achieved by making minor changes to river stage for each stress period until the hydrograph fluctuations matched in character and magnitude (Figure 4-27). The sharp changes observed in

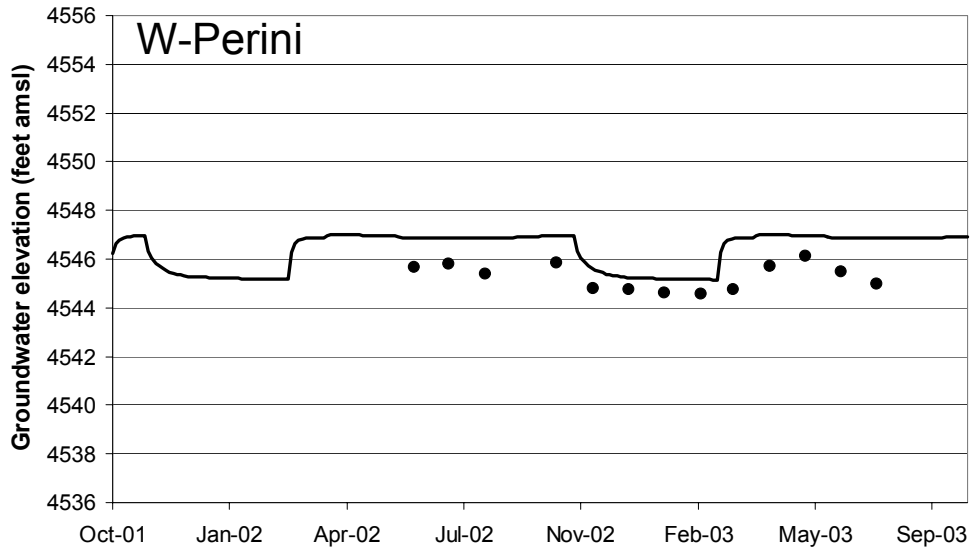
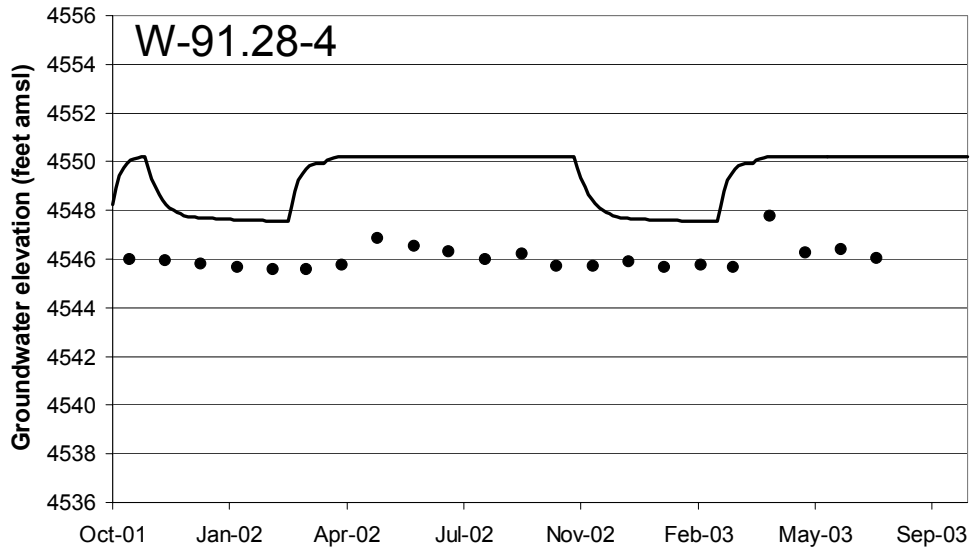
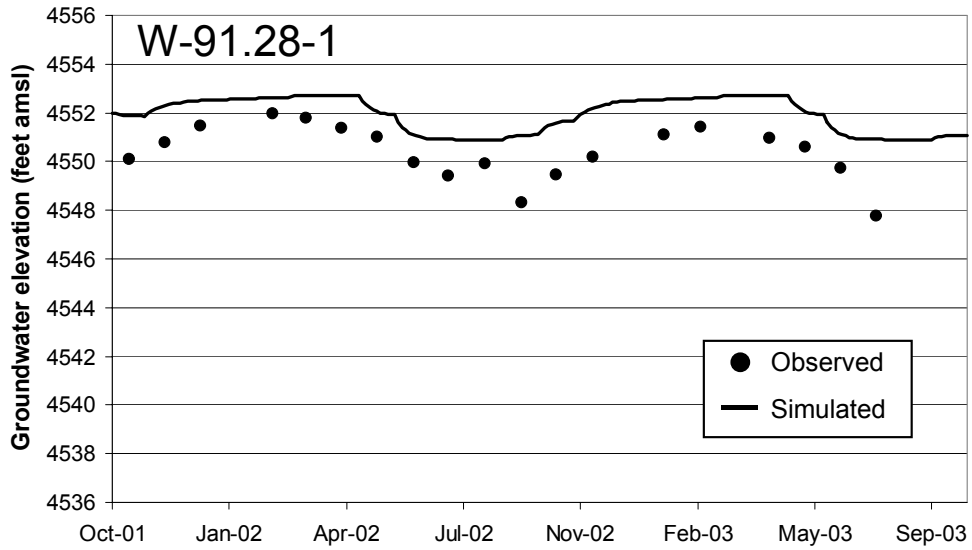


Figure 4-27: Simulated and observed heads at cross-section 91.28 and well W-Perini.

simulated water level elevation data were a result of stage and riparian evapotranspiration rate fluctuations and could have been reduced with the use of a shorter stress period (less than one month).

Transient-state simulated values of seepage were three percent lower than steady-state values (Table 4-4). Net boundary influx also decreased by 57 percent in the transient model. LFCC seepage increased by nine percent in the transient model run along with total evapotranspiration losses that increased by 21 percent. These changes in balance to the hydrologic system were caused by the application of crop irrigation (April through October) and the presence of water in agricultural drains and canals (March through October). Total inputs minus total outputs equaled a water budget in excess of 375 af/yr (4.6×10^{-5} m³/yr), 0.8 percent of the total inputs.

Groundwater Inputs	af/yr	m ³ /yr
River seepage	33,144	4.1E+07
Recharge	1,678	2.1E+06
Drains	7,602	9.4E+06
Net boundary influx	2,619	3.2E+06
TOTAL IN	45,043	5.6E+07
Groundwater Outputs		
LFCC seepage	34,729	4.3E+07
Evapotranspiration	9,939	1.2E+07
TOTAL OUT	44,668	5.5E+07
IN - OUT	375	4.6E+05

Table 4-4: Inputs and outputs to the water budget expressed as annual averages.

A time series plot of Rio Grande and LFCC seepage showed that the two surface water bodies were directly connected (Figure 4-28). When Rio Grande loss decreased, LFCC gains also decreased. Both observed higher losses between the months of April through October than in the winter months. Effects

of evapotranspiration were observed during the months of April through October when rates increased significantly (Figure 4-29).

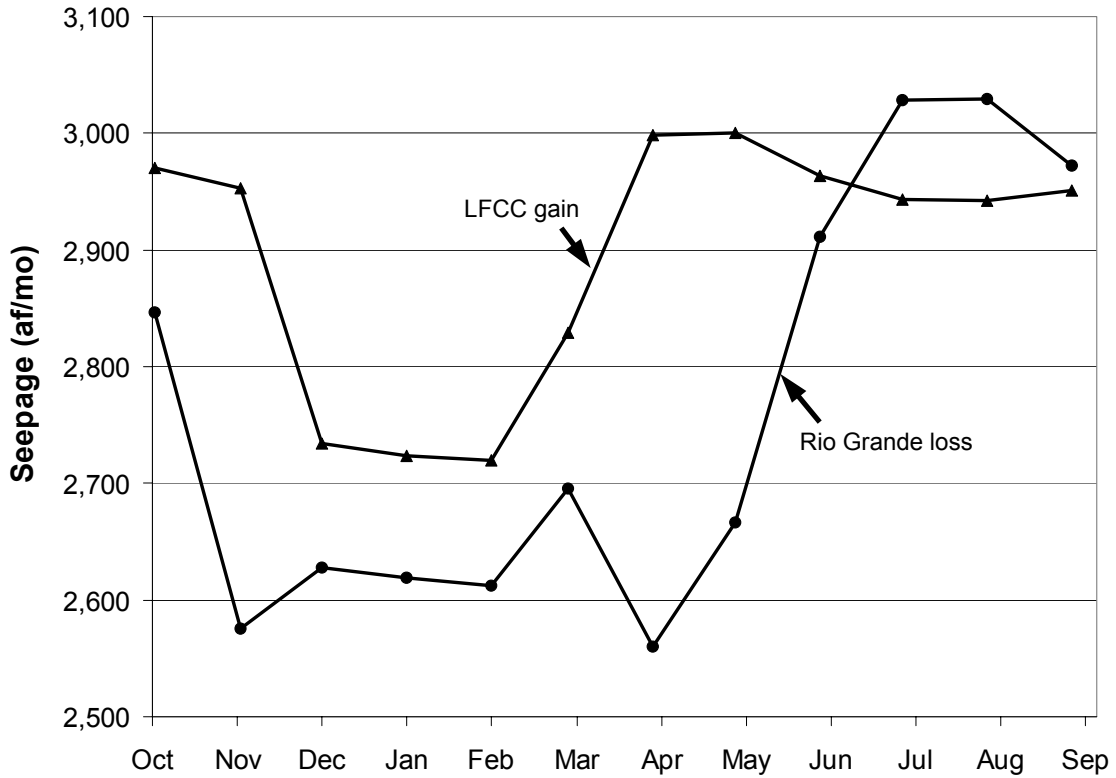


Figure 4-28: Simulated monthly average Rio Grande loss and LFCC gain for one year.

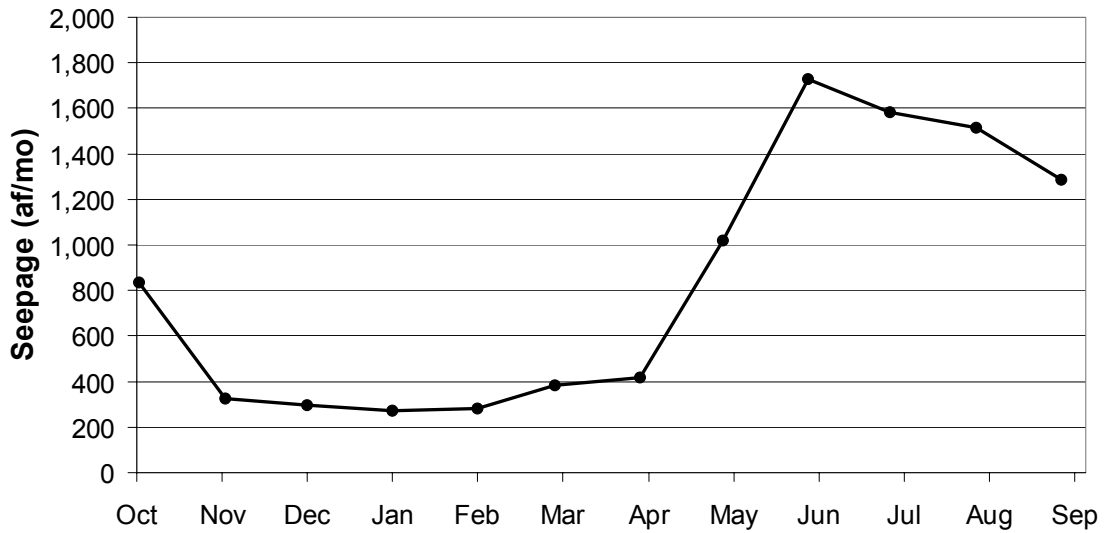


Figure 4-29: Simulated losses from the system due to evapotranspiration.

5. SENSITIVITY ANALYSES

Several assumptions were made during the geologic characterization for the telescopic model including:

- Three distinct geologic units of differing hydraulic properties existed.
- A continuous layer of lower permeability and conductivity sediment was located at approximately 30 feet (9 m) depth with constant thickness of two feet (0.6 m). It separated the upper and lower aquifers.
- Sediments underlying and between the LFCC and the Rio Grande possessed the same hydrologic characteristics as the surrounding valley alluvium.

These assumptions suggested that deeper screen wells (layer three) should display characteristics of a confined aquifer, as pump test results in Chapter 4.1.4 implied. Steady-state simulations were conducted to test assumptions about composition of the subsurface geology including changes in anisotropy and hydraulic conductivity. The first simulation tested effects of homogeneous and anisotropic sediments over the entire depth. The second displayed changes made to the system when the aquifer is heterogeneous and isotropic. Finally, the third simulation compared water level elevations in an anisotropic and heterogeneous aquifer with various hydraulic conductivity values.

5.1 HOMOGENEOUS ANISOTROPIC HYDROSTRATIGRAPHY

The first simulation tested the effects of the confining layer on water elevations by changing the vertical and horizontal hydraulic conductivities of layer 2 to match that of layers 1 and 3. This created a one-layer anisotropic and homogeneous model with horizontal and vertical hydraulic conductivities of 100 and 50 feet/day (31 and 15 m/d), respectively. All other inputs to the model remained constant from the initial steady-state run presented in Chapter 4.3.

Analysis of results produced elevated Rio Grande and LFCC seepage values compared to the original steady-state run, with increases in river loss and LFCC gains each by 4.4 cfs/mile ($1.3 \times 10^{-1} \text{ m}^3/\text{s}/\text{mile}$). Aquifer gains attributed to Rio Grande seepage and net boundary flux increased by 55 and 7 percent, respectively. Losses from the aquifer due to the LFCC and evapotranspiration increased by 60 and 2 percent, respectively. Total inflows minus total outflows equaled a difference of -92 af/yr ($-1.1 \times 10^5 \text{ m}^3/\text{yr}$), or 0.2 percent of the total inflows (Table 5-1).

Groundwater Inputs	af/yr	m ³ /yr
River seepage	52,864	6.5E+07
Net boundary influx	6,446	8.0E+06
TOTAL IN	59,310	7.3E+07
Groundwater Outputs		
LFCC seepage	51,056	6.3E+07
Evapotranspiration	8,346	1.0E+07
TOTAL OUT	59,402	7.3E+07
IN - OUT	-92	-1.1E+05

Table 5-1: Steady-state water budget for the telescopic model with homogeneous geology.

Water table maps and cross-sections of the homogeneous geology simulation compared with the initial steady-state map showed increased water elevations to the east of the Rio Grande and decreased elevations to the west (Figures 5-1 and 5-2). These patterns were attributed to the increased

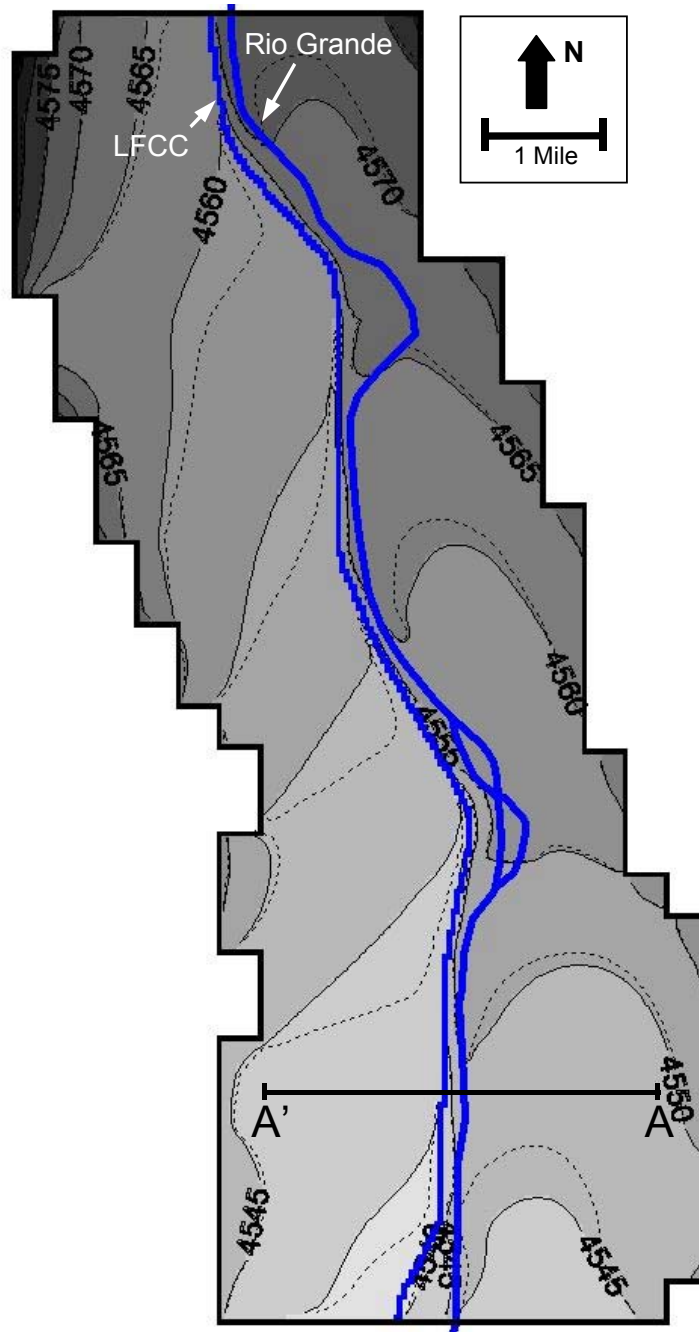


Figure 5-1: Simulated steady-state water table maps with homogeneous (solid) and heterogeneous (dashed) models.

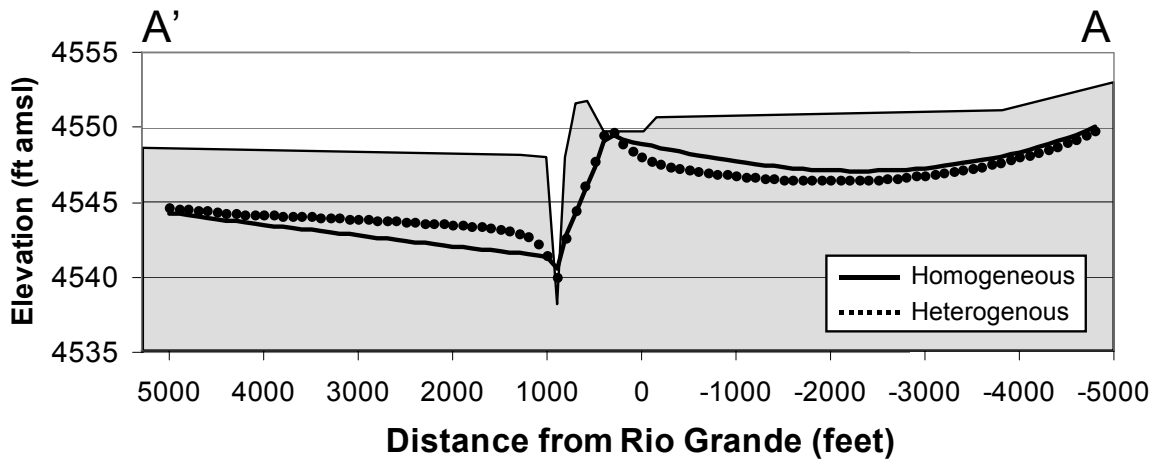


Figure 5-2: Cross-section of water level elevations at row 260 with simulations of homogeneous (solid) and heterogeneous (dashed) geology.

vertical connection between layers 1 and 3 in the absence of the clay layer. To the east of the Rio Grande, elevated water levels may have been a result of increased seepage from the river into the shallow aquifer. Decreased elevations to the west of the river were attributed to increased seepage from the shallow aquifer into the LFCC. Vertical gradients were plus or minus less than 0.1 foot (0.3 cm) with the exception of the region directly beneath the LFCC and Rio Grande channels.

A plot of simulated vs. observed heads for the homogeneous model suggested a good correlation between the two datasets with a root mean squared value of 5.57 feet (1.70 m) and an R-squared value of 0.97 (Figure 5-3). An RMS value of 5.57 feet indicated that simulated water levels for the homogeneous model (steady-state) were an average of 5.57 feet different than observed levels (measured in May 2003). This was 0.35 feet (1 cm) more different than the steady-state model run from Chapter 4.3 where the RMS value was 5.22 feet (1.59 m). This implies that simulated aquifer water level elevations were an average of 0.35 feet higher in the absence of the clay layer.

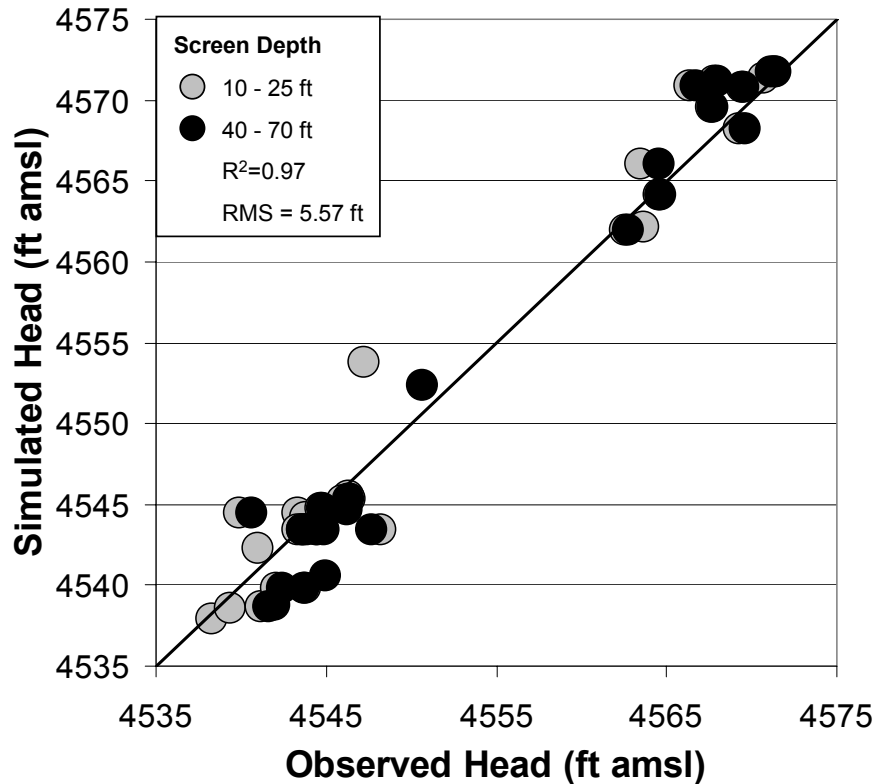


Figure 5-3: Steady-state simulated vs. observed water level elevations for the model with homogeneous geology.

In summary, the telescopic model was highly sensitive to changes in vertical connectivity between layers 1, 2, and 3. LFCC and Rio Grande seepage was also largely affected when the clay layer was removed from the system with changes in aquifer gain and loss of more than 55 percent.

5.2 HETEROGENOUS ISOTROPIC HYDROSTRATIGRAPHY

An isotropic and heterogeneous model was constructed to compare effects of anisotropy on the groundwater and surface water systems. Horizontal and vertical hydraulic conductivities for layers 1 and 3 were 100 feet/day (31 m/d), and 2 feet/day (0.6 m/d) for layer 2. All other inputs to the model were unchanged from the initial steady-state run presented in Chapter 4.3.

Results from the isotropic and homogeneous model simulations were similar, with slightly less magnitude of change observed with the isotropic model. Aquifer gains from the Rio Grande and net boundary flux increased by 47 and 4 percent, respectively, from the initial steady-state run. Groundwater outputs via the LFCC and evapotranspiration increased by 51 and 2 percent, respectively. Total inflows minus total outflows equaled a difference of -53 af/yr ($-6.5 \times 10^4 \text{ m}^3/\text{yr}$), or 0.09 percent of the total inflows (Table 5-2).

Groundwater Inputs	af/yr	m^3/yr
River seepage	50,113	6.2E+07
Net boundary influx	6,310	7.8E+06
TOTAL IN	56,423	7.0E+07
Groundwater Outputs		
LFCC seepage	48,161	5.9E+07
Evapotranspiration	8,315	1.0E+07
TOTAL OUT	56,476	7.0E+07
IN - OUT	-53	-6.5E+04

Table 5-2: Steady-state water budget for the telescopic model with isotropic geology.

Contour maps of water level elevation under isotropic conditions showed similar trends as the homogenous geology simulation (Figure 5-4). Water levels were elevated to the east of the Rio Grande and depressed to the west of the LFCC. These effects were due to the increased vertical connection within the shallow aquifer and supported results of the simulation in Chapter 5.1, where removal of the clay layer resulted in similar trends. Vertical gradients were also on the order of plus or minus 0.1 feet (3 cm). Total flow through the system increased by 41 percent.

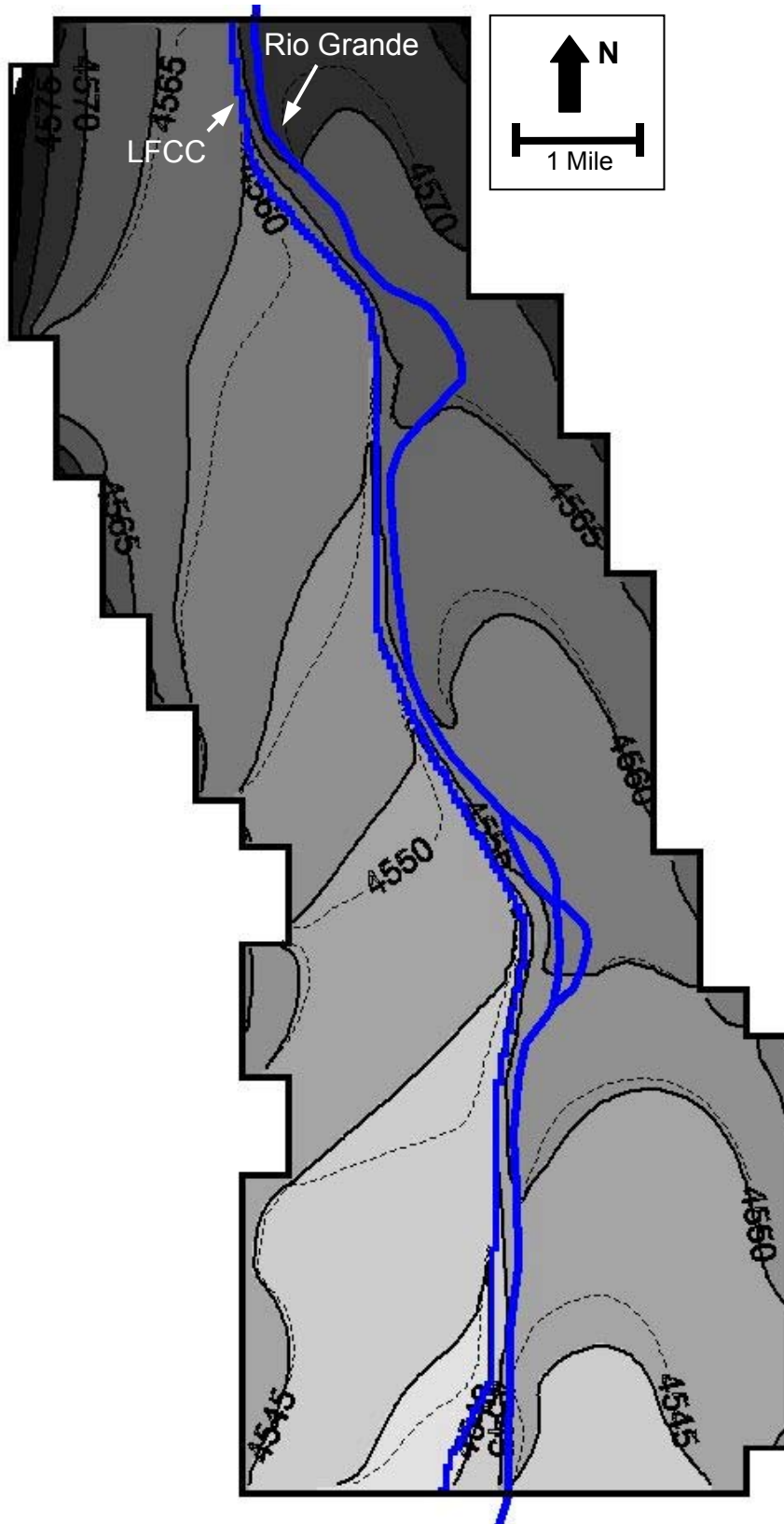


Figure 5-4: Simulated steady-state water table maps with isotropic (solid) and anisotropic (dashed) models.

5.3 ALTERATIONS TO HYDRAULIC CONDUCTIVITY

Simulations were conducted to observe effects of changes to hydraulic conductivity in a heterogeneous and anisotropic aquifer. This analysis was necessary because of the wide range of values obtained from aquifer tests at well W-Sichler and well HWY-W08EX (35 to 240 ft/d or 11 to 73 m/d).

Horizontal and vertical hydraulic conductivity were decreased by half (50 and 25 ft/d or 15 and 8 m/d, respectively) for layers 1 and 3 within the entire model, simulating values closer to those obtained from the aquifer test at Highway 380. These results were compared to water level elevations simulated with horizontal and vertical hydraulic conductivity values at two times the original value (200 and 100 ft/d or 60 and 30 m/d, respectively), more accurately representing values obtained from the aquifer test at well W-Sichler. Layer 2 horizontal and vertical hydraulic conductivity values were left unchanged at two and 0.1 feet/day (3.1×10^{-2} m/d), respectively, for both models.

Model results with decreased conductivity values yielded 34 and 40 percent declines in river and LFCC seepage, respectively. When hydraulic conductivity values were doubled, river and LFCC seepage rates increased by 50 and 61 percent, respectively. This suggested that the model was sensitive to changes in aquifer properties and that simulation accuracy could be improved with further stratigraphic analysis. The total water budget of Rio Grande seepage and net boundary gains minus LFCC and evapotranspiration loss equaled -86 af/yr (-1.1×10^5 m³/yr) for the decreased hydraulic conductivity model and -5 af/yr (-6.2×10^3 m³/yr) for the increased hydraulic conductivity

model (Table 5-3).

	1/2 K		2X K	
	af/yr	m ³ /yr	af/yr	m ³ /yr
Groundwater Inputs				
River seepage	22,360	2.8E+07	51,073	6.3E+07
Net boundary influx	4,121	5.1E+06	9,162	1.1E+07
TOTAL IN	26,481	3.3E+07	60,235	7.4E+07
Groundwater Outputs				
LFCC seepage	19,202	2.4E+07	51,477	6.3E+07
Evapotranspiration	7,365	9.1E+06	8,763	1.1E+07
TOTAL OUT	26,567	3.3E+07	60,240	7.4E+07
IN - OUT	-86	-1.1E+05	-5	-6.2E+03

Table 5-3: Steady-state water budget for the telescopic model with altered hydraulic conductivity values.

Water table elevations in the domain were decreased with lower hydraulic conductivities of layers one and three (Figures 5-5 and 5-6). Less change was observed at the boundaries of the model although this was likely caused by higher initial water level elevations prescribed for the model perimeter that were based on the regional model steady-state water table. Cross sections of water level elevations in layers 1, 2, and 3 at row 260 showed vertical gradients at a maximum near the LFCC and Rio Grande (Figure 5-7). Upward flow was in areas of dense riparian evapotranspiration and discharge from the LFCC and downward flow was in areas of zero evapotranspiration and recharge from the Rio Grande.

A linear relationship was observed between evapotranspiration, net boundary flux, and hydraulic conductivity (Figure 5-8). LFCC and Rio Grande seepage display similar trends with changes in hydraulic conductivity with slightly higher seepage values when hydraulic conductivity is 100 feet/day (31 m).

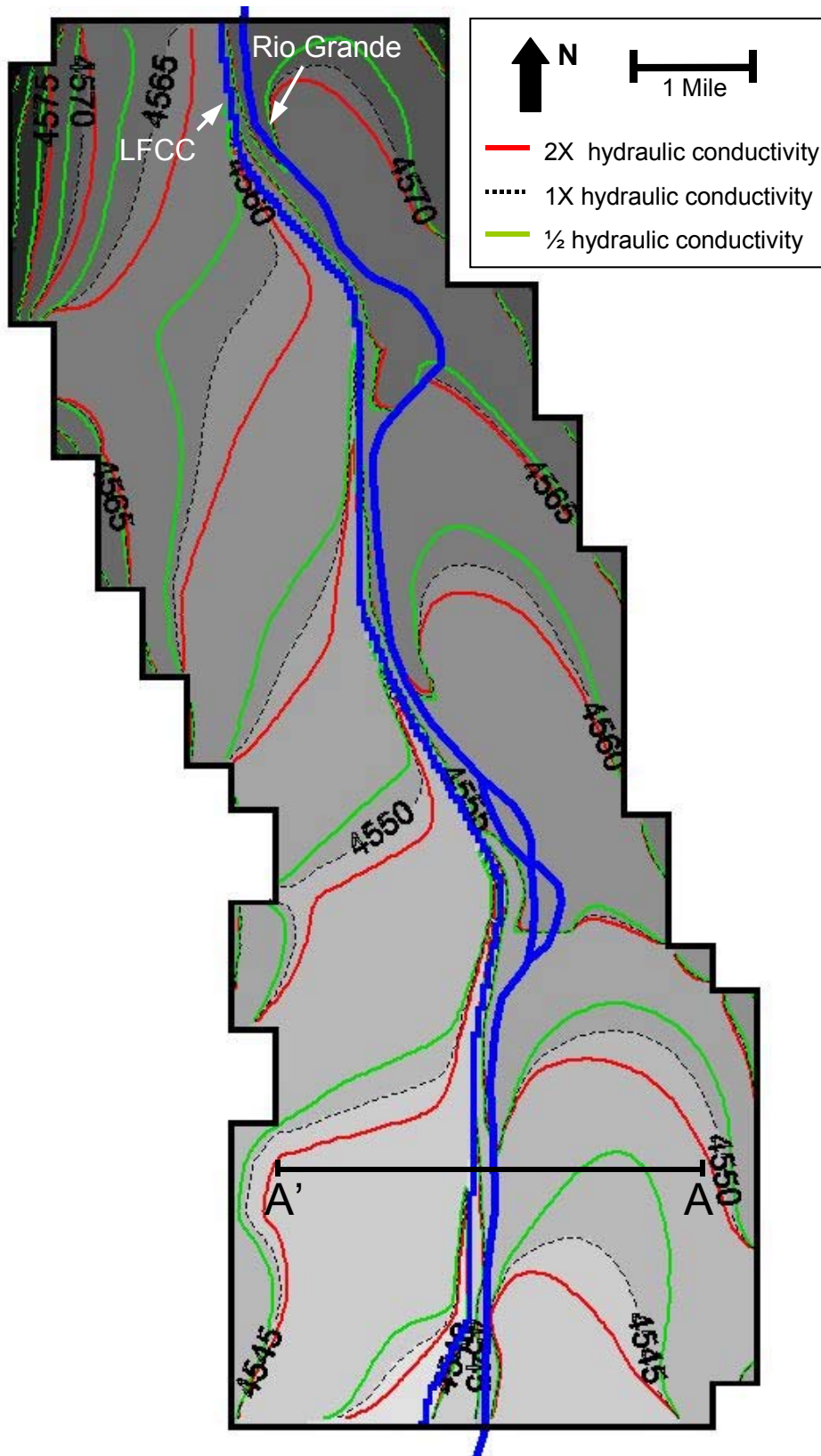


Figure 5-5: Simulated water table map using decreased (green), increased (red), and initial (dashed) values of hydraulic conductivity.

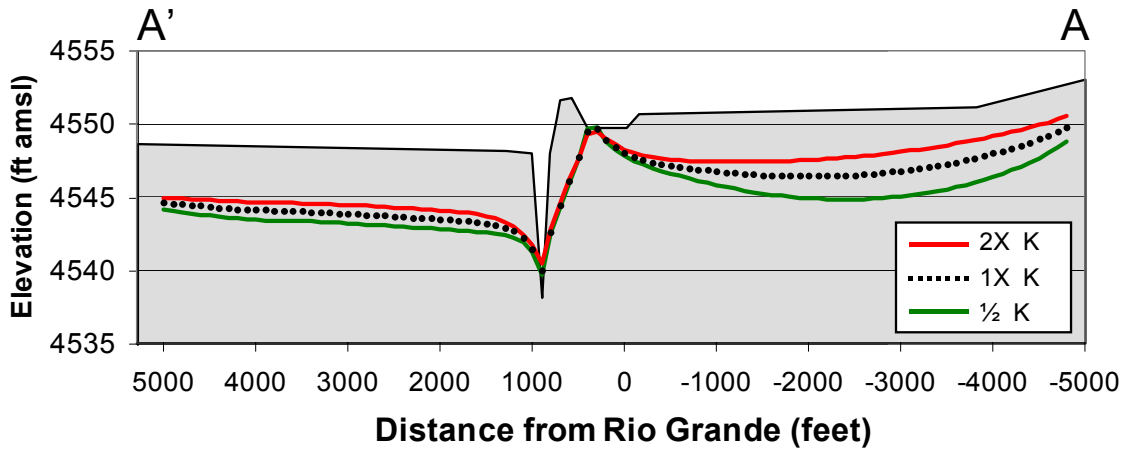


Figure 5-6: Cross-section of water level elevations at row 260 with simulations of decreased (green), increased (red), and initial (dashed) values of hydraulic conductivity.

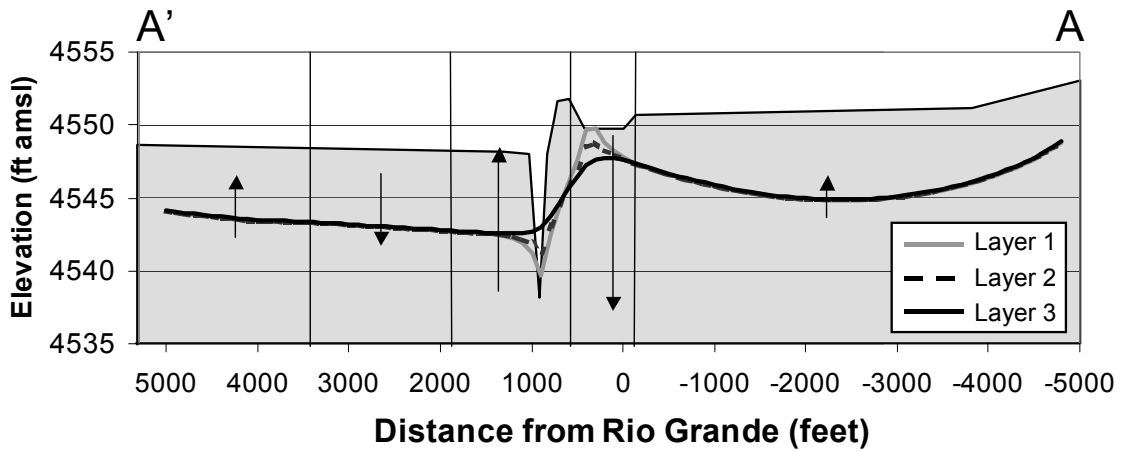


Figure 5-7: Cross-section of water level elevations in layers 1, 2, and 3 at row 260 when hydraulic conductivities of the sediments are decreased by one half.

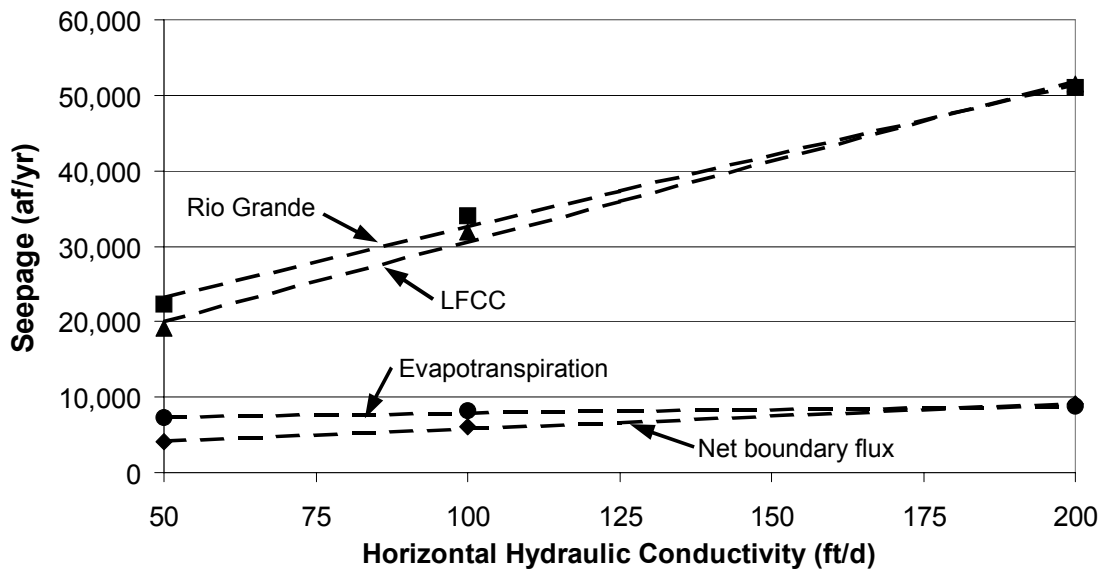


Figure 5-8: Seepage response to changes in hydraulic conductivity.

A plot of simulated versus observed heads for the model with decreased hydraulic conductivity in layers 1 and 3 suggested good correlation with a root mean squared value of 5.18 feet (1.58 m) and an R-squared value of 0.97 (Figure 5-9). A 5.18-foot RMS value indicated that simulated water level elevations were an average of 5.18 feet different than observed levels.

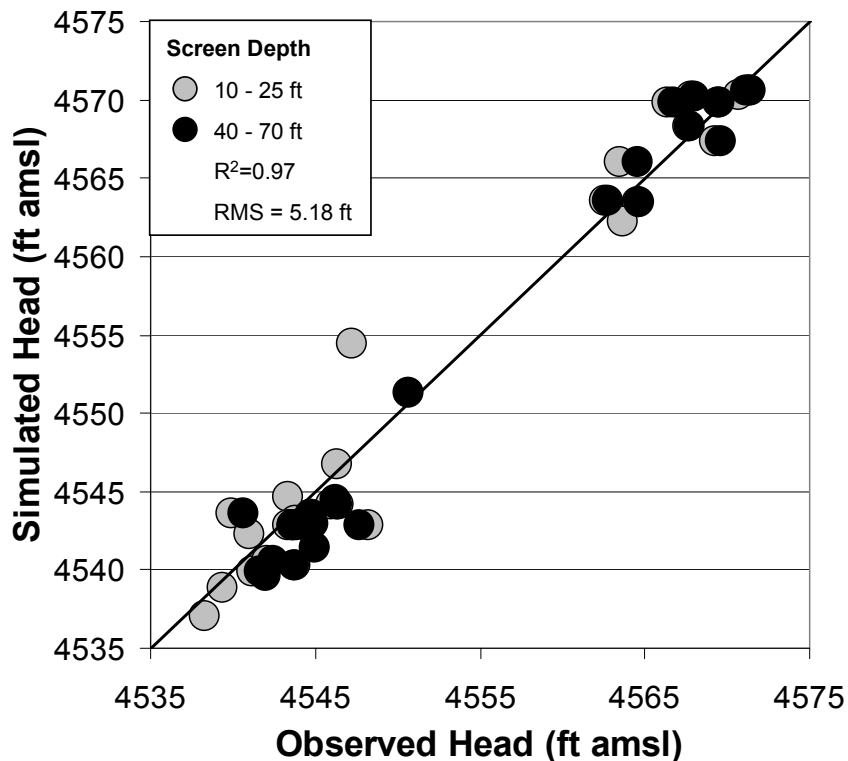


Figure 5-9: Steady-state simulated vs. observed water level elevations for the model with decreased hydraulic conductivity.

In conclusion, the system was found to be responsive to changes in hydraulic conductivity of subsurface sediments when anisotropy ratios remain consistent with the initial steady state run. Total flow through the system was decreased by 34 percent for the simulation with $\frac{1}{2}$ hydraulic conductivity and increased by 50 percent for the simulation with twice the value of hydraulic conductivity. These percentages implied that changes in hydraulic conductivity

cause less effect in the system than the simulations of Chapters 5.1 where total flow through the system increased by more than 55 percent.

6. MANAGEMENT ALTERNATIVES

6.1 EVALUATION OF THE SYSTEM PRIOR TO THE LFCC

6.1.1 Steady-state

A steady-state run of the model was conducted with no LFCC present. Surface water cells included in the river package were from the Rio Grande present day channel location and were assigned a constant stage value of two feet (0.6 m). Analysis of the steady-state results yielded a decrease in seepage from the Rio Grande of 76 percent. Net boundary flux decreased by 62 percent. Losses to evapotranspiration increased by 27 percent, caused by higher water level elevations in the shallow aquifer. The water balance equated to a net flow of -35 af/yr (-4.3×10^4 m³/yr) out of the system, 0.3 percent of the inputs (Table 6-1).

Groundwater Inputs	af/yr	m ³ /yr
River seepage	8,093	1.0E+07
Net boundary influx	2,273	2.8E+06
TOTAL IN	10,366	1.3E+07
Groundwater Outputs		
Evapotranspiration	10,401	1.3E+07
TOTAL OUT	10,401	1.3E+07
IN - OUT	-35	-4.3E+04

Table 6-1: Inputs and output to the system prior to LFCC construction.

A water table map and cross section generated with the Rio Grande as the only surface water system present (excluding the LFCC and irrigation canals and drains) yielded overall higher water levels within the floodplain than elevations generated with the initial steady-state model (Figures 6-1 and 6-2).

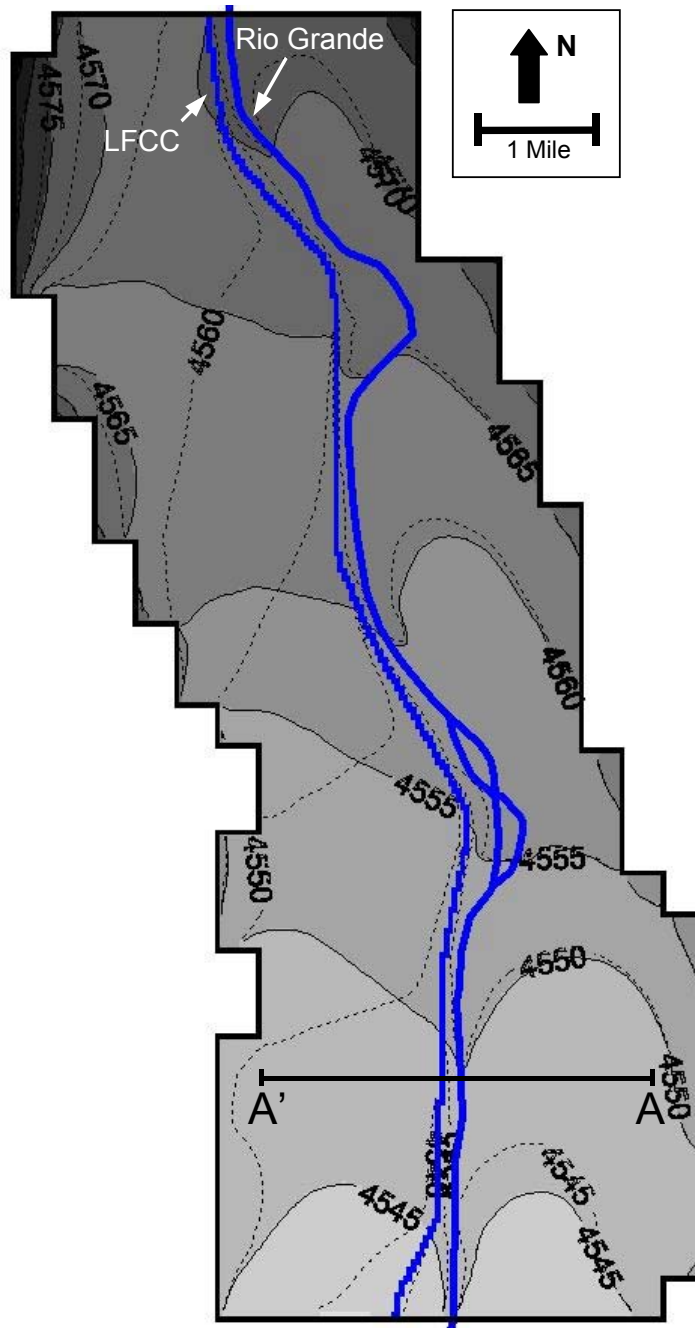


Figure 6-1: Simulated water table maps generated with (dashed) and without (solid) the presence of the LFCC.

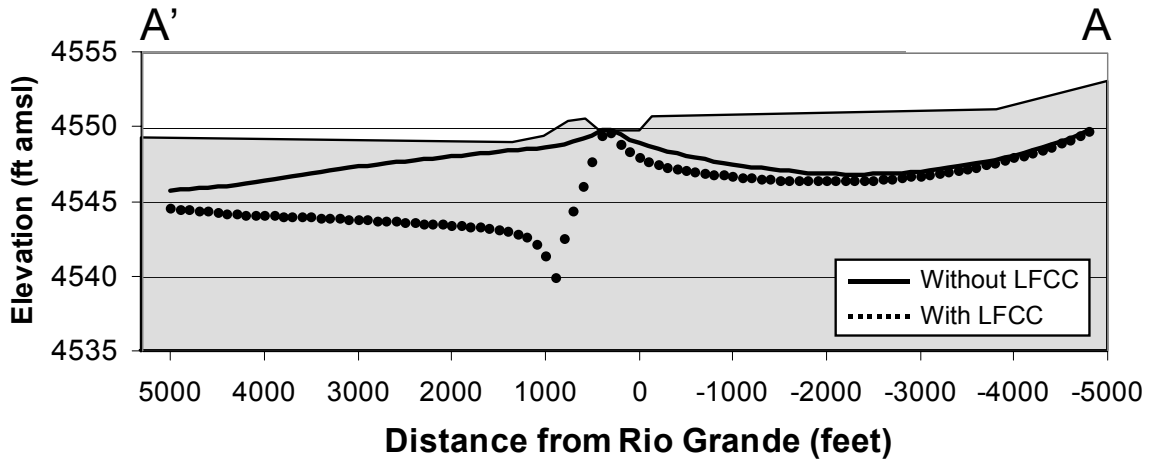


Figure 6-2: Cross-section of water level elevations at row 260 with (dashed) and without (solid) the presence of the LFCC.

This simulation showed that the Rio Grande recharged to the east and west and as distance from the Rio Grande increased, the magnitude of change in water level elevation decreased. Water level elevations in the floodplain to the west were significantly elevated in the absence of the LFCC with simulated values as much as 10 feet (3 meters) greater than those produced in the initial steady-state run. To the east of the river channel this change was not as extreme, but an increase in water elevations was still observed. The dampened response of water levels to the east from LFCC activity to the west was because of the hydrographic boundary produced by Rio Grande seepage. Vertical gradients were less than plus or minus 0.1 feet (3 cm), with the exception of directly beneath the river channel (Figure 6-3).

A plot of simulated versus observed heads indicated that average water level elevations in the study area were elevated when no LFCC was present (Figure 6-4). An RMS value of 9.19 feet (2.80 m) indicated that water elevations were an average of 3.97 feet (1.21 m) higher in the absence of the LFCC when compared to initial steady-state results.

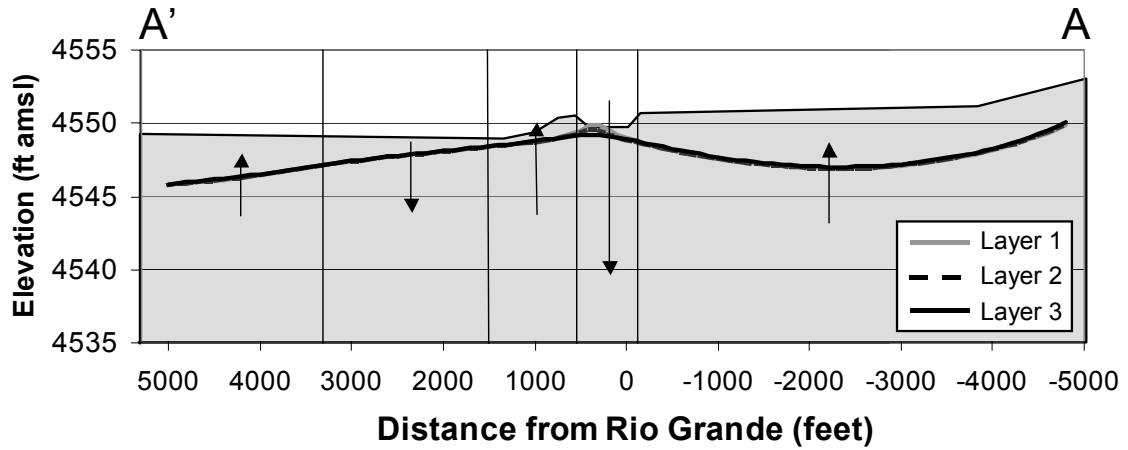


Figure 6-3: Cross-section of water level elevations in layers 1, 2, and 3 at row 260 in the absence of the LFCC.

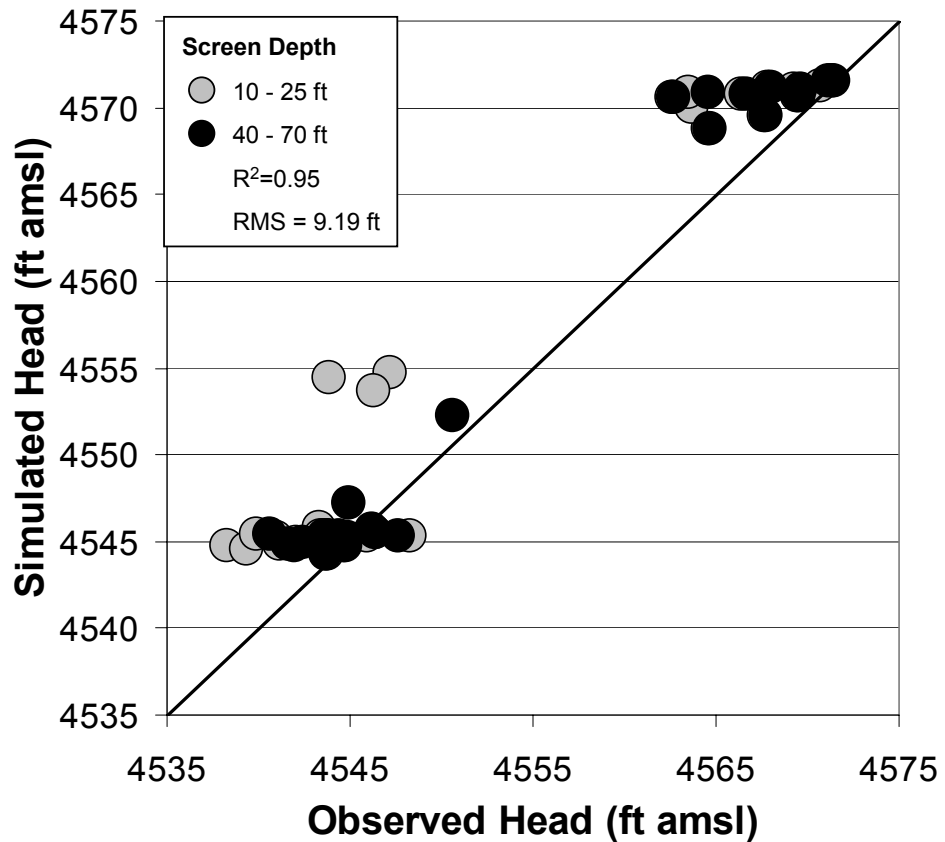


Figure 6-4: Steady-state observed and simulated heads in the absence of the LFCC.

6.1.2 Transient-state

A transient simulation was conducted to observe the hydrologic system over time with no LFCC present. Parameters that remained consistent with the initial transient model included crop recharge, Rio Grande stage and riparian evapotranspiration variations, and geologic discretization. Agricultural canals and drains except for the LFCC were included all with a constant stage value of two feet. Initial water level elevations for the model were taken from steady-state results presented in Chapter 6.1.1 where no LFCC was present.

The simulation produced water level elevations to the west that were higher than the transient run from Chapter 4.4 which included the LFCC (Figure 6-5). Water levels to the east at well W-91.28-1 showed an increase in elevation during the winter but decreased water levels in the summer compared to initial transient runs. Well W-87.62-3 was located 30 feet (9m) west of the present day LFCC location and showed an increase in water levels of five to eight feet (1.5 to 2.4 m). The pronounced step pattern in the hydrograph also indicated a more defined groundwater connection with the river in the absence of the LFCC. Well W-Perini, located near the western edge of the floodplain, exhibited the least change in water level elevations except for the months of November through March. Increased levels during these months indicated improved connection between the Rio Grande and the shallow aquifer to the west in the absence of the LFCC.

Results indicated that with no LFCC present, river seepage and net boundary influx decreased by 67 and 72 percent, respectively.

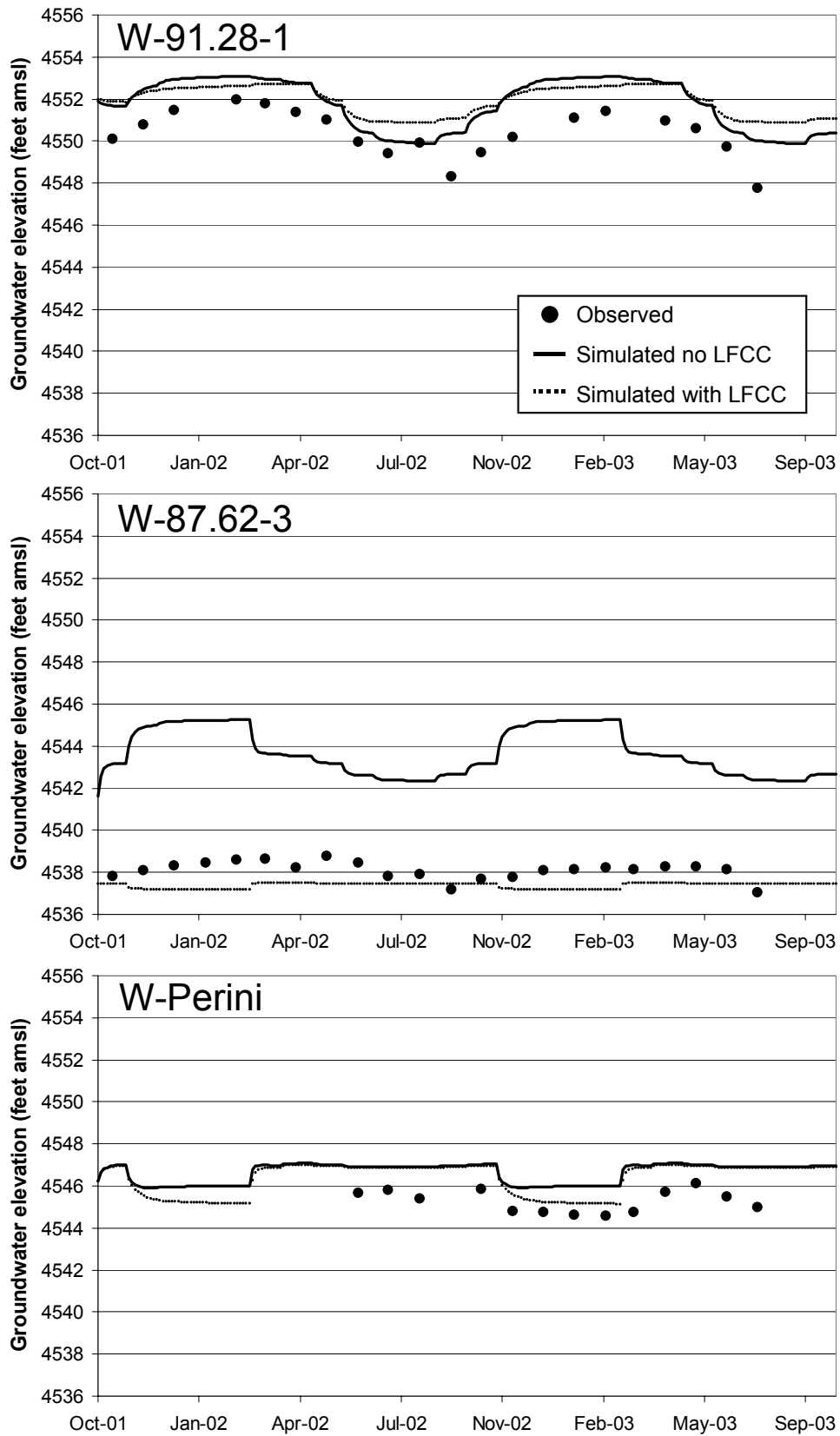


Figure 6-5: Transient-state observed and simulated water level elevations with (dashed) and without (solid) the presence of the LFCC.

Evapotranspiration increased by 8 percent due to elevated water levels in the shallow aquifer. Input to the aquifer from drains decreased by 138 percent, thus it was an output to the groundwater system with no LFCC present. Total inputs to the system minus total outputs equaled a deficit of 466 af/yr ($5.7 \times 10^5 \text{ m}^3/\text{yr}$) to the water budget (Table 6-2).

Groundwater Inputs	af/yr	m ³ /yr
River seepage	10,807	1.3E+07
Recharge	1,678	2.1E+06
Net boundary influx	733	9.0E+05
TOTAL IN	13,218	1.6E+07
Groundwater Outputs	af/yr	m ³ /yr
Drains	2,902	3.6E+06
Evapotranspiration	10,782	1.3E+07
TOTAL OUT	13,684	1.7E+07
IN - OUT	-466	-5.7E+05

Table 6-2: Inputs and outputs to the system in the absence of the LFCC.

A time series plot of river seepage with and without the LFCC present showed reduction in losses from the Rio Grande (Figure 6-6). Between the

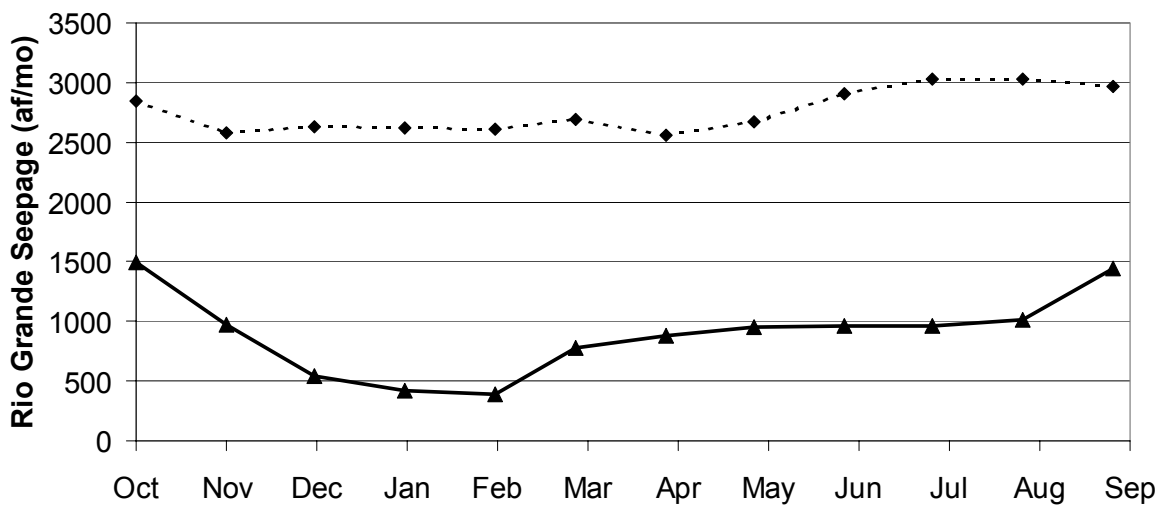


Figure 6-6: Time series plot of Rio Grande seepage loss with (dashed) and without (solid) the presence of the LFCC.

months of April and October, seepage loss values were elevated. In the winter, river leakage to the aquifer was approximately 6,000 af/yr ($7.4 \times 10^6 \text{ m}^3/\text{yr}$) less than in the summer. Rio Grande seepage also fluctuated by approximately 500 af/yr ($6.2 \times 10^5 \text{ m}^3/\text{yr}$) more in the absence of the LFCC than under present day conditions.

6.2 DECREASED RIPARIAN EVAPOTRANSPIRATION

In recent years several parties including the BDA NWR have put forth extensive effort and expense to control saltcedar and other non-native invasive vegetation (Tetra Tech Inc., 2003, p. vii). This has been done in hopes of restoring the ecosystem to a more natural state for resident wildlife and the overall health of the Rio Grande. Research conducted by Bawazir of New Mexico State University reported various evapotranspiration values for dense monotypic saltcedar and other vegetation types (2000). Some vegetation types were calculated to transpire approximately 20 percent less than monotypic saltcedar, however, it must be emphasized that these values were from established growth in various locations and not representative of a system that would be stripped of saltcedar and re-vegetated. Few studies have been published, to date, reporting percentages of decrease in evapotranspiration with saltcedar eradication and alternative species re-vegetation. For this reason, three management alternatives were evaluated with decreased rates of riparian evapotranspiration.

A steady-state model was created to evaluate the groundwater and surface water systems. Evapotranspiration values for riparian vegetation and

open ground applied in the initial steady-state run in Chapter 4.3 were decreased by 5, 20, and 50 percent. All other parameters remained the same as the initial steady state model.

For the model with a five percent decrease in evapotranspiration rate, losses from the Rio Grande and total flows through the system decreased by one percent (Table 6-3). Greater effect was observed when evapotranspiration rate was decreased by 20 percent with a two percent decrease in river seepage and a three percent decrease in total inputs and outputs. Largest effect was observed when evapotranspiration was decreased by 50 percent. This caused a six percent decrease in river seepage, a 21 percent decrease in net boundary flux, and a one percent increase in LFCC seepage. Total inputs and outputs to the system were decreased by eight percent. LFCC seepage was effected less by decreased values of riparian evapotranspiration rates than Rio Grande seepage because most of the riparian vegetation was located to the east of the river and this surface water body acted as a hydrologic boundary.

ET Reduction	5%		20%		50%	
Groundwater Inputs	af/yr	m ³ /yr	af/yr	m ³ /yr	af/yr	m ³ /yr
River seepage	33,841	4.2E+07	33,249	4.1E+07	31,956	3.9E+07
Net boundary influx	5,938	7.3E+06	5,600	6.9E+06	4,787	5.9E+06
TOTAL IN	39,779	4.9E+07	38,850	4.8E+07	36,743	4.5E+07
Groundwater Outputs						
LFCC seepage	31,969	3.9E+07	32,081	4.0E+07	32,364	4.0E+07
Evapotranspiration	7,835	9.7E+06	6,737	8.3E+06	4,415	5.4E+06
TOTAL OUT	39,804	4.9E+07	38,818	4.8E+07	36,779	4.5E+07
IN - OUT	-25	-3.1E+04	32	3.9E+04	-36	-4.4E+04

Table 6-3: Inputs and output to the system with decreased evapotranspiration rates.

Although it was not realistically possible for evapotranspiration rates to be decreased by 50 percent, it appeared that this was the only management alternative that would have made a significant impact on the system. Decreases in evapotranspiration by five and 20 percent did not show dramatic effects on Rio Grande seepage.

Water level elevations were slightly elevated with the reductions in evapotranspiration (Figures 6-7 and 6-8). More effect was observed to the east of the Rio Grande than to the west because riparian vegetation was denser (Figure 4-22).

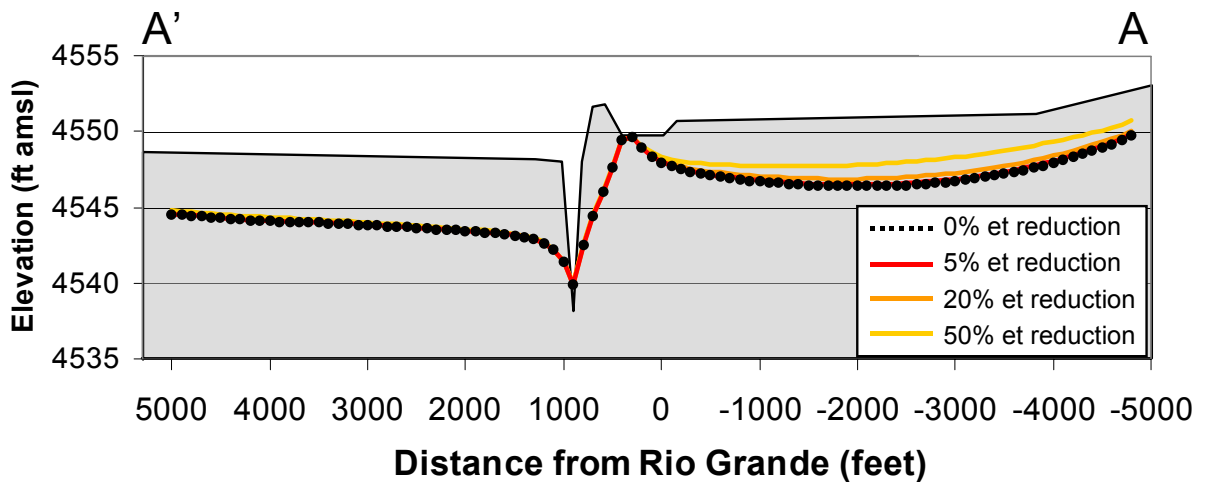


Figure 6-7: Cross-section of water level elevations at row 260 with varied rates of riparian evapotranspiration to the east of the Rio Grande.

A plot of observed versus simulated water level elevations for the model with 20 percent reduction in evapotranspiration rate produced a RMS value of 5.27 feet or 1.6 meters (Figure 6-9). This implied that water level elevations in the study area changed by an average of 0.5 feet (0.2 m). Most of the effect was observed to the east of the Rio Grande under riparian vegetation, and not in crop areas where it would bring great benefit to farmers.

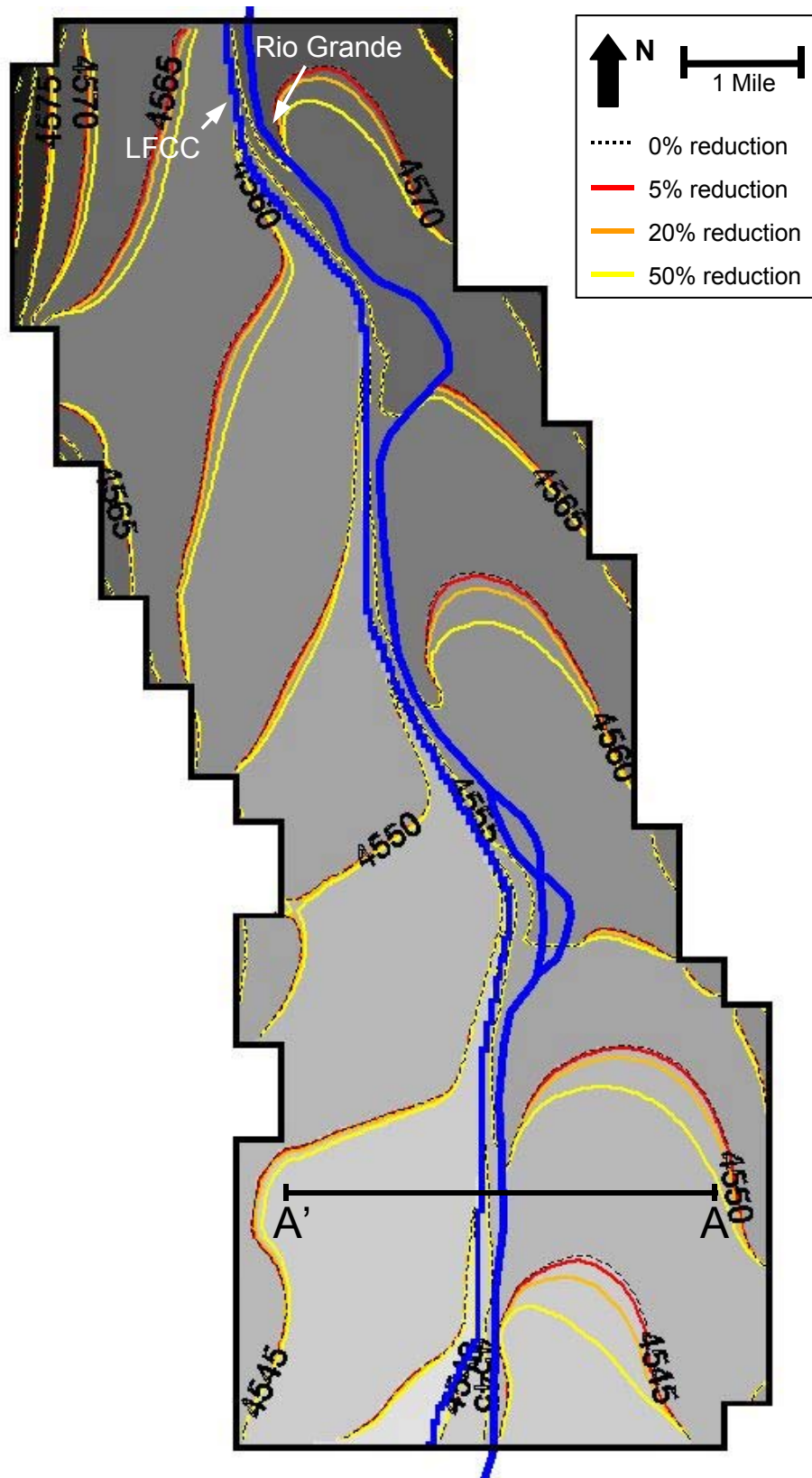


Figure 6-8: Simulated water table maps generated with decreased evapotranspiration rates.

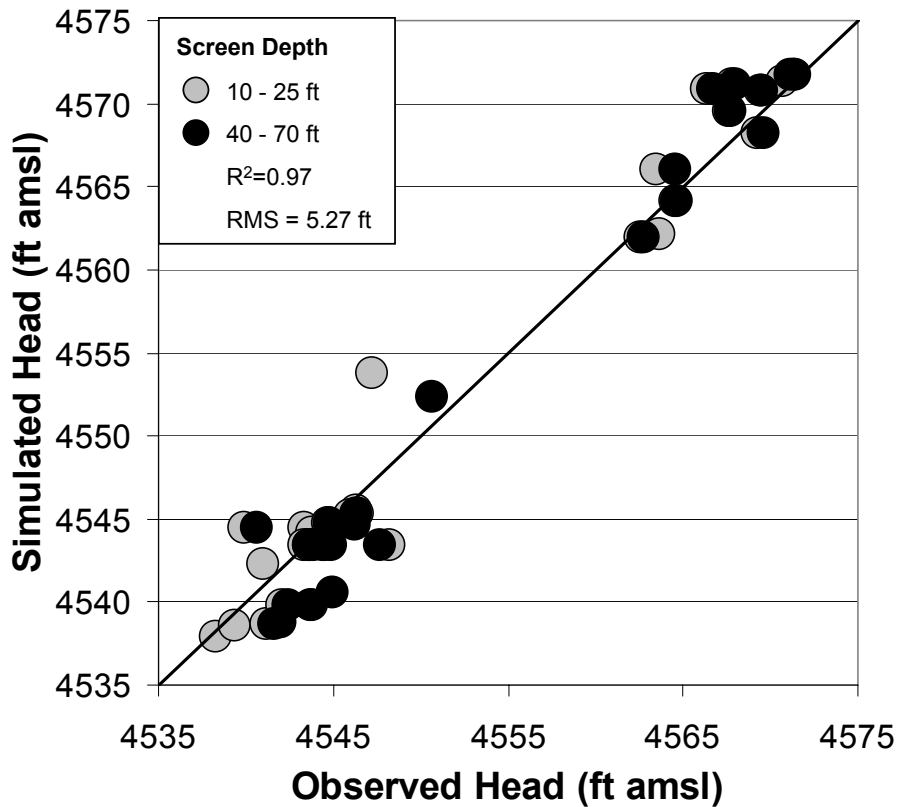


Figure 6-9: Steady-state observed and simulated water level elevations with 20 percent reduced evapotranspiration rate.

6.3 EVALUATION OF RELOCATION OF RIVER CHANNEL

Water table gradients between the LFCC and Rio Grande were steeper than those to the east of the Rio Grande or to the west of the LFCC (Figure 4-4). One possible management alternative for the Rio Grande was to shift the river channel further east in an effort to lessen the gradient and slow groundwater flow. It was hypothesized that widening of the channel would increase conveyance and restore the river to a more natural, pre-1950's state. Changes were made to the river between Neil Cupp and Highway 380. The change did not impede on any existing private structures that were farther east of the proposed location.

To simulate the system with a wider channel slightly shifted to the east, a new river file was created for the transient model (Figure 6-10). Input to the transient model was taken from the initial steady-state run (presented in Chapter

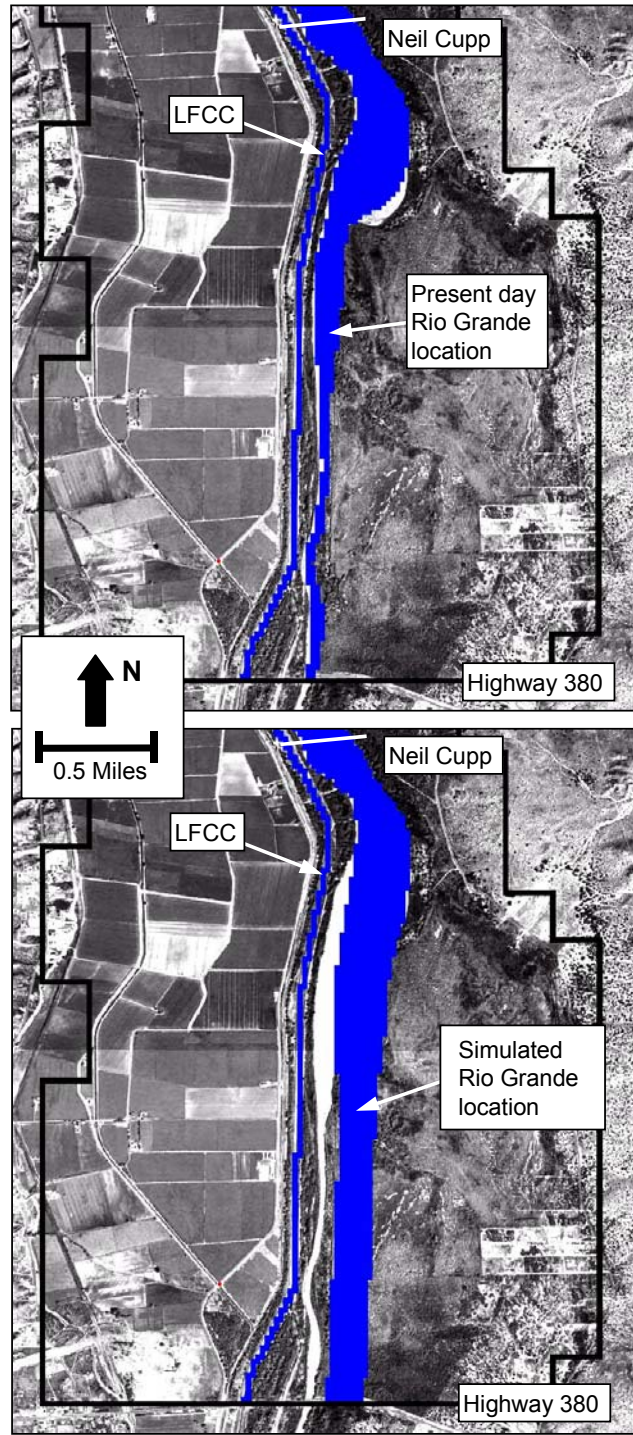


Figure 6-10: Present day and simulated locations of the Rio Grande channel.

4.3) where simulated heads were recorded with the LFCC and river in their present day configuration. River cells remained active for the entire year.

Results of the transient simulation indicated that Rio Grande and LFCC seepage decreased by 34 and 17 percent, respectively, after channel widening and relocation. Seepage from drains, all of which were located to the west of the LFCC canal, increased by 13 percent. Losses from the aquifer due to evapotranspiration decreased by two percent. Total inputs to the groundwater system decreased by 34 percent and total outputs decreased by 13 percent. This water budget imbalance equated to $-3,844$ af/yr (-4.7×10^6 m³/yr), 11 percent of the total inflows to the system (Table 6-4). The large difference of outputs and inputs observed in this simulation was because initial heads were taken from the steady-state and regional-scale model output of the river in its original location.

Groundwater Inputs	af/yr	m ³ /yr
River seepage	21,947	2.7E+07
Recharge	1,678	2.1E+06
Drains	8,622	1.1E+07
Net boundary influx	2,624	3.2E+06
TOTAL IN	34,871	4.3E+07
Groundwater Outputs		
LFCC seepage	28,978	3.6E+07
Evapotranspiration	9,737	1.2E+07
TOTAL OUT	38,715	4.8E+07
IN - OUT	-3,844	-4.7E+06

Table 6-4: Inputs and outputs to the hydrologic system with a new river channel location.

Water level elevations at W-91.28-1 indicated that levels were higher to the east of the Rio Grande with the new river channel simulation (Figure 6-11). It

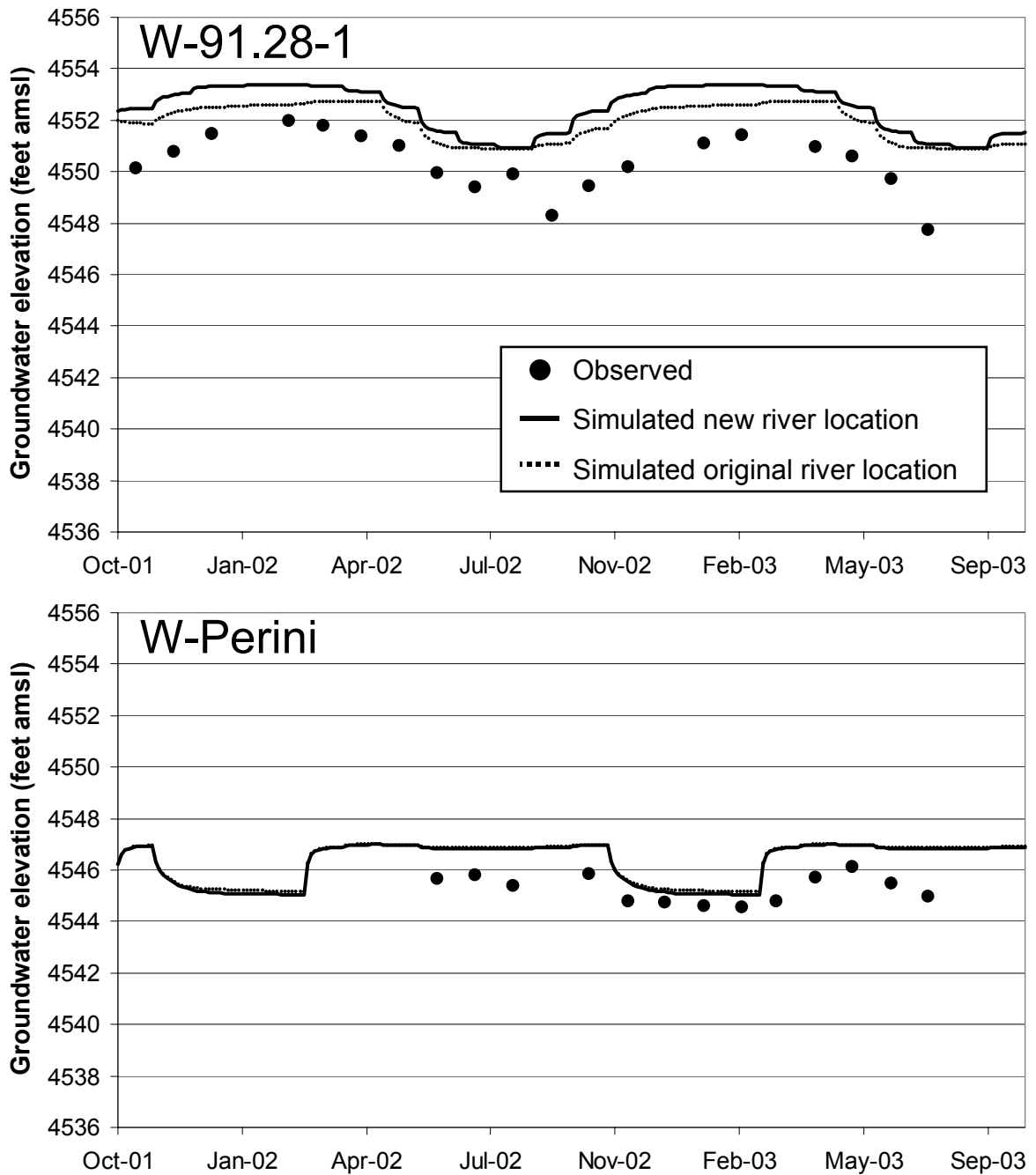


Figure 6-11: Simulated and observed water elevations for current and proposed river channel locations at W-91.28-1, W-87.62-1, and W-87.62-3.

was possible that elevated levels were observed to the south of this location, but there were no existing wells in that region to compare simulated and observed data. Elevations at well W-Perini were nearly identical to the original model output except for slightly depressed levels during the months of October through

March. This was because the LFCC acted as a hydrologic barrier between the Rio Grande and groundwater levels in agricultural lands to the west.

Plots of Rio Grande and LFCC seepage showed changes to the surface water and groundwater interaction made by a shift in river location (Figures 6-12 and 6-13). Rio Grande seepage losses from the proposed channel location

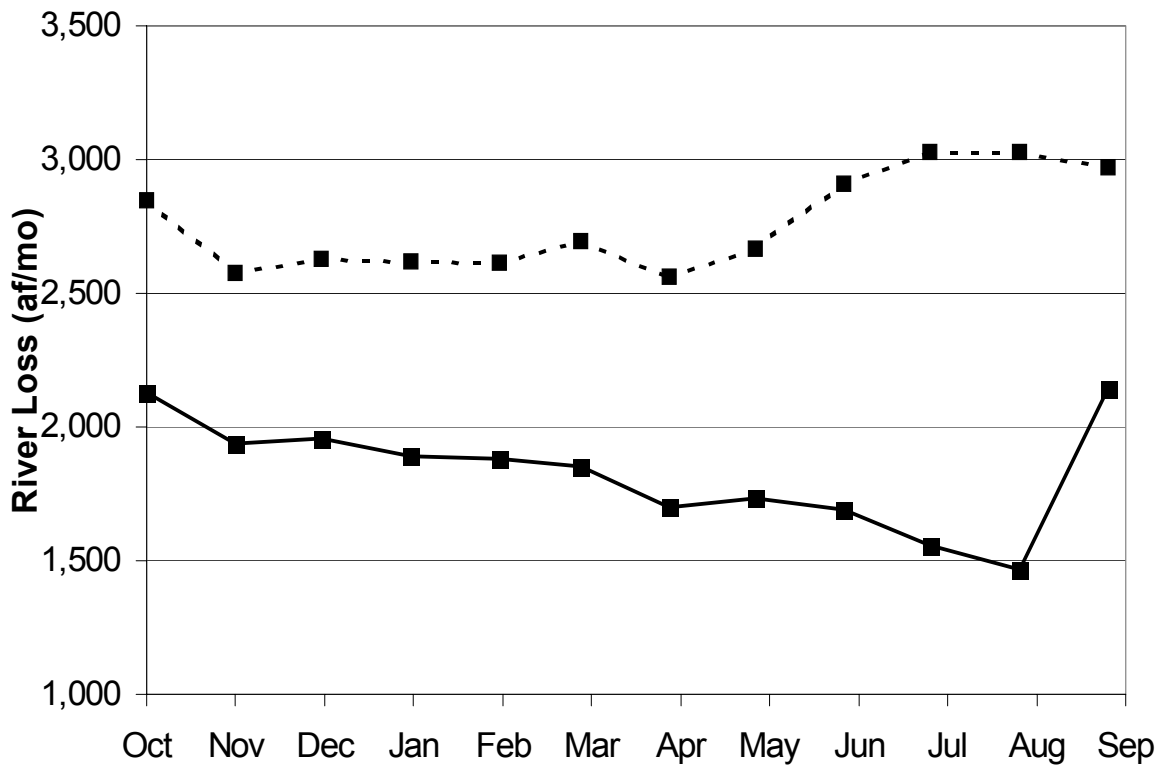


Figure 6-12: Simulated Rio Grande seepage for relocated (solid) and original (dashed) river channel locations.

differed in character from the original results of Chapter 4.3. Changes in seepage behavior indicated that aquifer gains from the Rio Grande decreased throughout the summer for the new river location (as stage height decreased) while in the original simulation these aquifer gains increased. This behavior might be attributed to the increased distance between the Rio Grande and LFCC channels. Character of fluctuations in LFCC aquifer loss with the new river

channel was nearly identical to those with the original Rio Grande location. The only difference was that seepage gain was less in magnitude by approximately 500 af/month ($6.2 \times 10^5 \text{ m}^3/\text{mo}$) with the new river location.

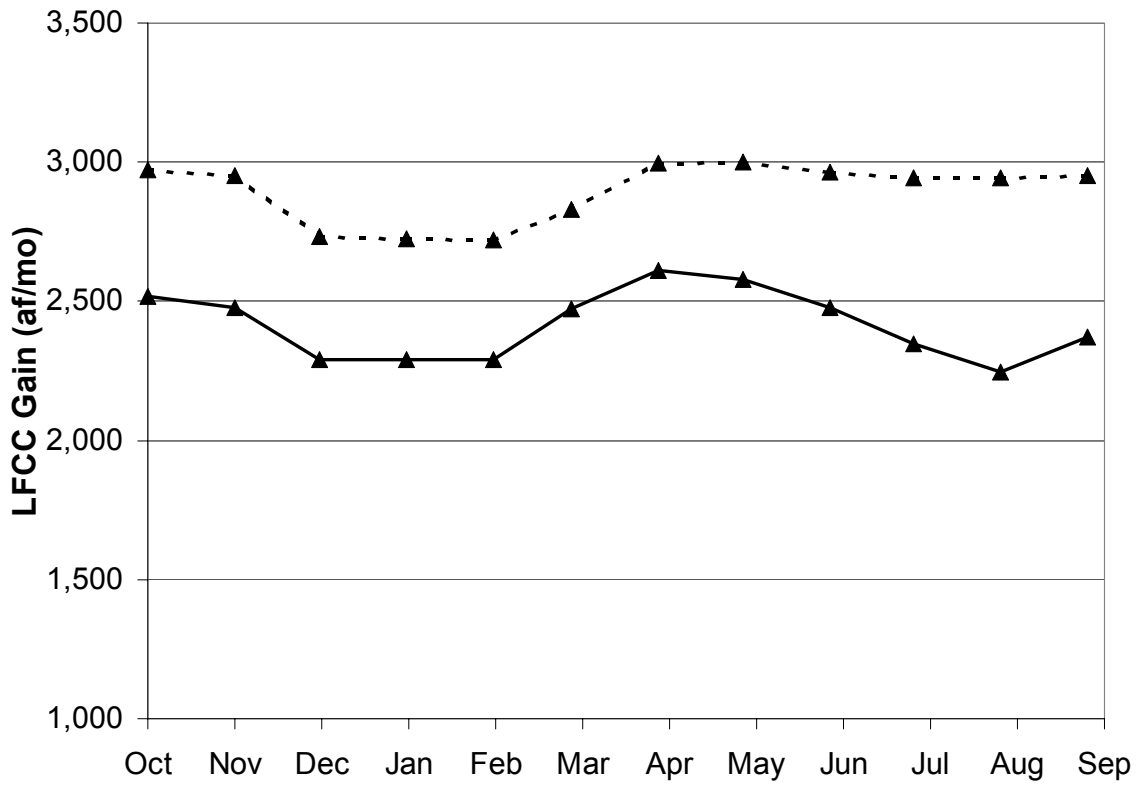


Figure 6-13: Simulated LFCC seepage for relocated (solid) and original (dashed) river channel locations.

7. CONCLUSIONS

High-resolution telescopic modeling was conducted along the Rio Grande and associated drains and canals to evaluate several management alternatives aimed at improving river conveyance efficiency. Simulation results indicated that the system was very responsive to changes in geologic properties, especially when such alterations improved vertical connectivity between layers. It was also shown that in the absence of the LFCC, water level elevations on the west side of the Rio Grande channel were significantly elevated. Simulations of the system with decreased evapotranspiration rates and a relocated river channel showed less magnitude of change.

Sensitivity analyses of the steady-state model were conducted to evaluate the effects of assumptions made during geologic discretization. Three simulations were performed. The first simulation was a homogeneous and anisotropic model where the clay layer (layer 2) properties were set equal to those of layers one and three. Results indicated that water levels were elevated by an average of 0.35 feet. Net seepage into the aquifer from the Rio Grande channel increased by 55 percent and losses to the aquifer from the LFCC increased by 60 percent. Changes in seepage rates and water levels were caused by an increase in vertical connectivity between hydrostratigraphic units

Isotropic and heterogeneous properties were tested in the second simulation where all hydraulic conductivity values were set to the horizontal value applied in the original steady-state model. This changed the vertical hydraulic conductivity of layer 2 from 0.1 feet/day (3.0×10^{-2} m/d) to 2 feet/day (0.6 m/d). Similar results were observed as the homogeneous model with increased river and LFCC seepage by 47 and 51 percent, respectively. Again, these changes were due to increased vertical connection between layers

Finally, in the third simulation, effects of decreasing and increasing hydraulic conductivity were tested while maintaining heterogeneities and anisotropy ratios from the original model. Fluctuations in water level elevation correlated with changes in hydraulic conductivity. When hydraulic conductivity values were decreased by 50 percent, total flow through the system declined by 34 percent. When double the hydraulic conductivity value was applied, total flows were increased by 50 percent.

This information, combined with the pump test data presented in Chapter 4.1.4, suggested justification for the presence of a clay layer at approximately 30 feet depth. In reality, the system was likely scattered with clay sills and fine sand lenses, representing ancient riverbed deposits. The geologic discretization applied to this model was an attempt to generalize and simulate what was most probably a highly complex system.

Management alternatives evaluated using simulations included:

- Evaluation and comparison of the system with and without the LFCC

- Decreased riparian vegetation and open ground evapotranspiration rates, based on current riparian management alternatives
- Evaluation of a possible relocation of the Rio Grande channel

These simulations were conducted to determine the magnitude of improvement that could be made to increase Rio Grande conveyance and groundwater elevations in the study area.

In the absence of the LFCC, average groundwater level elevations in the domain were increased by 3.97 feet (1.21 m). Total flows through the system decreased from 40,089 af/yr (4.7×10^7 m³/yr) to 10,366 af/yr (1.3×10^7 m³/yr). These results indicated that the presence of the LFCC recharges the shallow aquifer at the sacrifice of decreasing the volume of water conveyed through the system as a whole.

Riparian vegetation and open ground evapotranspiration rates were varied at 5, 20, and 50 percent of the original value. Resulting plots of water elevation showed increased levels (average of 0.5 ft or 0.15 m at 20 percent reduction) with decreased evapotranspiration rate. When evapotranspiration rates were decreased by 20 percent, a two percent decrease in river seepage and a three percent decrease in total inputs and outputs was observed. Changes in LFCC seepage gain were negligible because most riparian vegetation existed to the east of the Rio Grande canal. Because eradication of saltcedar and other invasive species is time consuming, expensive, and poorly understood, this management alternative was not recommended for this particular study area.

Relocation of the Rio Grande channel to the east of its present day location decreased river loss and LFCC gain by 34 and 17 percent, respectively. There was not enough data to see a significant change in groundwater elevation levels, although some increase was observed to the east of the Rio Grande. Little fluctuation was observed to the west of the LFCC, indicating that this channel acted as a hydrologic boundary between the Rio Grande and agricultural fields to the west.

Groundwater and surface water modeling can be a vital tool for watershed management. Having the ability to predict river flows and understand the dynamics of the system can help decision makers allocate a scarce water supply more efficiently. The credibility of a groundwater/surface water models is based upon the accuracy, quantity, and quality of the data used as input and initial conditions. As more assumptions are made regarding subsurface geologic parameters, flow conditions, evapotranspiration rates, and other parameters, the model loses its credibility. This telescopic model has been developed in an attempt to gain a better understanding of the flow system with the existing information and help future modelers create accurate, working models of the region in hopes of more efficiently allocating water among users.

8. RECOMMENDATIONS FOR FUTURE WORK

One of the primary concerns for groundwater/surface-water modelers is the quantity, quality, and accuracy of data. Inconsistencies in collection method, scarcity of data points, and lack of regular scheduled measurements lead to poor model calibration and inaccurate simulations. For the reach of the Rio Grande between Brown Arroyo and Highway 380, model calibration was hindered primarily by a lack of subsurface geological information and observed water level elevation data.

8.1 MODEL CONSTRUCTION

Two cross-sections of geologic split spoon sampling analysis were performed at the northern and southern ends of the model domain. Linear interpolation was used to estimate the depth to the top of layer two between well locations. This technique was also used to approximate the depth of layer two between the two cross-sections. This interpolation made many assumptions, including that the clay layer was a continuous geologic unit at the same depth along the reach. Ground surface elevation was determined from a 10-m DEM average applied to each 100 x 100 foot grid cell. Many assumptions were made in defining the geologic units applied to the model. Additional core analysis in the model domain would help refine an understanding of the stratigraphy.

Mathematical codes can be used to generate more realistic aquifer properties and distributions for a heterogeneous alluvial system (Regli et al., 2003).

Hydrogeologic parameters were determined from pump test results in two locations near the south of the model. Each test produced different values for hydraulic conductivity and the average of the results was used as input for the system as a whole. Properties of layer 2 were assigned to be standard values of clay taken from Freeze and Cherry (1979). Bed conductivity of drains, LFCC, and the river were obtained from the regional model. These values for aquifer and riverbed conductivity can be improved with further analysis of tracer tests, water chemistry, and refined modeling.

Refinement of geological and hydrological properties within the domain would increase our understanding of the interactions present and allow us to simulate the system more realistically.

8.2 INPUT DATA

Prior to October of 2001 data was not collected at regular intervals along this reach of the river. Several locations were measured intermittently in the 1950s through the 1980s, but many of the survey elevations of measuring points were rounded to the nearest 5-foot interval. Beginning in October of 2001, monthly water levels used in calibration of the telescopic model were recorded at ten locations within the domain. In May of 2003, monthly water level measurements were initiated in NMISC wells located at the northern and southern model boundaries. Datalogger files from these wells will provide vast amounts of detailed information regarding short and long-term fluctuations in

water elevation. Inclusion of these data as they are collected over the upcoming years can help generate more accurate models and simulate detailed processes.

Precipitation was not considered in this analysis of the hydrologic system. In Chapter 2.2, it is shown that rain and snow contribute minimal inputs to the shallow aquifer, relative to Rio Grande flows. In the future, this information, along with more accurate estimates of mountain front recharge, can be monitored within the study area and included as part of the model.

River flows for the telescopic model presented were determined from regional model boundary inputs. Stage was estimated to follow trends recorded at San Marcial. Values could be improved with installation and monitoring of gaging equipment which was initiated May 2003 as discussed in Chapter 4.1.2.

Evapotranspiration rates estimated from BDA NWR tower data were applied to the model as a monthly average where riparian evapotranspiration fluctuates while crop and sandbar rates remain constant. Accuracy of the model could be improved if evapotranspiration values for riparian and crop vegetation were monitored over time within the study area.

8.3 LINKING REGIONAL AND TELESCOPIC MODELS

The telescopic model presented gathers prescribed head values for the boundaries from the regional model at the first time step of the first stress period. Ideally, prescribed head values for the boundaries of the telescopic model domain would be extracted from the regional model at the beginning of each stress period. The model would be run based on these initial heads for a certain span of time steps until the regional model was called on again to determine an

updated set of initial conditions. This continuous link between the regional model and the telescopic model would help ensure consistency in final output for long-term scenarios and maintain the link between the large-scale and refined systems

REFERENCES

- Anderholm, S.K. 1987. Hydrogeology of the Socorro and La Jencia basins, Socorro County, New Mexico. U.S. Geological Survey Water-Resources Investigations Report 84-4342. Dept. of the Interior, Denver, CO.
- Bawazir, A.S. 2000. Riparian evapotranspiration studies of the middle Rio Grande. Dissertation. New Mexico State University, Las Cruces, NM.
- Cather, S.M. 1996. Geologic map of upper Cenozoic deposits of the Mesa del Yeso 7.5' quadrangle, New Mexico. Pending New Mexico Geology. New Mexico Bureau of Mines and Mineral Resources, Socorro, NM.
- Cather, S.M. 1997. Toward a hydrogeologic classification of map units in the Santa Fe Group, Rio Grande rift, New Mexico. New Mexico Geology vol. 19 No. 1:15-21.
- Chapman, D.C. and C.M. Canavan. 2002. Nutrients, phytoplankton, and hydrogen sulfide, in Elephant Butte reservoir, New Mexico. p. 94. In 105th Annual Meeting of the Texas Academy of Science program and abstracts. Laredo, Texas.
- Cleverly, J.R., C.N. Dahm, J.R. Thibault, D.J. Gilroy, J.E. Allred Coonrod. 2002. Seasonal estimates of actual evapo-transpiration from *Tamarix ramosissima* stands using three-dimensional eddy covariance. [Online]. Journal of Arid Environments v. 52:181-197. Available at: <http://www.sciencedirect.com/science/journal/01401963> (accessed 8 Dec. 2003) Elsevier Ltd, Orlando, FL.
- Freeze, A., and J. Cherry. 1979. Groundwater. Prentice-Hall, Inc., Englewood Cliffs, NJ.
- Gellis, A.C. 1992. Decreasing trends of suspended sediment concentrations of selected streamflow stations in New Mexico. p. 77-93. In Proc. of the 36th Annual NM Water Conf. New Mexico Water Resources Research Institute Report 265. Las Cruces, NM.

- Hantush, M.S. 1961. Drawdown around a partially penetrating well: Proceedings of the American Society of Civil Engineering, Journal of the Hydraulics Division, v. 87, no. HY4, p. 83-98.
- Hydrosphere Resource Consultants. August 2001. Investigation of surface water – groundwater interactions Rio Grande Low Flow Conveyance Channel, Socorro County, NM.
- Interstate Stream Commission and Middle Rio Grande Conservancy District. 2001. Middle Rio Grande Vegetation Classification – Summer 2000. Albuquerque, NM.
- McDonald, M.G., and A.W. Harbaugh. 1988. A modular three-dimensional finite-difference groundwater flow model. U.S. Geological Survey Open File Report 83. U.S. Geological Survey, Washington, D.C.
- Middle Rio Grande Conservancy District and Interstate Stream Commission. 2001. Middle Rio Grande
- Miller, R.S. 1988. User's guide for RIV2--A package for routing and accounting of river discharge for a modular, three-dimensional, finite-difference, ground-water flow model. U.S. Geological Survey Open-File Report 88-435. Denver, CO.
- Population Division, U.S. Census Bureau. New Mexico county population estimates: April 1, 2000 to July 1, 2002-Table CO-EST2002-01-35. [Online]. Available at: <http://www.census.gov> (accessed 4 July 2003) U.S. Census Bureau, Washington, D.C.
- Prudic, D.E. 1989. Documentation of a computer program to simulate stream-aquifer relations using a modular, finite-difference, ground-water flow model. U.S. Geological Survey Open-File Report 88-729. Denver, CO.
- Regli, C., M. Rauber, and P. Huggenberger. 2003. Analysis of aquifer heterogeneity within a well capture zone, comparison of model data with field experiments: A case study from the River Wiese, Switzerland. *Aquat. Sci.* 65:111-128.
- Roybal, F.E. 1991. Ground-water resources of Socorro County, New Mexico. U.S. Geological Survey Water-Resources Investigations Report 89-4083. U.S. Department of the Interior, Albuquerque, NM.
- S.S. Papadopoulos & Associates, Inc. 2002. Assessment of flow conditions and seepage on the Rio Grande and adjacent channels, Isleta to San Marcial, summer 2001. SSPA, Boulder, CO.

- S.S. Papadopulos & Associates, Inc. 2003. Recommendations for installation of extraction wells and observation wells, Rio Grande watershed study, phase 1. SSPA, Boulder, CO.
- Sanford, A.R. 1968. Gravity survey in central Socorro County, New Mexico. New Mexico Bureau of Mines and Mineral Resources Circ. 91. NMIMT, Socorro, NM.
- Shafike, N., R.S. Bowman, and L.J. Wilcox. 2002. Hydrologic modeling of the Rio Grande surface water / groundwater system from San Acacia to Elephant Butte Reservoir. p. F30. *In Proc. Conf. New Mexico Water Research Symposium*. Macey Center, Socorro, NM.
- Smith, R. 2002. New Mexico works to remove saltcedar. [Online]. Available at: http://southwestfarmpress.com/ar/farming_new_mexico_works/ (accessed 3 Nov. 2003; verified 8 Dec. 2003) Southwest Farm Press, Bellevue, NE.
- Swain, E.D. and E.J. Wexler. 1996. A coupled surface-water and ground-water flow model (MODBRANCH) for simulation of stream-aquifer interaction. Denver, CO.
- Tetra Tech, Inc. 2003. Hope for a living river, a framework for a restoration vision for the Rio Grande. The Alliance for Rio Grande Heritage, Albuquerque, NM.
- Western Regional Climate Center. Precipitation and snowfall monthly totals. [Online]. Available at: <http://www.wrcc.dri.edu> (accessed 10 July 2003) WRRC, Reno, NV.

APPENDICES

The following appendices contain data used for model construction and calibration in the region between Brown Arroyo and San Antonio, New Mexico. Well and surface measuring point locations are provided, with water level elevation data spanning the period of October 2001 through August 2003. Geologic logs written and compiled by S.S. Papadopulos and Associates are included for 24 boreholes within the study area.